648 | 2009

SCHRIFTENREIHE SCHIFFBAU

Florian Kluwe

Development of a Minimum Stability Criterion to Prevent Large Amplitude Roll Motions in Following Seas

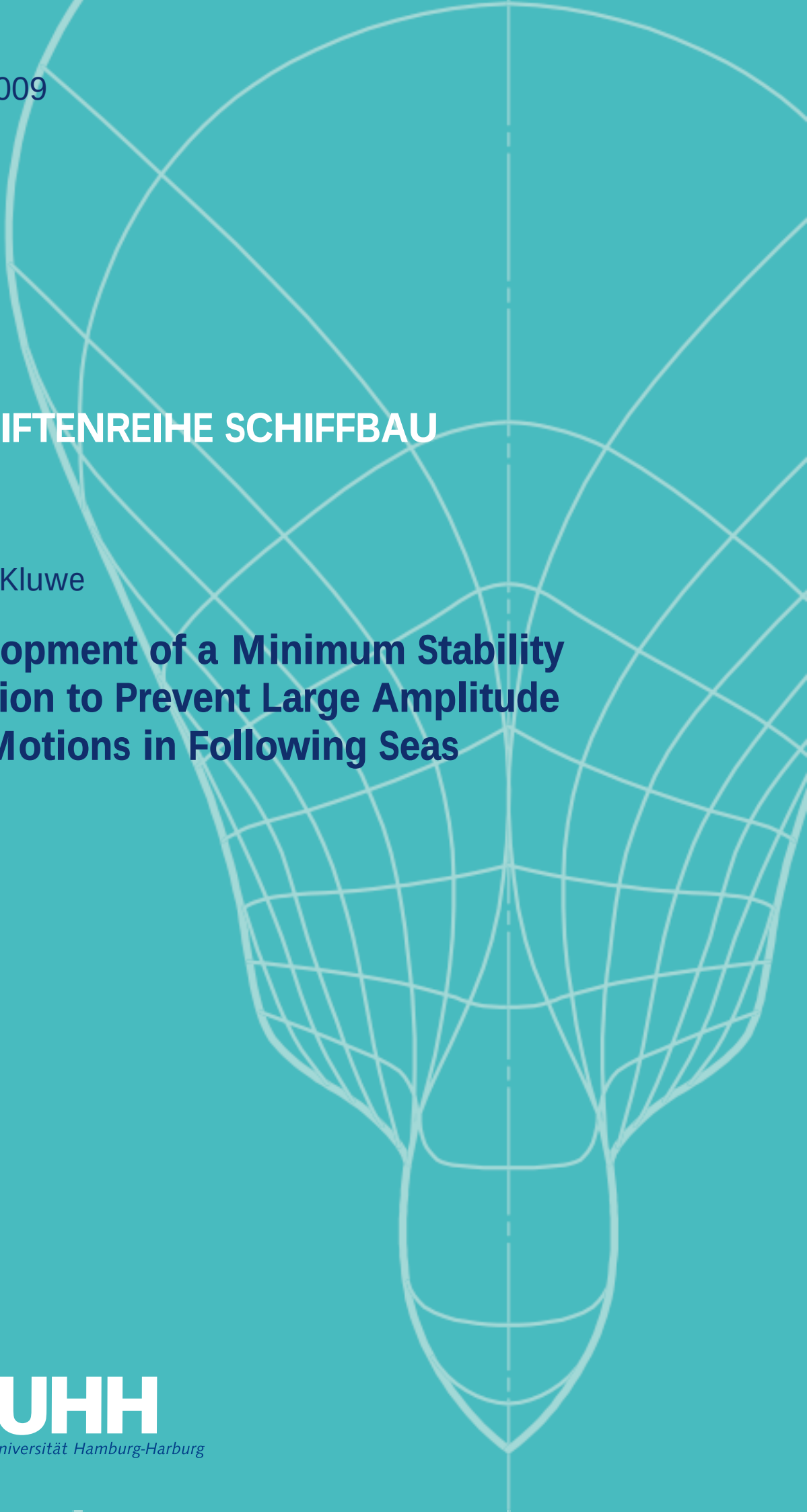

TUHH
Technische Universität Hamburg-Harburg

Development of a Minimum Stability Criterion to Prevent Large Amplitude Roll Motions in Following Seas

Florian Kluwe

1. Auflage, Hamburg, Technische Universität Hamburg-Harburg, 2009
ISBN 978-3-89220-648-4

Schriftenreihe Schiffbau
Schwarzenbergstraße 95c
D-21073 Hamburg

http://www.tuhh.de/vss

Development of a Minimum Stability Criterion to Prevent Large Amplitude Roll Motions in Following Seas

Vom Promotionsausschuss der
Technischen Universität Hamburg-Harburg
zur Erlangung des akademischen Grades

Doktor-Ingenieur (Dr.-Ing.)

genehmigte

Dissertation

von
Dipl.-Ing. Florian Kluwe
aus Kulmbach

2009

Vorsitzender des Prüfungsausschusses:

Prof. Dr.-Ing. Otto von Estorff

Gutachter:

1. Gutachter: Prof. Dr.-Ing. Stefan Krüger
2. Gutachter: Prof. Dr.-Ing. Moustafa Abdel-Maksoud

Zusätzliche Gutachter:

Prof. Dr.-Ing. Edwin Kreuzer
Prof. Dr.-Ing. Thomas Rung

Tag der mündlichen Prüfung:

09. 10. 2009

Technischen Universität Hamburg-Harburg
Schwarzenbergstraße 95c
D-21073 Hamburg

Bericht Nr.: 648

ISBN 978-3-89220-648-4

Dedicated to my father

Abstract

The intact stability of ships, their ability to withstand external forces and loads without capsizing, to date is still evaluated on the basis of empirical and semi-empirical criteria. A number of accidents in the past years show that these existing criteria do not provide a sufficient safety level, especially with respect to certain ship types, like RoRo-vessels and large Container Ships. In particular, the dynamic behaviour in longitudinal waves is not addressed by the existing criteria. In the present work a new type of intact stability criterion is developed, which is based on the direct assessment of ship responses in irregular short crested seaways. The idea behind the new approach is to evaluate the ship's behaviour in a representative number of possible operating conditions. For each operating condition a limiting wave height is determined by the *Blume-criterion*. Above this wave height a ship is considered to be unsafe. All unsafe situations contribute to the Insufficient Stability Event Index (ISEI) with their individual probability of occurrence. This index is a measure for the overall vulnerability of a ship in the dynamic wave environment. The threshold value for this index is obtained from the investigation and analysis of a number of capsizing accidents. Finally, a simplified criterion is derived from the simulation-based index in order to provide the findings obtained from the numerical simulations also in situations where direct calculations are not accessible. The simplified criterion is mainly based on lever arm alterations in waves.

Kurzfassung

Die Intaktstabilität von Schiffen, ihre Fähigkeit, Kräften und Momenten ohne Kenterung zu widerstehen, wird heutzutage immer noch auf Basis von empirischen und semi-empirischen Kriterien bewertet. Verschiedene Unfälle in den letzten Jahren zeigen, dass die bestehenden Kriterien kein ausreichendes Sicherheitsniveau bieten, insbesondere für verschiedene Schiffstypen, wie beispielsweise RoRo-Schiffe und große Containerschiffe. Vor allem das dynamische Verhalten in längslaufendem Seegang wird von den existierenden Kriterien nicht in ausreichendem Maße berücksichtigt. Die vorliegenden Arbeit beschäftigt sich mit der Entwicklung eines neuen Intaktstabilitätskriteriums, basierend auf der direkten Berechnung der Schiffsantwort in unregelmäßigen, kurzkämmigen Wellen. Die Idee hinter dem neuen Ansatz ist, das Schiffsverhalten in einer Anzahl repräsentativer Betriebszustände zu bewerten. Für jede Situation wird dabei mit Hilfe des *Blume-Kriteriums* eine limitierende Wellenhöhe bestimmt, wobei das Schiff oberhalb der Grenzwellenhöhe generell als unsicher angesehen wird. Alle unsicheren Betriebszustände tragen zum "Insufficient Stability Event Index" (ISEI) bei, der ein Maß für die Gefährdung des Schiffes in seinem dynamischen Umfeld darstellt. Der Grenzwert für den Index wird aus Unfalluntersuchungen gewonnen. Schließlich wird ein vereinfachtes, simulationsunabhängiges Kriterium abgeleitet, welches auf den Erkenntnissen aus der Simulation beruht und diese auch dort bereitstellt, wo Seegangssimulationen nicht verfügbar sind. Das vereinfachte Kriterium basiert im Wesentlichen auf den Hebelarmschwankungen in Wellen.

Acknowledgements

The thesis in hand is based on the research carried out during my time as research assistant at the Institute of Ship Design and Ship Safety of the Hamburg University of Technology. I would like to express my thanks and my gratitude to my adviser, Prof. Dr.-Ing. Stefan Krüger, who offered me the opportunity to research at his institute and who supported my work by continuous encouragement and valuable suggestions throughout the years.

Further I would like to thank Prof. Dr.-Ing. Moustafa Abdel-Maksoud for the evaluation of this thesis, as well as the additional evaluators, Prof. Dr.-Ing. Edwin Kreuzer and Prof. Dr.-Ing. Thomas Rung for their work.

Additional thanks go to Prof. Dr.-Ing. Otto von Estorff who chaired the doctorate commission.

The work on this thesis was carried out within the framework of the research project "Lasten auf Schiffe im Seegang" (LaSSe), which was funded by the German Federal Ministry of Economics and Technology (BMWi).

I also don't want to miss the opportunity to thank my colleagues of the institute M-6 for the good working atmosphere and the input of ideas as well as many fruitful discussions. Namely, I would like to express many thanks to Dr.-Ing. Felix-Ingo Kehren who was sharing the office with me, for the interesting and successful time we spent together.

Finally, I would like to express my deepest gratefulness to my family for their everlasting support and to Katja for sharing and supporting my life with great patience and constant encouragement.

Contents

List of Figures

List of Tables

List of Symbols

Δ	Displacement in tons
δ	Rudder angle
η	Sway displacement
λ	Wave length
μ	Encounter angle of waves
ω	Circular frequency of the wave
ω_e	Circular frequency of encounter between the ship and the wave
ψ	Yaw angle
ρ	Density
σ	Standard deviation
Θ_{xx}	Mass moment of inertia
ε	Phase shift of the wave components
φ	Roll angle
ϑ	Pitch angle
ξ	Surge displacement
ζ	Heave displacement
$\zeta(x, y, t)$	Time and place dependent wave elevation
$\mathbf{A}$	Matrix containing all added mass terms

A_H	Cross sectional area
A_{15diff}	Residual area between minimum and maximum lever arm curve up to 15 degrees heel
A_{40min}	Area below minimum lever arm curve up to 40 degrees heel
AP	Aft perpendiculum
$\mathbf{B}$	Matrix representing all damping components
B	Centre of buoyancy
BL	Base line
$\mathbf{C}$	Matrix containing all restoring forces and moments proportional to the displacement in the six degrees of freedom
C_B	Block coefficient
C_{WP}	Waterplane coefficient
CL	Centre line
d_L,d_Q	Linear and quadratic damping coefficient
E_R	Residual area below the lever arm curve
$\mathbf{F_E}$	Vector containing all exciting forces and moments
g	Gravity in m/s^2
$\delta h(\varphi)$	Lever arm alterations due to waves
H	Wave height
$h(\varphi)$	Transverse lever arm
$H_{1/3}$	Significant wave height (expected value of the one third highest waves)
H_{A0}	Mean limiting wave height
$h_{still}(\varphi)$	Still water lever arm

Θ_{xz}	Mass product of inertia
i'	Roll radius of gyration
J	Advance coefficient
k	Wave number
k_Q	Propeller torque coefficient
k_T	Propeller thrust coefficient
KG,VCG	Vertical centre of gravity
L_{bp}	Length between perpendiculars
LCG	Longitudinal centre of gravity
$\overline{GM}$	Metacentric height
$\mathbf{M}$	Mass matrix containing all solid mass components
m	Mass
M	Metacentre
P	Probability
p	Probability density
r	Turning rate
$R(v)$	Calm water resistance curve
R_A	Added ship resistance
R_T	Total ship resistance in calm water
r_{fail}	Failure rate
$S(\omega, \mu)$	Two-dimensional wave spectrum
T_1	Characteristic period of the waves

T_e	Encounter period in seconds
$\mathbf{u}$	Vector of motion containing all six degrees of freedom
v	Speed
$\hat{Y}_x$	Transfer functions

1 Introduction

In order to assure the safe operation of ships, it is necessary to provide sufficient intact stability, which is defined as the ship's ability to withstand external forces and loads without capsizing in undamaged conditions. For merchant ships, today, this is regulated by criteria and rules issued by the International Maritime Organization (IMO). Although IMO only recommends the fulfilment of these criteria, usually all newbuildings have to meet the requirements as they are made mandatory by the respective flag state authorities.

The IMO criteria are still based on an approach developed in the early 20th century, which mainly consists of a statistical evaluation of lever arm curves for a set of ships, whereas the ships' actual safety is judged by "expert knowledge", which means pure guess based on empirical observations. The set of ships mainly consists of small vessels below 100 metres in length. The hullforms are mainly standard types widely used at the time the investigation was made. The resulting IMO-criteria consist of a set of required minimum values with respect to lever arms and areas below the lever arm curve. Since the time the criteria were developed, the average ship size as well as the hullforms have changed significantly. As the criteria are limited to statistics without taking into account loads and responses directly, it becomes obvious that the applicability to large ships, modern hullforms and unconventional ships is very limited.

Today, it is a widely accepted fact that the general intact stability criteria formulated by the IMO neither assure a uniform nor a sufficient safety level in many cases. The reason for not facing more losses of ships due to intact stability failures, mainly lies in the damage stability regulations which provide more restrictive requirements in most cases. However, this can not be generalised to all ship types and, furthermore, it is unclear how the new damage stability regulations, coming into force in 2009, will affect the safety level in detail.

Besides the common understanding in general that the intact stability regulations must be revised in such way that they provide a sufficient and consistent safety level, it is also widely recognised that there is a need to take into account the dynamic behaviour of ships for future intact stability assessment directly. Especially the phenomena related to stability alterations in longitudinal waves, known for example as parametric rolling and pure loss of stability, can lead to the sudden occurrence of very large roll angles. In extreme cases this can end up in the total loss of the vessel. A number of accidents during

Figure 1.1: *MV Finnbirch* after cargo shift caused by heavy rolling in following seas. (Photo: MRCC)

the last years which were related to dynamic stability alterations, have clearly shown that the phenomena mentioned beforehand are a real problem for ship safety, in particular for modern hull forms. Currently, the IMO does not provide any regulation which outlines these failure modes, which obviously generates the need for new criteria in this field.

As a consequence of various accidents, a number of capsizing criteria have been proposed in the last decades, either based on model tests and simulations or on empirical observations. A brief introduction to a selection of these criteria, introduced by German research groups, is given in the first part of this work. All presented criteria intend to reduce the capsize-risk of ships in heavy weather, but most of these criteria do not consider the dynamic effects of ships travelling in rough seas. New techniques, such as numerical motion simulations in the time domain have improved our knowledge on the phenomena and the situations in which ships are endangered with respect to large roll angles. Today, this allows us to address exactly those dynamic aspects, which most of the older criteria are lacking.

Based on the direct assessment of ship responses with numerical simulations carried out in irregular short crested waves, a new criterion is developed within the scope of this work. The structure of the approach incorporates some ideas of the goal based standards, which according to the International Maritime Organization (IMO) shall be the preferred basis for future regulations. The idea behind the new criterion is to evaluate the ship's behaviour in a representative number of possible operating conditions. For each operating condition, a limiting wave height is determined by deterministic decision criteria. Above this wave height, a ship is considered to be unsafe. All unsafe situations contribute to an index value with their individual probability of occurrence. In consequence, this index is a measure for the overall vulnerability of a ship in the dynamic wave environment. In order to make use of the new criterion in the safety assessment of ships, it is necessary

to determine a threshold value below which the risk of a stability accident is considered to be acceptably low. This threshold value is determined on the basis of various accident investigations which give a comprehensive overview on the index values associated to safe and unsafe operating conditions, respectively.

Finally, a simplified criterion is derived from the simulation-based index in order to provide the findings obtained from the numerical simulations also in situations, where direct calculations are not accessible. The simplified criterion is based on the same basic approach as the simulation based one, but it replaces the determination of the limiting wave heights by a method which is mainly based on lever arm curves in waves. The simplified criterion is correlated in such way that it delivers the best possible consistence with the results obtained from the numerical simulations.

In combination, both criteria can be used as efficient and powerful tools to assess the dynamic intact stability of ships during design, approval and operation.

2 Hazards to Ship Stability in Heavy Weather

The constantly changing shape of the water surface represents a dynamic environment which causes transient external forces and moments to ships. If these forces and moments become large due to large wave amplitudes, they may endanger the ship. At this, two main categories of hazards can be identified. On the one hand, waves cause high local as well as global loads to the ship-structure which can result either in the immediate failure of certain structural components, or which can cause structural damage due to fatigue in the long term. On the other hand, the external forces and moments induce ship motions, which in certain conditions can reach large amplitudes and which can effect large accelerations, both potentially leading to severe damage to the ship, the cargo and the men on board. A comprehensive analysis of possible hazards and failure modes of ships in heavy seas can be found in Skjong et al. [64]. The present work focuses on the second category of hazards by addressing certain phenomena related to the dynamic intact stability of ships.

Dynamic intact stability means that the assessment of ship-stability takes into account the transient character of the exciting forces and moments as well as the dynamic response of the vessel. Hence, the fundamental equation describing the rigid body motion of the ship in waves reads:

$$(\mathbf{M} + \mathbf{A}) \cdot \ddot{\mathbf{u}} + \mathbf{B} \cdot \dot{\mathbf{u}} + \mathbf{C} \cdot \mathbf{u} = \mathbf{F_E} \tag{2.1}$$

Here, $\mathbf{u}$ denotes a vector, describing the displacement in all six degrees of freedom, while $\dot{\mathbf{u}}$ and $\ddot{\mathbf{u}}$ are the time derivatives describing the velocity and the accelerations, respectively:

$$\mathbf{u}^T = (\xi,\ \eta,\ \zeta,\ \varphi,\ \vartheta,\ \psi) \tag{2.2}$$

The translational degrees of freedom are surge (ξ), sway (η) and heave (ζ), whereas the second three elements of the vector represent the rotational degrees of freedom, namely roll (φ), pitch (ϑ) and yaw (ψ). Figure 2.1 illustrates the orientation of the individuell degrees of freedom.

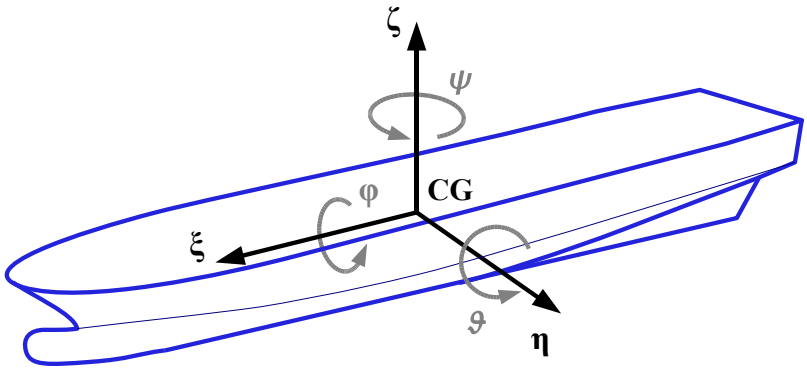

Figure 2.1: Ship motions in six degrees of freedom

Equation 2.1 consists of four elements describing the forces and moments that act on the ship. The first element represents all forces and moments which are linked to accelerations. Here, $\mathbf{M}$ denotes the mass-matrix containing all solid mass components of the ship and the cargo, while $\mathbf{A}$ contains all added mass terms, which represent the acceleration-dependent hydrodynamic forces and moments. The second element, which is the damping term of the differential equation, contains all speed dependent force components, represented by Matrix $\mathbf{B}$. Finally, the last element on the left hand side of Equation 2.1 is the stiffness term, containing the restoring forces and moments which are proportional to the displacements of the system. On the right hand side, the fourth element, represented by the vector $\mathbf{F_E}$, contains all external exciting forces and moments. Equation 2.1 forms a coupled system of six differential equations, describing the ship motions in the six degrees of freedom.

In the following we want to assess which degrees of freedom of ships are mainly affected by large amplitude motions and large accelerations. In case of ships with forward speed, the yaw motion is actively controlled via the available steering device, which under normal operating conditions is usually the rudder. Only if the manoeuvrability is lost, we observe large yaw amplitudes when the ship turns into beam seas. For the pitch motion, the stiffness of the system and the mass moments of inertia are large compared to the exciting moments, which is why we do not expect large amplitudes for conventional ship types. However, accelerations can become large due to the high stiffness. Finally, the roll motion is characterised by a small stiffness term compared to the other degrees of freedom and low damping. Depending on the actual stiffness provided by the up-righting moments, large amplitudes as well as large accelerations and also both hazards in combination are possible. As, in this work, we target minimum stability requirements in waves, large roll amplitudes associated to low stiffness are most important here. There are three main categories known which can induce roll motions of a ship. These are direct excitation via roll motions introduced by waves, parametric excitation due to lever arm alterations

in waves and, finally, the broaching of ships due to the loss of course control. These mechanisms are introduced in the following sections.

2.1 Direct Excitation of Roll Motions

This section provides an introduction to roll motions which are caused by external exciting moments initiated by waves approaching the ship from abeam. For demonstration reasons we simplify Equation 2.1 by neglecting all coupling terms and thus, obtain the following differential equation describing the uncoupled roll motion in one degree of freedom:

$$\Theta_{xx} \cdot \ddot{\varphi} + b \cdot \dot{\varphi} + \Delta \; g \; h(\varphi) \cdot \varphi = \Delta g h_e \tag{2.3}$$

Here, Θ_{xx} denotes the mass moment of inertia around the longitudinal x-axis, including the solid mass elements of the ship and the cargo as well as the added mass fraction. φ is the roll angle, Δ represents the displacement in tons and b represents roll damping. In the simplest case, b is modeled as constant damping coefficient. Further, $h(\varphi)$ denotes the lever arm curve of the ship. On the right hand side of Equation 2.3 we can find the exciting moments.

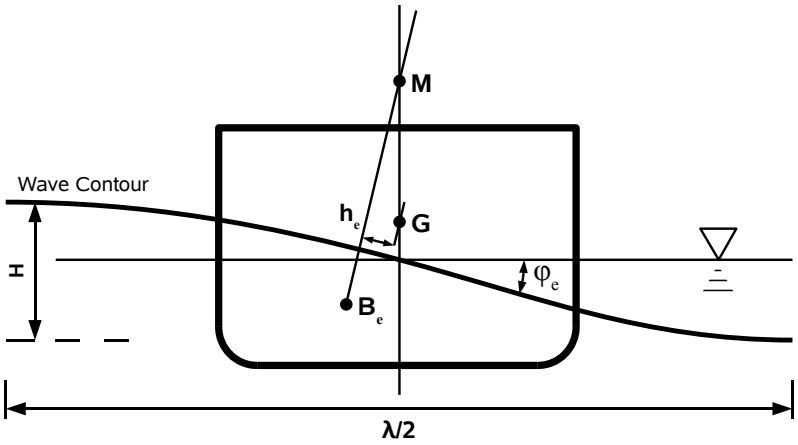

Figure 2.2: Approximation of the heeling lever induced by a transverse wave by the wave-steepness

To explain the basic principle how a beam wave induces roll moments to a ship, we consider a simple cross section as drafted in Figure 2.2. Obviously, the wave causes a shift of the centre of buoyancy similar to a static inclination of the ship by the angle φ_e. Replacing

the wave profile by a straight line in way of the cross section, this angle approximately equals the angle of the transient wave slope, determined by:

$$\varphi_e = \arctan\left(\frac{\pi H}{\lambda} \cdot \cos(\omega t)\right) \tag{2.4}$$

Where H denotes the wave height and λ is the wave length. As the wave passes the hull this virtual heeling angle varies between 0 and the maximum wave slope φ_e^{max} for $\cos(\omega t) = 1$. Consequently, the heeling arm h_e is obtained from the normal still water lever arm curve:

$$h_e = h(\varphi_e)$$

This very simple model considers only the hydrostatic forces, neglecting all hydrodynamic influences due to the wave velocity and due to the disturbance of the wave by the ship as well as any forces exerted on the water by the ship motions. Moreover, any coupling to the other degrees of freedom in this case especially sway and yaw, are neglected. While the model delivers a satisfying approximation for small wave-steepnesses, the waves cause the ship to drift at larger steepnesses, which dissipates a significant amount of the wave energy. In such cases a model without considering the drift motion delivers far too large roll amplitudes.

In order to estimate the danger caused by direct excitation to the ship, we must have an idea of the expected roll amplitudes. The largest roll amplitudes always occur in resonance conditions, but for larger merchant vessels roll resonances in beam sea conditions are mostly impossible. The reasons for this, is that in this case the resonances are found at very long waves, which introduce only very small exciting moments. This might be illustrated by the following example. We consider a ship with a mean natural roll period of about 20 seconds. In order to meet the resonance condition, the wave length of a regular wave then must equal:

$$\lambda = \frac{T_e^2 \cdot g}{2\pi} = \frac{(20s)^2 \cdot 9.81 m/s^2}{2\pi} = 624,8m$$

Assuming an extreme wave height of 25 metres, this would deliver a maximum virtual heeling angle of ca. 4.6 degrees, which is almost neglectable. Moreover, such large wave lengths are very unlikely to occur.

Nevertheless, there are situations where a ship can be endangered by direct excitation. In case the ship has excessive stability, possible resonance is shifted to shorter waves which are more probable. Direct, resonant roll excitation in connection with high stability can result in large accelerations. Additionally, smaller vessels are endangered by steep and breaking waves which can lead to an immediate capsize in one wave cycle. This

scenario in particular affects smaller fishing vessels travelling in very rough weather, often in combination with shallow water. However, both scenarios described are not of interest for the assessment of minimum stability, because neither their probability of occurrence, nor the severity of the consequences can be reduced by increasing the stability.

To conclude, roll moments introduced by waves can lead to relevant roll motions, but capsizing is very unlikely to occur under these conditions, as resonance conditions are usually not met and because steep waves induce drift motions which dissipate parts of the wave energy. In a realistic environment with irregular, short crested waves, these direct roll moments are always present and they always contribute to the resulting roll motion.

2.2 Excitation of Roll Motions by Dynamic Stability Alterations

We now consider the case that the ship is travelling in longitudinal waves, which means that the waves approach from ahead or astern. In long-crested waves, this would mean that the exciting term on the right hand side of Equation 2.3 becomes zero. Even though we do not have any exciting term anymore, we can observe the occurrence of very large roll angles under certain circumstances. The reason for this phenomenon is that the wave changes the ship's stability while passing by. To exemplify this, we consider a ship in a wave equalling almost the ship length, as shown in Figure 2.3.

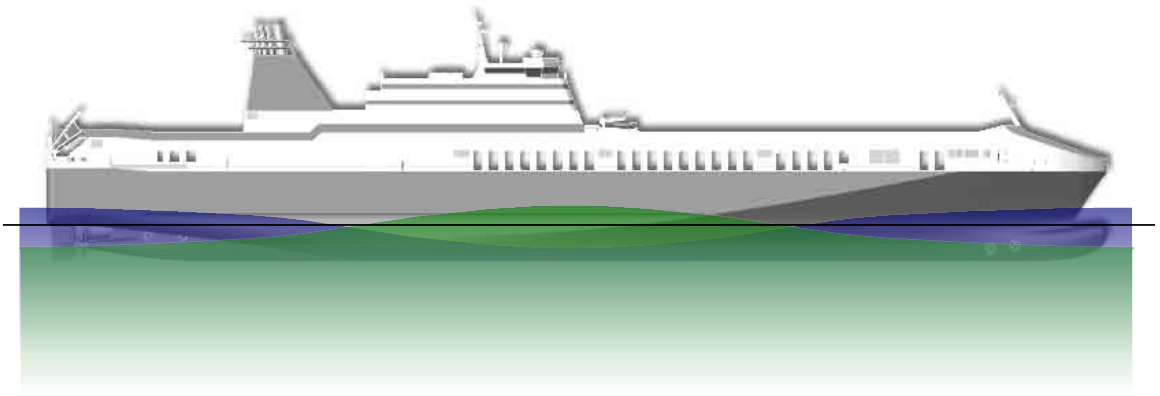

Figure 2.3: The drawing shows a ship situated in a wave with $\lambda \approx L_{bp}$. The sketch shows wave trough condition (blue) and wave crest condition (green).

2.2.1 Lever Arm Alterations and Roll Motions

The lever arm curve of the vessel is now calculated for still water conditions as well as for the situation where the ship is situated in the wave, at which we consider two situations: One lever arm curve is calculated for the situation where the wave crest is situated amidships, which is called wave crest condition in the following. A second curve is calculated for the situation that a wave crest is located at both ends of the ship, whereas the midship section is situated in a wave trough. We refer to this as the wave trough condition.

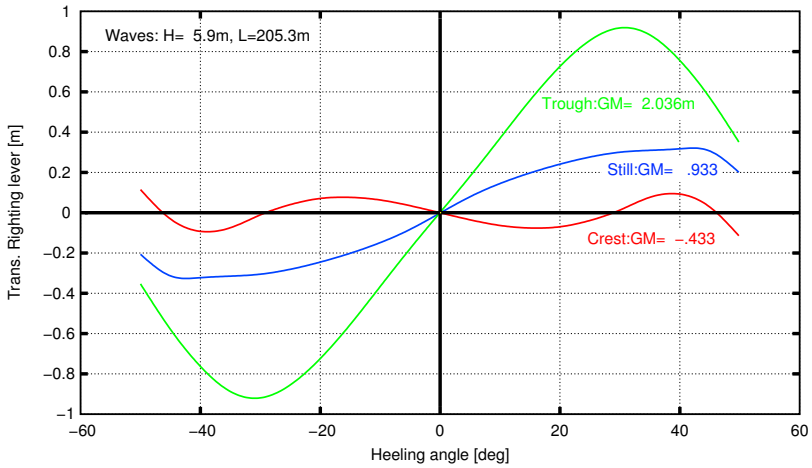

Figure 2.4: Lever arm curves of the ship in still water, wave trough and wave crest conditions.

Figure 2.4 shows the resulting righting lever curves. Obviously, the ship has significantly more stability in the wave trough condition than in still water, whilst the stability on the wave crest vanishes almost completely. This alteration of the righting lever arms results from the changing shape of the underwater hull. Figure 2.5 illustrates this mechanism. The left hand side shows the submerged parts of the hull for the wave crest condition and the right hand side those of the wave trough condition. The wave crest and the wave trough condition as introduced here, usually represent the extreme values of the lever arm alterations. When the waves are passing along the hull, the actual righting levers oscillate periodically between these two extremes. The frequency of this oscillation equals the encounter frequency between the ship and the waves.

A simple model for this mechanism can be formulated with the following differential equation, derived from Equation 2.3. Again, we consider only one degree of freedom and assume regular waves:

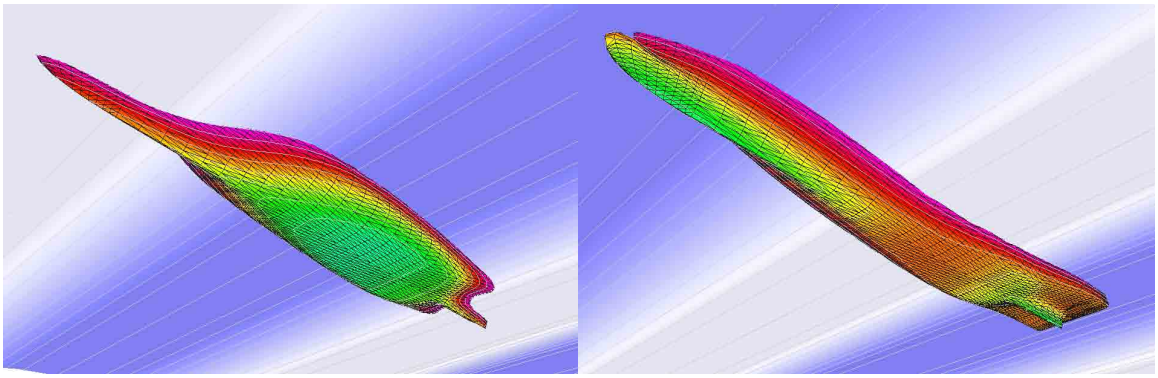

Figure 2.5: Variation of wetted surface and waterline area for a ship in wave crest (left) and waved trough (right) conditions.

$$\Theta_{xx} \cdot \ddot{\varphi} + b \cdot \dot{\varphi} + \Delta \; g \;\; [h_{still}(\varphi) + \delta h(\varphi) \cdot \sin(\omega_e t)] \cdot \varphi = 0 \tag{2.5}$$

This type of differential equation, which is characterised by the oscillating stiffness-parameter, is called *Mathieu-equation*. Even though this differential equation does not have an element of directly exciting moments on the right hand side, roll motions can be excited by the periodically oscillating stiffness term. As the driving force for the roll motions is the varying parameter in the stiffness term, this type of excitation is commonly called "parametric".

2.2.2 Characteristics of Parametrically Excited Roll Motions

In order to demonstrate the principle behaviour, Equation 2.5 is applied to three different, generic examples of lever arm curves with different characteristics. Figure 2.6 shows the development of the roll motion with identical initial conditions, ship data and GM, but with different lever arms. The original lever arms shown in the middle of Figure 2.6 are taken from a mid-size container vessel, displacement 47238 tons with a limiting GM of 0.2 metres. The two other sets of curves are transformed clones of the original lever arms, while the wave trough curve remains unchanged. The wave crest curve is varied in the range between 20 to 50 degrees so that we obtain different magnitudes of lever arm changes. The length of the regular wave is set to 215 metres, which equals the ship length between perpendiculars. The wave height is 4.0 meters. The wave encounter frequency is chosen so that it is approximately twice as large as the natural roll frequency of the vessel. This results in a forward speed of 17.35 knots. On the left hand side the extreme values of the lever arm curves are shown, representing wave crest and wave trough conditions, respectively. On the right hand side the resulting time series of roll angles are plotted.

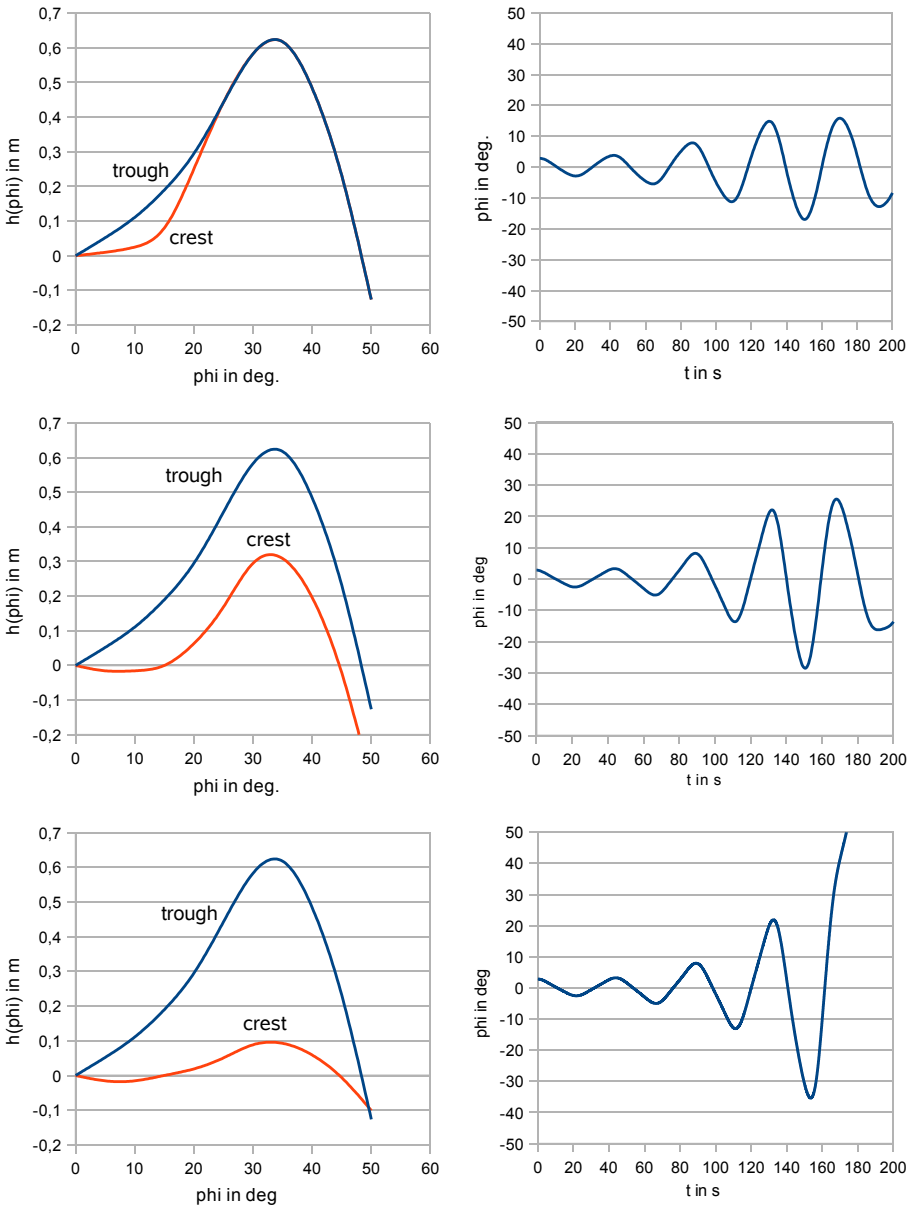

Figure 2.6: Generic example for a parametrically excited roll motion solved for 1 degree of freedom numerically, taking into account the non-linear lever arm curve. Responses shown for three different lever arm characteristics; $\lambda = 215$m, v = 17.35kn.

Visibly, increasing lever arm alterations lead to increased amplitudes, whereas the negative lever arms at small angles accelerate the development of large roll angles. The solution for the first two examples always remains within certain limits and thus, never leads to capsizing, while the roll motion in the last example rapidly grows until the ship capsizes.

The examples show the two possible types of solutions of the *Mathieu-equation*. Depending on the frequency of the stability alterations and depending on their amplitude as well as on the roll damping, we obtain stable solutions in some cases, which are also called bounded solutions. In contrast, for some combinations of parameters, the equation delivers un-stable, un-bounded solutions, like in the last case of our example.

In order to get un-bounded solutions, the lever arm alterations must exceed a certain threshold value. This depends on the individual characteristics of the hullform and usually occurs when the wave length lies approximately within the range of 0.7 and 1.3 times the ship length. However, the most severe ship reactions are observed in the shorter waves in tendency. Further, the occurrence of un-bounded solutions is connected to resonance conditions. Two conditions are of interest in particular. They are defined by the encounter frequency of the waves being equal to, or twice the natural roll frequency, called 1:1 and 2:1-resonance, respectively. The latter one, equalling the situation in the previous example, is considered to be the more dangerous situation. This is because the ship always meets the wave crest condition with low stability, which is the reason for the fastly increasing roll amplitudes, when the ship is reaching its up-right floating condition. In case of the 1:1-resonance, this occurs every second up-right position.

In connection with resonance conditions it is important to note that the natural roll period of a ship never is a constant value. First of all it depends on the actual roll amplitude due to the non-linear shape of the lever arm curve. Secondly, the lever arm curve itself is subject to change in waves as explained above. Thus, in practise it is not possible to determine a constant value for the natural roll period. In consequence, resonance conditions sometimes can be found in regions quite different from those determined by linear approximations.

The 2:1-resonance does only occur at low ship speeds in head as well as following seas. The main difference between head and following sea conditions is the ship stability at which the resonance is met. Low ship stability is always associated with small roll-eigenfrequencies and high ship stability with larger ones. In following seas the encounter frequency is lower than in head seas and this is why the 2:1-resonance is met at low stability values. In head seas the stability has to be significantly higher to meet the resonance situation. Thus, a 2:1-resonance in head seas is mainly characterised by short roll periods, which can lead to large accelerations in connection with large roll amplitudes. In contrast, the scenario in following seas is dominated by extreme roll angles. In this situation the ship faces a significant risk of capsizing. The accelerations typically are much smaller due to longer roll periods. The 1:1-resonance condition can usually be observed only at higher speeds

in following seas. These situations are slightly less critical, because the larger ship speed leads to increased roll damping and the excitation is less powerful. Nevertheless, this situation also can lead to capsizing, if the stability is low enough.

Additionally, in following seas the remaining stability of the vessel in wave crest conditions becomes important. Some ships show negative levers over the entire range of heeling angles in this situation. When the ship rests on the wave crest for a relatively long time in following seas, the development of large roll angles is supported. In the case that the encounter frequency gets close to zero, which occurs if the ship speed becomes almost the same as the speed of wave propagation, the time the ship rests on the wave crest becomes very long. In such a situation it is possible that the ship simply capsizes within one roll period. This failure mechanism is called "pure loss of stability".

2.2.3 Behaviour for Irregular Waves

All statements made above presume regular waves, which practically do not exist in nature. Nevertheless, the same phenomena and mechanisms can be observed in natural seaways as well. In this case, the lever arm alterations are no longer sinusoidal and the critical encounter frequencies are usually met only for a limited number of wave groups. Research projects carried out in Germany in past years, see for example Cramer and Krüger [18] and Billerbeck et al. [7], have investigated the occurrence of large amplitude roll motions in natural seaways. The results confirm the existence of parametrically excited roll motions also in these conditions. However, in detail the behaviour of the ships and the characteristics of the phenomena are different to the situation in regular waves, mainly due to the wider band of different frequencies and encounter directions existant in a natural seaway.

One important finding is that it is not possible to separate the different phenomena as in regular waves. The excitation of large roll angles always contains direct as well as parametric excitation. This also explains why excessive roll angles develop much faster in irregular, short crested waves than in regular waves, because the direct excitation always delivers a sufficient initial disturbance to initiate parametric rolling. Therefore, a very small number of roll cycles is sufficient to build up extreme roll amplitudes in irregular, short crested waves.

A second important point to be taken into account, is that the region of parameter combinations in which large roll angles can occur is much larger in irregular waves than in regular waves. To exemplify this, a container ship ($L_{bp} = 260$m) is investigated in following, stern quartering and beams seas at different speeds. Figure 2.7 shows the limiting wave heights at which a maximum roll angle of 50° is just not exceeded. The calculation is carried out for regular waves, irregular long crested and irregular short crested

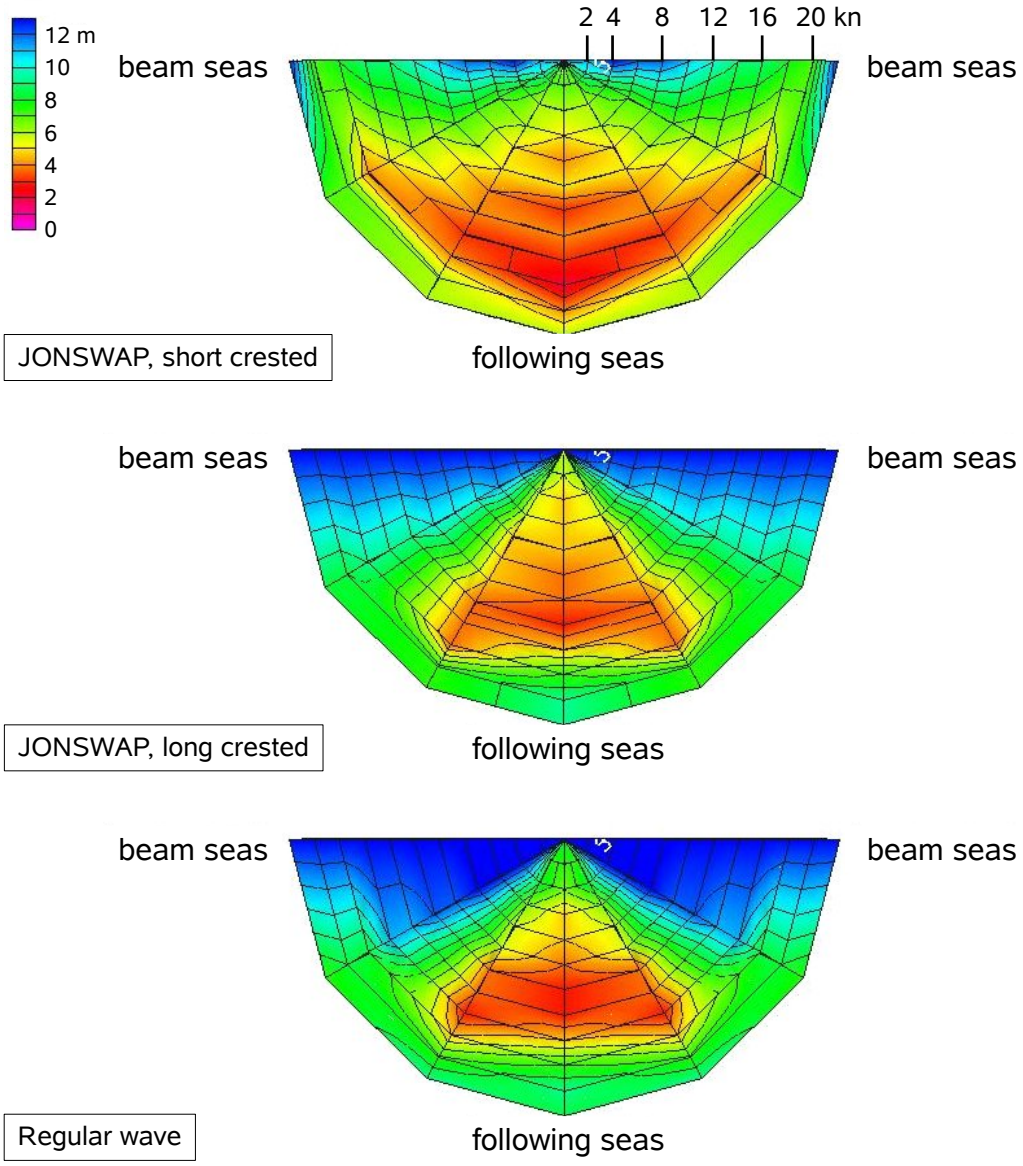

Figure 2.7: Polar diagram showing the limiting wave heights in following and stern-quartering waves for a container ship ($L_{bp} = 260$m). The wave length, or characteristic wave length, respectively, equals the ship length ($\lambda = 260$m). The first polar diagram shows the results for short crested seaway according to a JONSWAP spectrum. The second polar diagram shows the results for the same spectrum, but long-crested waves and the last diagram results from the simulation in regular waves.

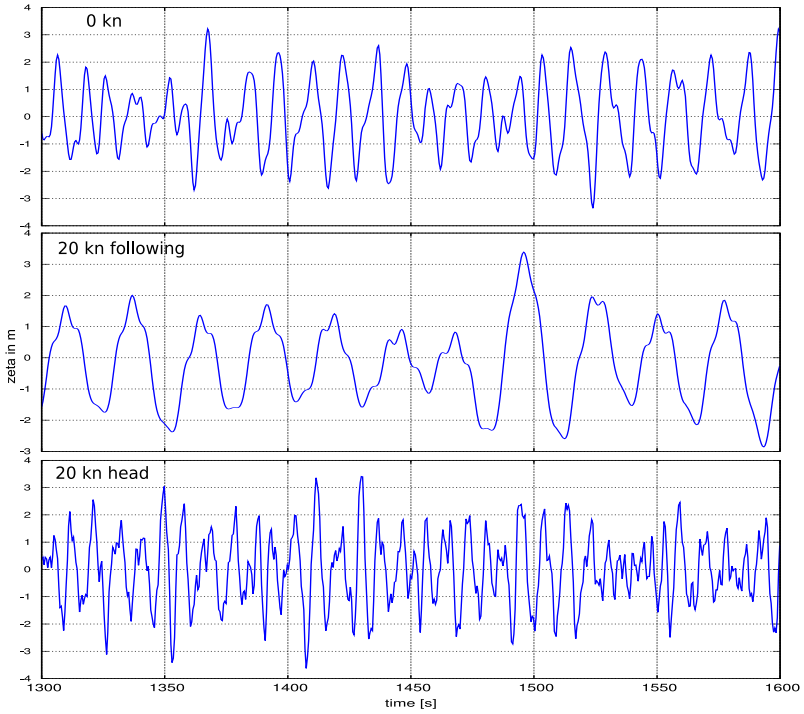

Figure 2.8: Irregular waves ($H_{1/3} = 5m; T_1 = 11s$) seen from a point moving with different speeds. Topmost diagram shows a stationary point, whilst the two lower time series show points moving with a speed of 18 knots with and against the waves, respectively.

waves. The wave length, or the characteristic wave length, respectively, equals the ship length. The irregular seaway is modelled by applying a JONSWAP spectrum.

In regular waves the boundaries of the region with large roll angles are relatively sharp and clearly limited, resulting in a narrow sector with respect to the ship's speed and the encounter angle. Long-crested, irregular waves lead to a wider range of encounter frequencies that the ship faces. This widens the range of ship speeds, where large roll angles occur. Finally, when a ship is facing short-crested waves the stability alterations as well as direct excitation always exist in parallel, because the waves approach the ship not only with various encounter frequencies, but also from different encounter angles. Thus, the boundaries of the critical regions not only get blurred in the speed domain, but also within the range of encounter angles. To conclude, large roll angles under the influence of stability alterations are observed in a far wider range of speeds and encounter angles in a natural seaway than in regular waves.

Another interesting observation is made by Paulling in [53]. He shows that the character of a natural seaway observed relatively from a moving point, gets a more regular character

when travelling in the same direction as the waves, whilst a point moving against the incoming waves leads to a more irregular appearance. An example of a time series of irregular waves seen from a point travelling with different speeds with and against the waves is shown in Figure 2.8. The visual impression is confirmed by the wave spectra plotted over the encounter frequency. In case of following seas, which equals a point travelling with the waves, the spectrum gets significantly more narrow banded, while in head seas, the spectrum is spread over a wider range of frequencies. This is generally known in physics as doppler-effect. Consequently, for increasing forward speed resonance conditions in head seas become more unlikely to be met and they are more unstable, which reduces the probability of large roll angles. In contrast, in following seas we receive a more regular excitation, typically in connection with smaller stability and longer times on the wave crest. This is another reason why capsizing is more often observed in following than in head seas.

2.3 Broaching of Ships

If large roll angles and capsizing in following seas is addressed, another phenomenon can become important. In certain situations, it is possible that waves approaching the ship from astern or from stern quartering directions lead to violent yaw motions, resulting in a very fast change of course. This high turning rate in turn produces very high centrifugal forces which often lead to capsizing. Characteristically, the yaw motion in such situations can no longer be controlled by the available steering devices. Following this observation, the loss of course control is considered as one of the elements defining the broaching phenomenon. Umeda et al. [75] gives the following definition, used for the detection of broaching:

$$\delta = -\delta_{max},\ r > 0,\ \dot{r} > 0 \tag{2.6}$$

Here, δ is the rudder angle and r denotes the turning rate. This definition says that broaching is present, if the ship's turning rate is positive and further increasing, even though the counteracting rudder force has reached its maximum already.

Broaching is suspected to be closely related to small flow velocities at the rudder which typically occurs either, if the encounter frequency between the ship and the waves tends towards zero, or if the ship is accelerated by the waves while resting on the wave crest, which is commonly known as surfriding. Unfavourably, the ship has only small up-righting stability in this situation and consequently the centrifugal forces cause large heeling moments.

However, from its nature the broaching phenomenon is not a classical problem of intact stability. Neither the alteration of certain design parameters, for example in order to

reduce lever arm alterations, nor the simple increase of up-righting stability, reduces the probability of occurrence of broaching and also does not attenuate the consequences substantially. Therefore, broaching has to be considered as a problem of manoeuvring and, hence, of operating and operator guidance, but not as a relevant failure mode for a minimum stability criterion.

3 Intact Stability - History, Contemporary Regulations and Future Development

The mechanical fundamentals of ship stability in terms of positive righting moments have already been known for a very long time. In the year 1747 *Bouguer* published his work "Traité du navire" where he defines the metacentre as the crossing point of two adjacent buoyancy vectors for the first time. And in 1757, *Bernoulli* discovered the relationship between the metacentric height (GM) and the roll period of ships. Next, *Moseley* introduced the first dynamic approach based on the energetic considerations with respect to the area under the lever arm curve. In principle all necessary knowledge to evaluate the dynamic stability of ships exists since this point in time and thus, the problem of ship stability was widely considered as being solved around the year 1900. However, this primarily meant that the theoretical fundamentals were complete, but not that the intact stability of ships was sufficient in reality. The main problem remaining up until the last decades of the 20^{th} century was the practical calculation of the equilibrium floating condition and of the related righting levers, due to the complex geometry of ship hulls. Several approximation procedures were invented over the years to overcome this problem, but the final solution for it came not until the introduction of numerical approaches supported by the appearance of computers. In the meantime, the stability of ships was judged mainly based on the metacentric height (GM), as the effort necessary to calculate this value is low compared to the whole lever arm curve. Also nowadays, ship stability is still wrongly viewed as being mainly a question of the initial metacentric height.

The first extensive statistical investigations into ship stability were carried out by *Rahola* in 1939. He analysed the still water lever arm curves of ships that were capsized. He discovered that many of the ships had righting levers which were below the minimum values recommended by the experts of his time. He identified three groups of ships: Ships that had too small righting levers according to the maritime board of enquiry and the experts, ships that had "critical" lever arm curves and ships which clearly had sufficiently large lever arms. Rahola's investigations resulted in the definition of a "standard" lever arm curve defined by minimum levers at 20 and 30 degrees heel, the maximum lever

being reached at 35 degrees heel and the angle of vanishing stability being 60 degrees. All lever arm curves with an enclosed area up to 40 degrees of the same amount or larger as the standard curve are accepted as equivalent. Rahola's investigations were widely recognised and have been subsequently the basis for many minimum stability regulations introduced over the years. Even the present minimum intact stability requirements of the International Maritime Organisation according to Resolution A.749(18) (see also Section 3.1) are based on Rahola's considerations. This is important to note due to two reasons: First, the categorisation into substandard, critical and sufficient stability is not directly based on physical considerations, but was taken from the subjective judgement during the accident investigations. Second, ships that capsized due to dynamic influences like cargo shift and resonant rolling, were put into the category "safe" during Rahola's analysis as they usually had sufficiently large still water lever arms according to the experts' opinion. Thus, dynamic effects are neither considered directly, nor indirectly in Rahola's minimum requirements.

3.1 Criteria recommended by the International Maritime Organisation (IMO)

All recommendations and regulations relating to ship intact stability and safety against capsizing issued by the International Maritime Organisation (IMO) nowadays are consolidated in the IMO-resolution A.749(18) [29]. As an exception of this, there are additional provisions in various other resolutions for certain types of ships, for example ships carrying grain in bulk as cargo. These are affected by an increased risk of encountering large cargo shifting moments and such are treated separately. As those, other regulations do not refer directly to seakeeping related problems and they shall not be presented in detail here. The A.749(18), which was adopted in 1993, replaces the older resolution A.167. The regulations in the A.749(18) are not mandatory so far, but the code on intact stability is undergoing a major revision at the moment. It is planned that the revised code, becoming effective from 2009, will contain a mandatory as well as an non-mandatory part. The intact stability criteria will be contained in the first part and thus get the same status as the damage stability regulations contained in the SOLAS. The basic concept of the general intact stability criteria is closely related to the ideas of *Rahola* and, as well as his concept, they are based on accident statistics. As data in sufficient quantity was only available for smaller ships when A.167 was developed, the resolution was applicable only to ships smaller than 100 metres in length. The requirements in the A.167 consisted of a minimum GM value, a minimum lever arm value at 30 degrees heel and three minimum areas below the lever arm curve. Dynamic effects were not taken into account.

General Stability Criteria The A.749 inherits the general intact stability criteria almost unchanged from the A.167. These are:

- Minimum metacentric height: $GM \geqq 0.15m$
- Minimum lever arm at 30 degrees heel: $h(\varphi = 30°) \geqq 0.20m$
- Maximum of lever arm curve beyond 25 degrees heel: $dh/d\varphi(\varphi = 25°) = 0.$
- Integrated area below the lever arm curve has to reach the following minimum values:
  - $\int_0^{30} h(\varphi)\ d\varphi \geqq 0.055mRad$
  - $\int_0^{40} h(\varphi)\ d\varphi \geqq 0.090mRad$
  - $\int_{30}^{40} h(\varphi)\ d\varphi \geqq 0.030mRad$

All these general intact stability requirements are applicable to ships of 24 metres in length and larger. Surprisingly and in contrast to the old regulation A.167, they also apply to ships of more than 100 metres in length, although the majority of the ships represented in the statistical sample on which the requirements are based, has a length of less than 60 metres. A detailed overview on the statistical sample and the development of the aforementioned criteria can be found in the draft for explanatory notes as shown in [30].

It is a widely accepted fact that the general intact stability criteria in their current form do neither provide a sufficient safety level for large ships, nor do they assure a uniform safety level for ships of different size or type (see Söding [71]). One major reason for these problems is the fact that the minimum requirements are not being scaled with the ship size. In practise this leads to the situation that a large container vessel of 300 metres in length is allowed to sail with the same minimum GM of 15 centimetres as a small coaster with a length of approximately 80 metres. Applying Froude's similarity law, it follows that lever arms increase with the geometrical scale λ with increasing ship size. Thus, in order to provide the same ability to resist heeling moments in the above mentioned example, the GM value would have to be increased for the large ship by the factor $300m/80m = 3.75$.

Figure 3.1 impressively illustrates the order of magnitude between an righting lever of 0.2 metres and a post-panmax container ship. As the righting lever is so extremely small compared to the overall ship dimensions it lies in the same order of magnitude as the uncertainties in the hydrostatical calculations. Taking further into account the changes of the lever arms, for example as a result of waves, then it becomes obvious that the given

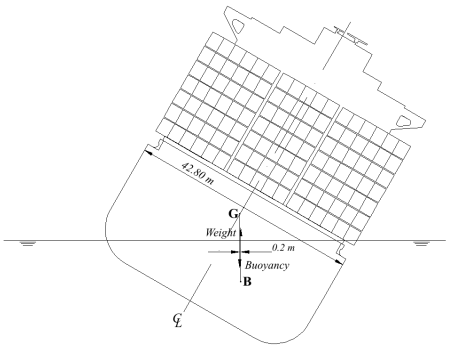

Figure 3.1: righting lever of 0.2m for a post-panmax container ship

small threshold values are not sufficient to provide an adequate safety level for large ships. The reason for not experiencing more insufficient stability accidents can be found in the damage stability regulations, which usually exceed the intact stability threshold. However, this is of course not an acceptable situation.

Severe Wind and Rolling Criterion (Weather Criterion) The "severe wind and rolling criterion", originally introduced by IMO res. A.562(14) in 1985, nowadays is also part of the IMO-resolution A.749(18). The main aim of this criterion is to assure that ships are able to withstand heeling moments due to incoming waves and wind without exceeding certain roll angles. The original formulation of this criterion goes back to stability requirements of the Soviet register of shipping from 1947 [58]. The structure of the criterion is prescriptive as well, whereas the threshold values are based on statistical long-term evaluations of accidents made since the first formulation in 1947. The critical KG value is adjusted to fit the mean of all KG values of ships in the statistics, which where considered to be safe in operation. The scenario the ship has to survive according to the criterion is illustrated in Figure 3.2.

The ship faces an initial heeling moment (lw1) due to beam wind which is given by a static pressure. The criterion assumes that the resulting lever arm is constant over all heeling angles. From this initial floating condition (Φ_1) the ship performs a wave induced roll motion to the opposite, luffward side. The absolute value of this roll angle (Φ_1) is determined by an regression formula which contains factors accounting for the ship's block coefficient, the draft to breath ratio, the linearised roll period and the roll damping in a simplified way. Having reached the leeward turning point of this roll motion a wind gust hits the ship resulting in a total heeling lever of 1.5 times the value of the initial static lever (lw2). Employing the area under the lever arm curve as a measure for the amount of potential energy stored in the inclined system, the criterion requires that the area under the lever arm curve beyond the new static equilibrium heeling angle must be at least of

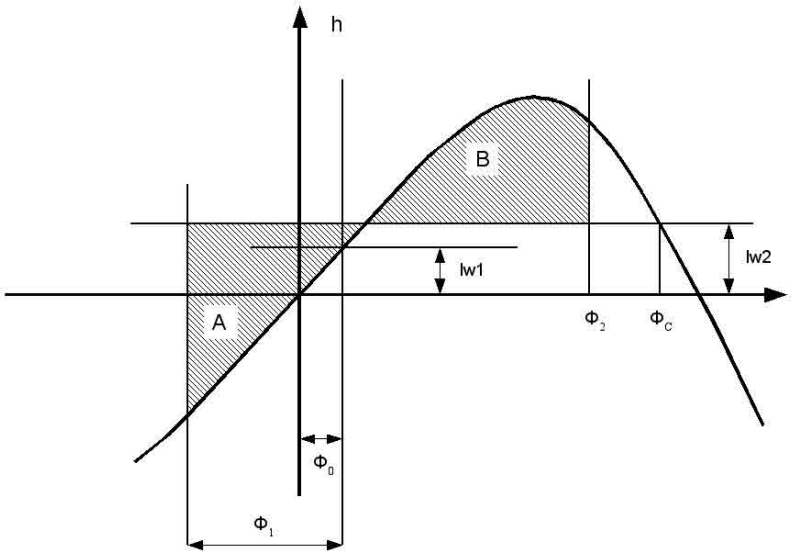

Figure 3.2: Heeling levers and areas below lever arm curve according to the IMO weather criterion

the same size as the area under the curve integrated from the luffward turning point up to the new equilibrium. The integration limit on the leeward side is given by the angle of vanishing stability, the angle where progressive flooding occurs or a maximum angle of 50 degrees, whichever is less.

The weather criterion is the only one amongst all of the IMO-criteria taking into account the influence of waves and the only one being based on a balance between heeling and righting levers. Although it considers the dynamics of ship roll motions, at least in a simplified way, this prescriptive scenario is not suitable to assess the phenomena endangering ships in head, following and quartering waves and it also never was intended to be used in such a way.

The weather criterion was already criticised shortly after its introduction. The main point of critics was, beside the partly unrealistic simplifications regarding the constant heeling lever due to wind and the wave induced roll motion, that the criterion is calibrated for "old-fashioned" ship types with traditional hull forms and moderate to small lateral areas and small B/T-ratios. These deficiencies were one initiating factor for the discussion about future requirements and standards for new criteria within the IMO. Discussion and development is still going on, but there is a significant trend towards performance based approaches. These recent developments are presented in more detail in Section 3.4.

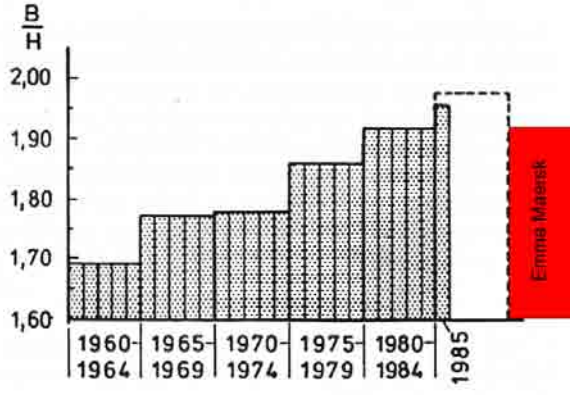

Figure 3.3: Development beam-to-depth ratio of ships analysed by Blume and Wagner compared to the largest container vessel of the container fleet in 2006.

Alternative stability criteria for container ships of more than 100 metres in length
As a consequence of the container ship development in the early 1980's, a clear trend could be noted to ship designs with increasing beam of the ships, without similar increase of the depth. This is simply due to the fact that this type of ship typically carries large amounts of deck cargo resulting in relative large vertical centres of gravity. Under the pressure to optimise the ships economically, designers usually try to maximise the number of containers carried on deck. To fulfil the minimum stability requirements it is an appropriate meassure to increase the ship's beam and thus, to maximise the waterline area of the vessel. This results in larger initial stability, but reduced form stability, whereas an increase in depth is always unfavourable for the initial (not for the **form**-) stability of the vessel. The lever arm curves of the resulting ship designs are then characterised by large initial stability, low additional form stability and a relatively small range of positive righting levers. Prior to the introduction of the IMO Res. A.749 the German Seeberufsgenossenschaft (SeeBG) which represents Germany as responsible flag state authority, required the fulfilment of some intact stability criteria in excess to the IMO Res.A.167. These required a minimum range of positive righting levers of 60 degrees. From today's point of view this would be a sensible extension also to the requirements made in the IMO A.749.

Having recognised that containerships had hullform characteristics significantly different from traditional designs which were mainly the statistical basis used for the development of the general IMO intact stability criteria, Wagner [82] concluded that new criteria should be developed, in order to compensate the more unfavourable beam-to-depth ratio of the modern designs by increased stability.

Figure 3.3 shows the trend as it was predicted by Wagner. For a comparison the beam-to-depth ratio of Emma Maersk, a 11000-TEU class container vessel built in 2006 by Odense Staalskibsværft is appended to the diagram. The trend predicted from Wagner

is more or less confirmed although the increase in beam-to-depth ratio proofs not to be as extreme as predicted by Wagner, but the trend is still significant. Further, as already shown previously in Figure 3.1, the absolute magnitude of the righting lever is extremely small with respect to the inaccuracies in calculations or other effects such as the alteration of that righting lever in waves. In 1986 Soeding and Tonguc [72] demonstrated already that the righting lever is about 1% of the vessels beam, which they concluded is too small with respect to possible inaccuracies in the calculation. For the 2006-vessel the same required minimum righting lever is only about 0.35% of the vessels breadth and thus lies within the range of the typical calculation accuracy.

Therefore, Blume and Wagner conducted systematic model tests for several container vessels to demonstrate that such a vessel could easily capsize in case the stability was adjusted according to the relevant minimum standard. During these model tests, Blume [11], [12] tried to establish a criterion for the minimum stability of a vessel in rough weather. To distinguish a vessel from clearly being safe or unsafe in a specific condition, he developed a statistical criterion with respect to the residual area under the stillwater righting lever curve which is presented in more detail in Section 5.3. Blume then tried to find a correlation between certain characteristics of the righting lever curve, derived from the Rahola parameters, and the statistical collective divided into safe and unsafe samples, and he found out the following:

- The only parameters which showed significant correlation with capsizing events occurring or not, were the maximum righting lever of the stillwater righting lever curve and the area under the righting lever curve.

- All other Rahola parameters such as initial GM or position of the maximum righting lever did not show any influence on the safety against capsizing.

Blume, Wagner and Hattendorff also tried to correlate the righting levers of the ship situated in wave crest condition for a wave equalling the ship's length with the Rahola parameters. They did not succeed as the results were at least not better than those obtained for the correlation with the still water lever arm curve. The influence of the lever arm alterations between the two extreme situations, namely the wave-crest and the wave-trough condition, was not part of their investigation. Thus, in order to keep their criterion simple and to avoid extra effort for calculating the lever arms in waves, which from their point of view was not necessary, they decided to calibrate their form factor, called C-factor, on the basis of the still water levers. This allowed the C-factor to be introduced as an addition to the minimum requirements of the Rahola parameters, but fully in line with the calculation procedures already in use. The concept of the resulting criterion then was not to use the constant, ship independent threshold values according to the IMO A.167, but to adjust them with the ship specific C-factor. This means that for example the minimum stillwater righting lever at 30 degrees should according to Blume

not take the constant value of 0.2 m, but a constant value divided by C, where the so called C-factor is to be determined by the following regression formula (see Blume [10]):

$$C = \frac{T \cdot D'}{B^2} \cdot \sqrt{\frac{T}{KG}} \cdot \frac{C_B}{C_{WP}} \cdot \sqrt{\frac{100}{L}} \tag{3.1}$$

Here, T denotes the draft, D' a modified depth including hatches, KG is the centre of gravity above base line, C_B and C_{WP} denote the block and the waterline coefficient, respectively. The C-factor tries to define different minimum requirements for the righting levers with respect to the following design features of container vessels, which were according to the model tests related to the capsizing of the vessel:

- Hull forms having large values of B/T and B/D need larger righting levers than conventional hull forms. This may be explained by the reduced form stability combined with the larger alteration of the righting lever in waves.
- It was found that in bow or stern quartering seas, those vessels were endangered where the centre of gravity was significantly higher than the still water line. Therefore, the C-factor decreases with increasing T/KG- ratio. The explanation might be that the difference between the alternating restoring moment due to the wave action and the heeling moment takes larger values.
- Hull forms having a large ratio of waterline coefficient over block coefficient are suspected to have large righting lever alterations in waves and are therefore more vulnerable to rolling.

Today the C-factor criterion is part of the IMO Res. A.749, the Code on Intact Stability, as an alternative assessment of intact stability for container vessels above 100m in length, but as the whole code it is not mandatory so far. Therefore, container vessels are usually designed according to the weaker general intact stability criteria, as there is no measure to force the use of the stricter C-factor concept.

As explicitly intended for container vessels above 100m, the C-factor concept is restricted to those types of ship and to the related phenomena, accordingly. Recent investigations of Krüger [40] and Hass [24] have shown that beside the parameters covered by the C-factor, also the L/T-ratio plays an important role, which has the same importance as the B/T or B/D-ratio. Further, the C-factor actually fails for vessels like RoRo- or RoPax-ferries, because the large stability loss on the crest due to the barge-type aftbodies is not correctly represented by the C_B/C_{WP} -ratio. Further, from today's point of view it seems to be unsatisfactory to consider the still water lever arm curve only, as it is not sufficiently representative for seakeeping problems. This shows that the C-factor concept may not be generalised for other ship types than those the C-factor was intended for, but the concept as such and the conclusions drawn from the model tests have been a big step forward and are still valid today.

3.2 Intact Stability Criterion of the German Federal Navy (BV1033)

As a consequence of capsizing incidents in the late 1950's and early 1960's, including the *Pamir*, the *Irene Oldenddorff* and the *Lohengrin*, Wendel [83] and his research-group developed a concept where the minimum required stability of a ship should be attained on the basis of an individual balance of righting and heeling levers. Later, the concept was further developed and investigated by Arndt [2] and Boie [14]. Based on the results of this research work, *Wendel* developed an intact stability criterion for the German Federal Navy, which was first issued as BV 103 in 1964 (see Arndt [4]). This standard was revised in 1969 and was subsequently published as BV1033 which is still valid today, including smaller enhancements made over the years. The BV1033 standard was also adopted by the Royal Dutch Navy. To date, the intact stability criterion of the German Federal Navy is the only one which explicitly takes into account the influence of waves on the static stability of ships.

The basic idea behind the BV1033 stability standard is to make up a stability balance of individual righting and heeling levers acting on the ship. In the resulting equilibrium condition the vessel must not exceed a certain heeling angle. Additionally, the residual righting lever at a certain reference heeling angle has to exceed a minimum limit. Although keeping in mind the change of heeling levers in waves as shown in the next paragraph, the BV1033 does not assess dynamic phenomena like parametric rolling directly. Nevertheless, this approach provides a significantly higher safety level with respect to capsizing than the IMO criteria as shown by Lichtenberg [45]. The minimum requirements depend on the desired area of operation and the operational profile of the respective vessel.

Righting arms In total the BV1033 requires the calculation of eleven cross-curves of stability. Those are the cross-curves in still water conditions and additionally ten cross-curves with the ship being situated in waves, while the location of the wave crest is varied. Being more specific the locations of the wave crest shall be at $-0.5L$,$-0.4L$, ...,$0L$, ...,$0.4L$, $0.5L$ from amidship. The wave length shall be equal to the ship's length ($\lambda = L$), whereas the required wave height is determined by applying a design wave approach delivering the steepmost wave to be expected for the given wave length. Formula 3.2 is provided in the BV1033 for the wave height calculation. It is based on statistical and probabilistic considerations.

$$H = \frac{\lambda}{10 + 0.05\lambda} \tag{3.2}$$

The resulting cross-curves are averaged over all 10 situations and subsequently compared with the still water values. The lowest curve is taken for the stability balance against the heeling levers.

Heeling arms and stability balance The BV1033 considers heeling arms due to

- free liquid surfaces
- wind
- crowding of people on board
- centrifugal forces in the turning circle
- replenishment at sea and
- transverse forces under towing conditions.

Here, only the wind criterion, keeping in mind the heeling levers due to wind and free liquid surfaces shall be presented exemplarily. For the calculation of the influence of free liquid surfaces in tanks two formulae are given in the BV1033. The first one, to be considered as "standard" formula reads:

$$k_F = \frac{\sum_{j=1}^{n} \rho_j i_j}{\Delta} \sin\varphi \tag{3.3}$$

Here, k_F denotes the heeling arm due to the free liquid surface, calculated according to the theory of small heeling angles by correcting the free surfaces based on the geometrical moment of inertia in the tank (i_j). Further, ρ_j represents the individual density of the fluid contained in a tank and φ is the current heeling angle. As this formula delivers exact solutions only for small heeling angles or for tanks with vertical walls, as long as the free surface does not intersect the tank bottom or top, there is the requirement for exact calculation of the heeling moment according to the actual fluid shifting moments in case the resulting heeling lever exceeds 0.3 metres at 30 °heel. Then, the formula to be used is:

$$k_F = \frac{1}{\Delta} \sum_{j=1}^{n} m_j a_j \tag{3.4}$$

The heeling arm due to wind is calculated with a semi-empirical formula as follows:

$$k_w = \frac{A_w \left(z_A - 0.5T_m\right)}{g\Delta} p_w \left(0.25 + 0.75\cos^3\varphi\right) \tag{3.5}$$

Here, A_w denotes the lateral area of the ship above the waterline level which is given by the mean draft T_m. The regulation allows to account for geometric properties by multiplying

parts of the projected area with resistance coefficients, for example circular shapes can be multiplied with a factor 0.6. z_A represents the vertical distance from the base line to the centroid of the lateral area A_w. Further, the equation contains the displacement Δ, the gravity g and the wind pressure p_w, which is prescribed in the standard depending on the respective area of service.

The total heeling moment consisting of the influence of the free liquid surfaces and the wind is then balanced against the minimum righting lever arm curve. The resulting heeling angle in the equilibrium floating condition is then φ_{ST}. The wind criterion according to BV1033 requires that the residual righting lever h_{res} has to amount to at least a minimum value as defined in equation 3.6.

$$h_{RES} = \begin{cases} 0.1 & \text{if} \quad \varphi_{ST} \leqq 15\,\text{deg} \\ 0.1\varphi_{ST} & \text{otherwise} \end{cases} \tag{3.6}$$

This minimum righting lever h_{RES} has to be evaluated at a specific reference heeling angle φ_{REF}, which is determined as follows:

$$\varphi_{REF} = \begin{cases} 35\,\text{deg} & \text{if} \quad \varphi_{ST} \leqq 15\,\text{deg} \\ 5\,\text{deg} + 2\varphi_{ST} & \text{otherwise} \end{cases} \tag{3.7}$$

The idea behind this concept is that the vessel sailing in waves with a constant list due to steady wind influence still has sufficient residual stability to withstand additional heeling moments, for example due to wind gusts and dynamic rolling, without capsizing.

3.3 DNV Rules for Naval and Naval Support Vessels

As it is common practise, the Norwegian classification society *Det Norske Veritas* (DNV) references the IMO Res. A.749 in those parts of its classification rules which target intact stability requirements. One exception are naval and naval support vessels. The IMO-regulations generally do not apply to naval vessels at all, why the DNV class rules [19] contain a set of intact stability requirements which are based on a momentum balance. The basic concept as such is very similar to the ideas published by Wendel, as implemented in the BV1033. The stability must be demonstrated for two loadcases, namely "Full load condition" and "Minimum Operating Condition", where the load items to be taken into account for both loadcases are defined in detail in the class rules.

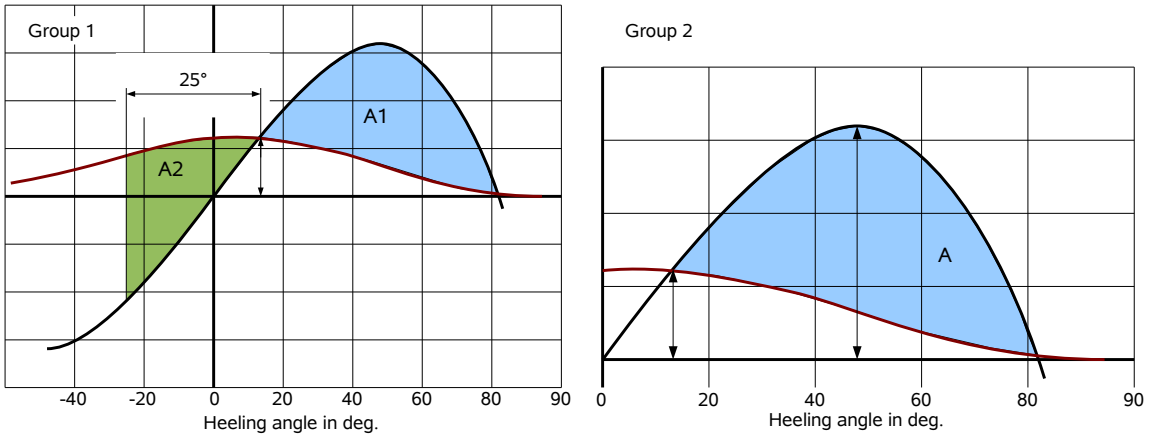

Figure 3.4: Intact stability requirements for naval and naval support vessels according DNV-class rules.

External Loads

The class rules require to take into consideration five different types of external loads which generate heeling moments. They are split into two groups which are treated separately from each other. The first group contains primarily the influence of beam wind. Additionally icing has to be considered, if the ship is to operate in such conditions as well. The second group contains moments due to crane loads, moments due to centrifugal forces in the turning circle and heeling moments due to the concentration of personnel on deck.

Minimum Stability Requirements

The criterion formulates different requirements with respect to minimum stability for the two groups of heeling moments. The first group of moments related to wind and icing is used for an approach which contains elements of the IMO weather criterion, assuming that the vessel rolls to the windward side by a fixed angle of 25 degrees, starting from the equilibrium floating condition. The scenario is visualised in Figure 3.4 on the left hand side. The rules require that the total heeling moment containing the contributions from wind and icing, must not be larger than 0.6 times the maximum righting lever at the equilibrium floating condition. The heeling angle corresponding to the equilibrium floating condition has to be smaller than 15 degrees and the righting lever curve must have a range of at least 70 degrees. Finally, the rules require that the area with the index A_1 in Figure 3.4, left hand side, has to be larger than 1.4 times the area A_2. The last requirement considers the dynamic rolling of the ship similar to the IMO weather criterion.

For the second group of heeling moments the requirements are further simplified, now corresponding to the sketch on the right hand side of Figure 3.4. Again, the heeling moment must be smaller or equal to 0.6 the maximum righting lever in the equilibrium floating condition, which must lie below 15 degrees. The remaining dynamic stability, represented by the effective area A between the righting arms and the heeling arms must not be less than 0.4 times the total area below the initial righting lever curve.

Guidance note for stability in waves

For the momentum balance the normal still water lever arm curve is used by default. The influence of waves, either by direct excitation, or by the change of the lever arm curve in waves is not taken into account by default. However, the DNV rules contain a guidance note, which recommends the correction of the lever arm curve according to Wendel's scheme. For this, a trochoidal wave of the length λ, equalling the ship length is used. The wave height is then calculated according to the same formula as used in the BV1033 (Equation 3.2).

For the righting lever curve used to make up the momentum balance, the mean values of the wave trough and wave crest conditions shall be used. Using the mean lever arm curves for the momentum balance neglects the energy introduced into the system by the dynamic changes of the righting levers. Consequently, the criterion is not suitable to provide sufficient safety against phenomena caused by dynamic lever arm alterations, such as parametric rolling.

3.4 IMO Development Principles for Safety Related Regulations

When taking a look at the history of the development of international safety regulations, it becomes obvious that new or enhanced regulations usually are reactions to major accidents. All safety codes currently existant under the responsibility of the International Maritime Organisation were originated in this way, which might be exemplified by the following list:

- **Titanic (1912):** Long before the IMO was founded in its present form, this accident eventually lead to the introduction of the first SOLAS (Safety of Life at Sea) in 1929.
- **Torrey Canon (1967):** This tanker ran aground off the coast of England and caused a serious pollution by major oil spill. In consequence, the IMO introduced the first version of International Convention for the Prevention of Pollution from Ships, MARPOL in 1973.
- **Herald of Free Enterprise (1987):** The capsizing of this ferry close to the harbour of Zeebrugge did not only lead to several amendments to the SOLAS Chapter II-1, but also marked the starting point for the development of the International Management Code for the Safe Operation of Ships and for Pollution Prevention (ISM)
- **Estonia (1994):** This severe accident with the loss of more than 850 lives again brought major changes to SOLAS, especially related to RoRo-ships and additionally lead to the Stockholm Agreement, formulating additional damage stability requirements for ferries operating in Northern Europe.

In consequence to the history of their development, most of the requirements contained in the IMO-codes are still based on experience and lessons learned from accidents and related statistical evaluations. With increased safety awareness of people, these traditional approaches seem to be outdated and no longer acceptable as methods of best practise. Indeed it appears to be somewhat cynical to wait for a sufficient number of fatalities to make up a statistics which is reliable enough to develop safety standards out of it. The traditional approach to react on accidents by tailor made regulations which aim to prevent future accidents by prescriptive requirements contains another major drawback. As these regulations are based on statistics and prior experience, they can be only valid for exactly those types of ships and problems which are contained in the statistics. New ship types or unconventional vessels, ships of significantly different size and ships with different operational profiles often can not be covered sufficiently by such instruments. A prominent example for such problems are the general intact stability requirements in

the IMO Res. A749 [29], which were originally developed from a collective of small ships shorter than 100 metres in length. Most of the ships were fishing boats, but today exactly the same prescriptive requirements are applied to container vessels of more than 300 metres in length, which leads to a very poor safety level for those ships.

In order to reduce and to overcome these problems, IMO today forces the development of regulatory frameworks for the future rule development. These new approaches aim to assure a more pro-active rule development, by use of direct calculation methods and the introduction of performance-based goals which address the related failure modes and underlying physical phenomena directly. Two recent major developments related to these efforts are presented in the following.

3.4.1 Goal Based Standards

In contrast to prescriptive safety standards, goal based regulations do not prescribe the way to achieve compliance, but they set goals, leaving open several ways to demonstrate compliance. For example, a prescriptive damage stability regulation could state "The ship shall be equipped with 10 transverse bulkheads", whilst a goal based standard would read "The ship shall survive the collision with another ship". A general introduction to goal based standards can be found in Penny et al. [54].

Industry today often optimises the achievement of the prescribed standard, sometimes at the expense of the real safety level achieved. The responsibility in case of an accident is often seen at the institution which issues the safety regulations, as the prescriptive requirement in such cases is judged to be insufficient. In contrast, goal based standards put the responsibility to proof compliance with the regulation to the user and always refer to the current best practise. At this, they also help to overcome the problems with unconventional designs and the insufficient consideration of the advancing state of the art in science and technology as introduced above.

Although the development is still in progress, IMO has started to introduce Goal Based Standards (GBS) for some special subjects since the year 2000. Nevertheless, there is still no systematic procedure or schedule dealing with the general introduction of GBS into the IMO rule making process. Examples for Goal Based Approaches in the regulatory framework of the IMO to date are the revised Chapter II-2 in the SOLAS, dealing with fire protection and the new structured framework for the holistic assessment of the safety of large passenger ships as introduced in 2002.

Since 2002, a working group within the IMO works on a structured framework for Goal Based Standards for ship design and construction. The methodology is based on a "five-tier system" (see Hoppe [27]):

Tier I: Goals The Tier I formulates the generic high level goals to be met by the underlying criteria. For example, IMO formulates for the design and construction of ships: "Ships are to be designed and constructed for a specified design life to be safe and environmentally friendly, ..., in intact and damage conditions throughout their life."

Tier II: Functional Requirements The functional requirements deliver a more detailed definition of the terms used in Tier I. For example, the design life is specified to have a minimum duration of 25 years and the environmental conditions shall be chosen equivalent to long term statistics of the North Atlantic Ocean.

Tier III: Verification of compliance This Tier shall provide the instruments necessary for demonstrating that the detailed rules and requirements defined in Tier IV are sufficient to meet the goals and the functional requirements defined in Tiers I and II. As such, this tier will be used as quality control for the detailed regulations.

Tier IV: Technical procedures and guidelines Tier IV contains the detailed requirements, which have to be fulfilled by the ships. At this, the requirements can be formulated in form of deterministic as well as probabilistic approaches. In case of unusual designs which are not covered by the standard regulations, Goal Based Standards always incorporate the possibility of using alternative ways to demonstrate compliance with goals and functional requirements.

Tier V: Industry standards, codes of practise and safety and quality systems This finally contains industry standards, design and building practises which are introduced by industry and classification societies to assure the compliance with Tier IV.

Today, goals (Tier I) and functional requirements (Tier II) are available since the 80th session of the Maritime Safety Comitee (MSC) in 2006, while work on the Tiers III to V is still under progress. To date, it is somewhat unclear how Tier III could be implemented. Another subject of ongoing discussions is, whether Tier IV should contain preferably risk based criteria or whether deterministic approaches are also acceptable. Currently, the development focuses on Goal Based Standards for ship design and construction, but there are plans to extend structured framework for GBS to all aspects of ship safety in the long term.

3.5 Requirements towards Future Intact Stability Criteria

As shown in the previous chapter, ships can be endangered by the occurrence of large roll angles in certain situations due to various failure modes. Especially roll motions in longitudinal waves can occur very quickly and violently, resulting in excessive roll amplitudes up to the point of capsizing. The physical phenomena behind these failure modes are not covered by intact stability criteria so far, although the frequency in which they occur as well as the consequences are significant. This is supported by several accidents which have happened during the last decades (see also Chapter 7). In order to increase ship safety under direct consideration of the environmental influences, new approaches need to be developed. In contrast to the traditional intact stability criteria which have deterministic, prescriptive character, future criteria shall follow the idea of goal based standards as described in Section 3.4 by applying first principle calculations of the ship's behaviour in waves. According to the IMO-definition of goal based standards (see Hoppe [27]), the following Tier I goals are relevant:

- The ship shall have adequate stability to minimise the risk of loss or pollution to the marine environment.
- The above made requirements apply for the whole design life of a ship. Design life is the nominal period a ship is exposed to operating and environmental conditions.

Further, the following set of failure modes as introduced in Chapter 2 can be defined. These failure modes must be covered by future intact stability criteria taking into account the behaviour of ships in waves in order to meet the goals mentioned above.

- Excessive roll moments introduced to the ship
- Parametric, resonant rolling excited by lever arm alterations
- Pure loss of stability
- Cargo shift or other heeling moments
- Broaching

These conditions typically happen in a sea state under the influence of arbitrary loads, which might come from wind and waves. Based on this set of possible failure modes it is possible to refine the definition of goals to a more detailed level. According to these standards, ships shall fulfil the following requirements in order to avoid large roll angles and large accelerations:

- Sufficient ability of the ship to withstand dynamic heeling moments in an arbitrary seastate.

- Sufficient roll damping, especially for ships with large mass moments of inertia.
- Avoidance of critical resonances in operating range, making dangerous situations less probable.
- Sufficient course keeping and steering ability for safe operation in heavy weather.

In this context, a large rolling angle is defined as an event which may lead either

- to the capsizing of the vessel
- to the submergence of major non weathertight openings
- to the malfunctioning of an important system
- to severe cargo shift
- or to any situation that will cause an even larger rolling angle.

According to this definition, a large rolling angle is therefore defined as an event which may lead to the total loss of the vessel. Large rolling angles can occur either at low values of stability, or if resonance conditions are met, or during broaching situations. As broaching phenomena are related to the ship's coursekeeping abilities in heavy weather, broaching can hardly be avoided by modifying the intact stability of the ship. Thus, broaching is a manoeuvring problem and must be treated accordingly. In all other cases the avoidance of large rolling angles directly corresponds to the establishment of minimum stability limits.

A large acceleration is defined as any event which causes:

- massive cargo loss
- severe damage to machinery or major safety relevant systems
- structural overload of safety relevant members
- severe discomfort or injuries to passengers or crew

Therefore, a large acceleration is an event which may result in severe damages to the ship but not necessarily in a total loss. It is important to note that large rolling angles are not necessarily accompanied by large accelerations and also large accelerations can occur at relatively small rolling angles. Furthermore, depending on the stability values of the ship, the same seastate, course and speed settings may either result in large rolling angles, or large accelerations, or both. Large accelerations typically occur at high stability values, whereas large rolling angles typically occur either at low stability or during broaching situations.

Obviously, not all goals can be covered by one intact stability criterion, as the fundamental requirements derived from the goals are different and in parts contradictory. This may

be illustrated by the following example: In order to avoid large accelerations, the stability must not be too high, as excessive stability values always lead to short roll periods and in consequence to large accelerations. Therefore, a suitable criterion for the avoidance of large accelerations has to address the upper limit of permissible GM-values. In contrast, a criterion assessing large roll angles would have to ensure minimum stability values, as large roll angles are typically associated to low stability. Additionally, not all failure modes can be covered completely during the design of a ship. For example, the avoidance of resonance conditions and the avoidance of situations with high risk of broaching are clearly related to operating standards and on-board guidance.

Taking all this into account, a comprehensive framework of criteria and minimum requirements is necessary to ensure a sufficient safety level of ships with respect to dynamic intact stability. This framework then would distinguish between permissible and non-permissible operating conditions by defining a set of limiting boundaries comparable to the limiting KG curves calculated from the present intact stability criteria. Additionally, a set of operating instructions and tools for on-board guidance should be made available to supplement the design criteria during operation. The proposed structure for the new dynamic criteria, as derived from the previously defined failure modes and goals, is as follows:

- Criteria to avoid large rolling angles (Minimum Stability requirement)
- Criteria to avoid large accelerations (Maximum Stability limit)
- Criteria to guarantee sufficient roll damping in dead ship condition (Minimum Damping requirement)
- Criteria to avoid broaching (Minimum Course keeping requirement)

The present work concentrates on the first element of the overall framework, the criteria for the avoidance of large roll angles in a dynamic environment. The evaluation procedure developed in the following would then represent a possible Tier IV implementation of the goal based safety standard.

In this context, we focus on the most critical situations. As shown before, these usually occur when ships are travelling in longitudinal waves. Keeping further in mind that the idea is to find a *minimum* stability requirement, we can limit the assessment to ships in following and stern-quartering waves (see Section 2.2). This is supported by the accident statistics. Nearly all accidents caused by a failure of intact stability in heavy seas and which end with capsizing and the total loss of the ship are observed in following and stern-quartering seas. Beam-sea accidents are very unusual for larger merchant ships, but they represent a certain hazard to smaller ships operating in short and steep, or breaking waves.

Accidents related to large amplitude roll motion in head seas are usually observed for relatively large vessels, most of these are container ships. The characteristic course of

events is that a ship suddenly faces very large roll angles, developing within very few roll cycles. This usually results in the loss of a significant number of deck containers. After another few roll cycles the roll motion dies out. The damage to ship and cargo on board is significant in most cases, but there are nearly no documented cases where a large container ship has been totally lost by parametric rolling in head seas.

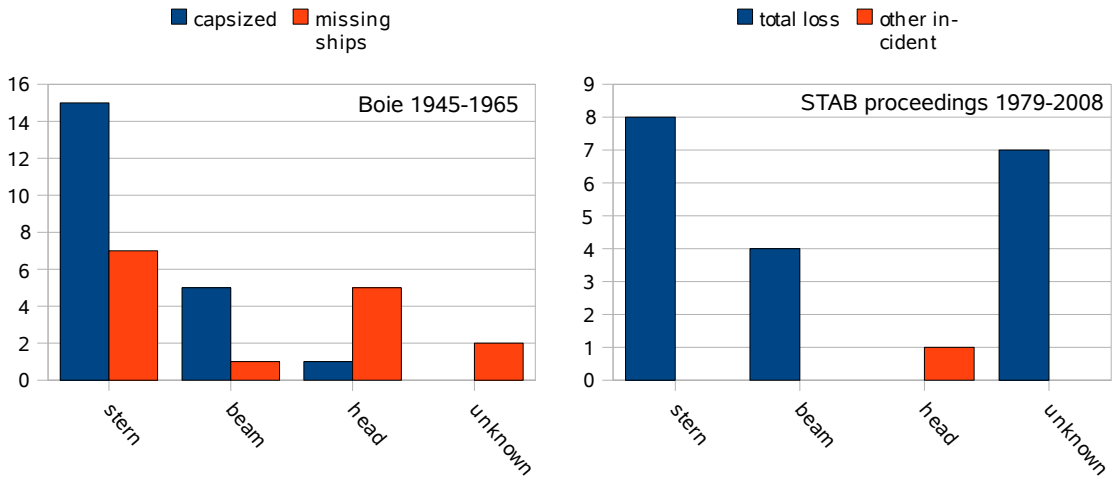

Figure 3.5: Left hand chart: Capsized and missed ships in heavy weather sorted by encounter direction. Accident statistics taken from [15]. Right hand chart: Intact stability related accidents in heavy weather presented in papers on STAB conferences and workshops in the years 1979 to 2008. Data taken from [55]

Although statistical material on the wave encounter direction for intact stability accidents in heavy wheather is hardly available, the data given in Figure 3.5 might support the statements made above. The left hand chart shows rather old data, collected in Germany in the years between 1945 and 1965. The data is taken from a publication of C.Boie [15], published in 1965 giving an overview of the capsizing accidents in German waters. The right hand chart is derived from a paper presented on the 10th International Ship Stability Workshop (STAB) in 2008, which gives an overview on all accident investigations presented on STAB workshops and conferences in the years from 1979 to 2008. Only these accidents were considered for this statistics which are clearly related to an intact stability problem in heavy weather. Unfortunately, more comprehensive and more recent statistical data are not available as the large accident databases (like Lloyd's casualty database) usually do not record the main encounter direction of the waves in case of a capsizing accident. Both statistics clearly state that the danger of capsizing and subsequent total loss is by far largest in following and stern-quartering seas. Although not representative, the trend clearly shows that a minimum intact stability criterion first of all has to address the stability loss and stability alterations in following seas.

4 Assessing Ship Motions in Waves by Numerical Simulations

In Chapter 2, a number of hazards are presented which potentially endanger a ship travelling in waves. In order to assess the individual failure modes, appropriate tools are necessary which are capable to deliver the ship response in waves. This provides the possibility to study the ships motions as such, as well as to make a judgement upon the ships safety under certain operating conditions, which is our main interest here. Numerical simulations are a flexible and powerful tool for the purposes mentioned above. However, not all numerical methods are suitable for the assessment of large roll angles, but certain minimum requirements have to be fulfilled to cover the relevant failure modes. The most important of these requirements are presented briefly in the following section. Afterwards the method *E4-ROLLS* is presented briefly, which provides a tailor-made solution for the assessment of large amplitude roll motions.

4.1 Minimum Requirements with Respect to Large Amplitude Rolling

Numerical codes, used to assess large amplitude roll motions, have to meet some specific requirements in order to be able to cover the relevant failure mechanisms. In Section 2 the important failure modes have been introduced, which are direct excitation by external moments and parametric excitation by stability alterations in waves. The assessment of broaching is not taken into consideration for the minimum requirements in the present context, as we treat it not as a problem of minimum stability.

Although our main interest lies on the roll motion, a numerical code in principle must assess all six degrees of freedom to account for the couplings as far as they are relevant for the roll motion. The six degrees of freedom can be split into two groups, namely the symmetric degrees of freedom, which are heave, pitch and surge, and the antisymmetric ones, namely roll, sway and yaw. In the linearised case these two groups are not coupled with each other. For a more realistic treatment of the roll motion additional terms containing the

mass product of inertia Θ_{xz} have to be considered which generates a coupling between heel, pitch and yaw motion.

Beside the inertial moments, the roll motion equation contains further elements because of external exciting moments and restoring moments. While the external moments due to waves are considered to be small, the restoring forces are very important for the correct treatment of the roll motion. They have to fulfil three requirements in particular:

- Realistic modelling of the righting lever characteristics in dependency of the roll angle.
- Correction of the righting arms for the instantaneous position of the vessel with respect to pitch and heave motions.
- Consideration of the influence of waves on the righting levers.

The first point mentioned above is required, because the linearised treatment of the restoring arms, usually implemented by using the initial metacentric height via $GM\varphi$, is not capable to model capsizing events at all. Due to the same reasons, the righting moments would become highly unrealistic at large roll angles. This also would lead to unrealistic resonance conditions, because the natural roll frequency is falsly determined. The restoring forces do not only depend on the instantaneous heeling angle, but they are also influenced by trim and draft and thus, linked to heave and pitch motions, which creates another important coupling between these degrees of freedom. Finally, the environmental influence of the waves has a significant effect on the restoring arms of a ship as well. The principles of this mechanism were already introduced in Section 2.2. Only numerical codes which account for this wave-induced change of the lever arms are able to assess parametrically excited roll motions. Additionally, it has to be taken into account that the instantaneous shape of the wavy surface around the ship is influenced by the relative position between ship and waves. This creates another coupling between the surge motion and the restoring moments. All this leaves us with a non-linear restoring term, which is time dependent, coupled to pitch, heave and surge motion, and which is dependent on the shape of the wavy surface along the ship's waterline. The non-linear couplings and the non-linear treatment of the restoring forces of the roll motion prevent the use of response amplitude operators (RAOs), because these transfer functions can only account for a linear relationship between exciting forces and the system response. Along with this, the problem can not be treated in the frequency domain anymore, but time domain simulations become necessary. The method *E4-ROLLS*, which is developed to account specifically for these problems while omitting time consuming but, for the roll motion, less important calculations, is presented in Section 4.3.

4.2 Wave Model

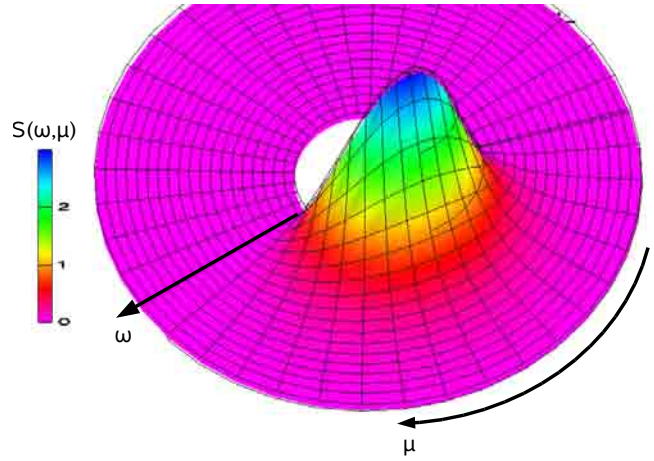

Figure 4.1: Three-dimensional visualisation of the spectral energy for irregular, short crested wind sea.

The realistic assessment of ship motions in waves also requires a suitable model for the natural environment itself. The following introduces the superposition model used for the generation of natural seaways in this work. The basic idea of the superposition-model is that irregular seaways, long crested as well as short crested, are considered to be a random superposition of an infinite number of regular wave components. Consequently, accepting a certain, small error, a natural seaway can be generated by superposition of a discrete number of N components. At this, the wave components each have different frequencies ω_j, different phase angles ε_j and in case of short crested waves also different encounter angles μ_j. Limitations and uncertainties of this methodology will be discussed later in this section.

The energy distribution in a natural seaway is given by wave spectra. For long crested waves they depend only on the circular wave frequency ω, whilst the energy in case of short crested waves is also spread over a range of encounter angles μ. Figure 4.1 shows a three-dimensional plot of a wind-sea spectrum that shows the energy distribution in a short crested seaway. The frequencies are plotted in radial direction and the encounter angles in the angular direction. In order to transform a given energy-spectrum into discrete wave components for superposition, we make use of the quadratic relationsip between the wave amplitude $\hat{\zeta}$ and the mean energy of the wave, which leads to the following equation for the instantaneous elevation of the water surface dependent on place and time, in dependency of the spectral value $S(\omega, \mu)$:

$$\zeta(x,y,t) = \sum_{N} \sqrt{2S(\omega_j,\mu_j)\Delta\omega_j\Delta\mu_j} \cdot \cos(\omega_j t - k_j(x\cos\mu_j + y\sin\mu_j) + \varepsilon_j) \quad (4.1)$$

At this, N is the overall number of discrete wave components, whereas each component has an individual circular wave frequency ω_j, an individual encounter angle μ_j and a specific phase angle ε. Further, $S(\omega_j,\mu_j)$ denotes the value of the spectrum at a certain point and $\Delta\omega_j$ as well as $\Delta\mu_j$ each represent a certain interval in the frequency and the angular direction, respectively. Different strategies for the splitting of the overall spectrum into the desired number of intervals are discussed in the following. Figure 4.2 shows an example of a times series recorded at a fixed point for a time interval of 1000 seconds for irregular, short crested waves, generated according to Equation (4.1) from a JONSWAP spectrum.

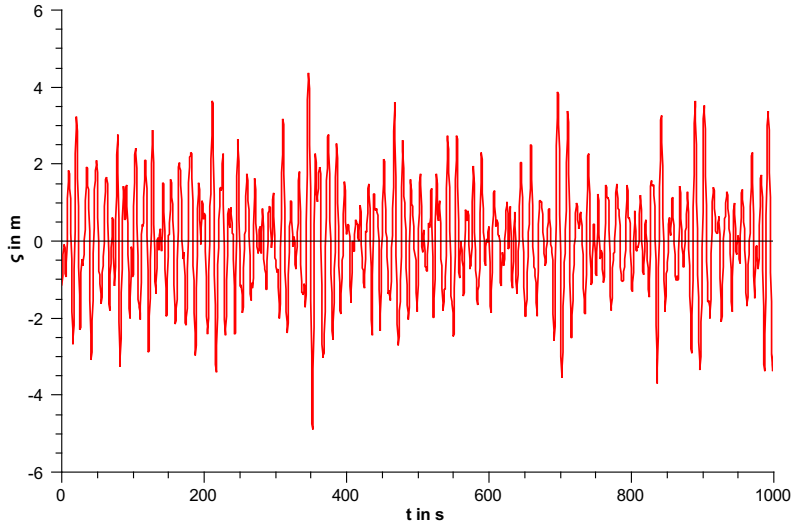

Figure 4.2: Wave elevation at a fixed point, for a irregular, short crested seaway, which was generated from a JONSWAP spectrum.

4.2.1 Discretisation of the Frequency Range

Starting from a minimum frequency ω_{min} up to a maximum frequency ω_{max}, the energy spectrum is split into N parts equalling the number of wave components desired. The straight-forward solution is to subdivide the domain by N equidistant strips of the uniform width $\Delta\omega$. The amplitude for each wave component is calculated according to Equation

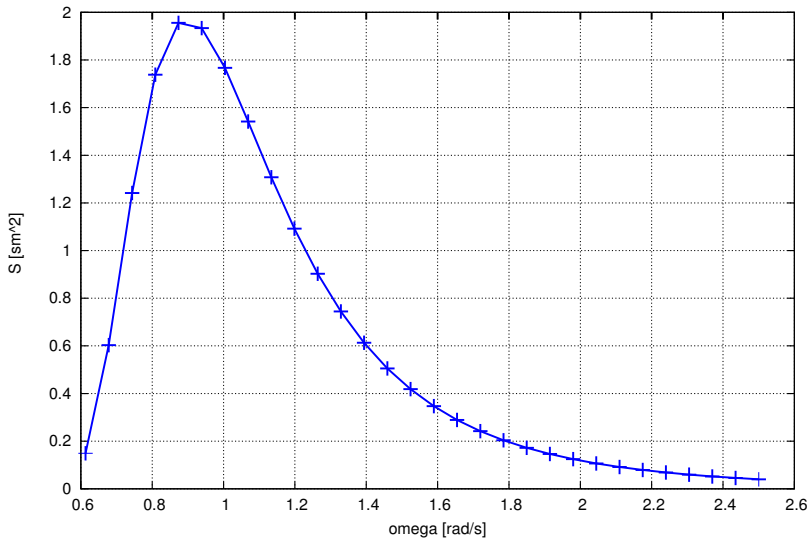

Figure 4.3: Equidistant discretisation of a JONSWAP spectrum in the frequency domain

(4.1), but without considering the angular distribution at this point. The frequency ω_j for each component is chosen within the respective strip by applying a random number algorithm, whereas the frequencies within the strip are assumed to be equally distributed. In case of the phase shift ε_j, the phasing of a component is randomly chosen between 0 and 2π, again assuming a constant probability density function. Figure 4.3 shows a JONSWAP spectrum discretised with equidistant frequency-spacing. This algorithm assures a realistic distribution of amplitudes and delivers also a good resolution of frequency-ranges with low energy shares compared to the overall spectrum. This is particularly of importance if the shape of the sea surface itself is subject of the main interest.

For seakeeping simulations the focus is different. One reason is that in this case the number of discrete frequencies used to model the spectrum is much smaller than in case of oceanographic applications, governed by the need to reduce computational effort. Secondly, the ship motions are induced by those ranges of frequencies which contain most of the wave energy. Areas of low energy are of minor interest in this case and thus, components are "wasted" for frequencies with very low amplitudes, which influence the ship motions only to a small or even negligible degree.

In case of a equidistant frequency spacing the resolution of the areas with high energy contributions gets poor, if the number of components is small. Additionally, the energy contents of a single strip in these regions become very large, which again results in unrealistically high wave amplitudes. Often a single wave component then dominates the ship response. This can lead to wrong conclusions on the ship's behaviour, especially if any of the ship's natural motion-frequencies come close to this area.

These problems can be overcome by splitting the spectrum into strips of equal energy content, resulting in N wave components with constant amplitude. The energy content of one strip then becomes:

$$\Delta\bar{E} = \rho g \, \frac{1}{N} \int_{\omega_{min}}^{\omega_{max}} S(\omega) d\omega \tag{4.2}$$

For practical applications the upper boundary of a strip can be estimated from the following relationship:

$$\omega_u = \frac{\Delta\bar{E}}{\rho g S(\omega_l)} + \omega_l$$

Here, ω_l denotes the known lower boundary of the strip and ω_u is the upper boundary. This type of discretisation algorithm is illustrated in Figure 4.4, showing clearly the improved resolution of the peak-area. The procedure avoids unrealistic high wave components and provides a good representation of the areas of high energy content. However, the areas of low wave energy are modelled with very few components and thus, the strips become wider. This potentially can be a problem if one of the ship's degrees of freedom shows a resonant response in the respective range of frequencies, because the single wave component is far higher than expected in a "real" seaway.

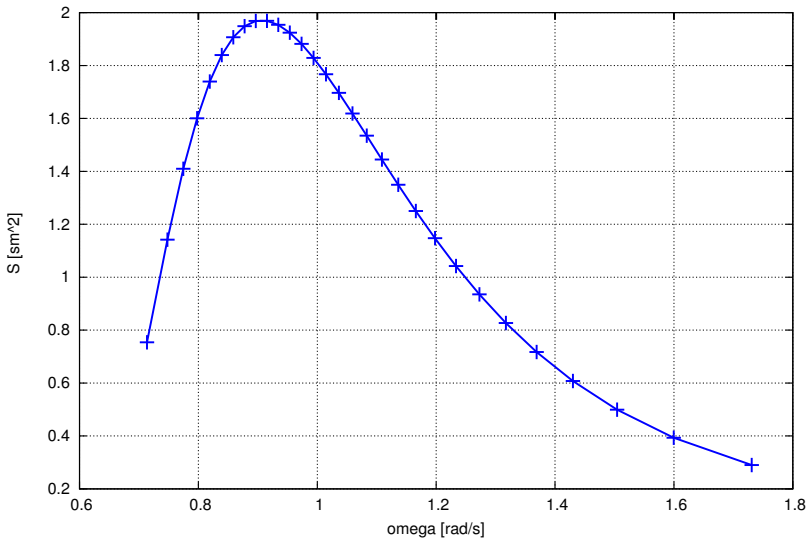

Figure 4.4: Equienergetic discretisation of a JONSWAP spectrum in the frequency domain

4.2.2 Discretisation of the Angular Range

In case of short crested waves the overall energy of the seaway is not only distributed over a range of wave frequencies, but also over a range of encounter angles. The encounter angles are spread over a certain interval around the main direction of wave propagation. When using standard spectra, the angular distribution is usually implemented by using a spreading function. Here, we use the common $\cos^2$-approach to spread the spectral energy over a certain range of angles, which can be formulated as follows:

$$D(\mu) = \frac{2}{\mu_R} \cdot \cos^2\left(\frac{\pi\,(\mu - \mu_0)}{\mu_R}\right) \text{ for } |\mu - \mu_0| \leqq \frac{\mu_R}{2} \tag{4.3}$$

Here, μ_R denotes the total range over which the spectral energy is distributed in the angular direction. The factor $2/\mu_R$ assures that the area below the curve always amounts to 1 in order to preserve the total energy of the spectrum. Finally, μ_0 represents mean direction of wave propagation and μ is the actual encounter angle. Other approaches for spreading functions were published for example by Pierson [57] or Mitsuyasu et al. [49], which are based on certain powers of the cosine function. A three dimensional representation of a spectrum, as shown in Figure 4.1, can be generated by multiplying the two dimensional spectrum with the spreading function:

$$S(\omega, \mu) = S(\omega) \cdot D(\mu) \tag{4.4}$$

This means that a two-dimensional spectrum $S(\omega, \mu)$ has to be discretised for both parameters ω and μ with n frequency components and m angular components. One possible approach for the discretisation is, to split the spectrum into M angular components first. For each of these encounter angles a one dimensional spectrum, scaled by the spreading function, is set up. In the next step the frequencies are discretised as described above, either using equidistant or equienergetic spacing. Figure 4.5 illustrates this approach. This approach is currently implemented in the numerical code *E4-ROLLS*. As for the frequencies and the phasing, the encounter angles are also scattered randomly within the given intervals in order to obtain a more realistic seaway.

4.2.3 Limitations and Errors

The irregular seaway, as used here, has two main sources for errors and limitations. On the one hand the superposition-principle presumes the use of a linear wave theory, which results in the superposition of sine-waves. On the other hand the limited number of components and the transformation of the spectrum into discrete strips represents a source of errors.

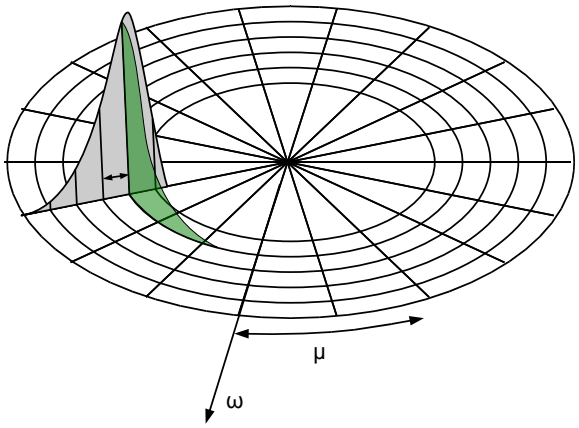

Figure 4.5: Quasi-2D discretisation of a three-dimensional spectrum.

In case of the linear wave theory all non-linear terms in the kinematic and dynamic surface boundary conditions are neglected. This introduces a certain error to the wave surface and an exact solution is only obtained for the still water level $z = 0$. According to Stempinski [74], the error is governed by the term $e^{k_j z}$, where k denotes the wave number for the component j out of N wave components and z represents the actual wave elevation above still water level. Especially the wave components with high frequencies are affected by this type of uncertainty, which becomes manifest in unrealistic speed components in the wave crest. According to [34], the velocities in the wave crest are exaggerated by 15 % and the accelerations were exaggerated by up to 30 %. This is definitely important when calculating impact-loads on the ship structure, however in this context only the influence of the error on the ship motions is of interest. With respect to the roll motion, Stempinski [74] concludes that there is no significant influence on the roll angle, as the local speed components in the wave crest are not considered by the method ROLLS.

Another problem to be avoided is the periodicity of the seaway. This means that after a certain time interval T the sequence of irregular waves repeats itself again. Given an equidistant and regular spacing $\Delta\omega$ between the discrete wave frequencies ω_j and applying the theory of beating waves, the time interval of repetition yields:

$$T = \frac{2\pi}{\Delta\omega} \tag{4.5}$$

The spectrum shown in Figure 4.3, which is discretised with 29 components in a range from $\omega_l \approx 0.6$ to $\omega_u \approx 2.5$, delivers a frequency interval of $\Delta\omega = 0.0655$. Applying Equation (4.5), it results in a period of about 96 seconds after which the wave sequence starts again. This is far to short for our purposes, as we typically use simulation times of 10000 seconds. The periodicity can be visualised by calculating the autocorrelation

function of the wave sequence:

$$R_{\zeta\zeta} = \lim_{T_m \to \infty} \frac{1}{T_m} \int_0^{T_m} \zeta(t)\ \zeta(t+\tau) dt \tag{4.6}$$

Figure 4.6 shows an autocorrelation function, where the seaway is periodic with an interval $T \approx 180s$ and the periodicity can be observed easily by the peaks in the function. In contrast, the autocorrelation function of a real irregular seaway would drop very fast to zero with increasing τ.

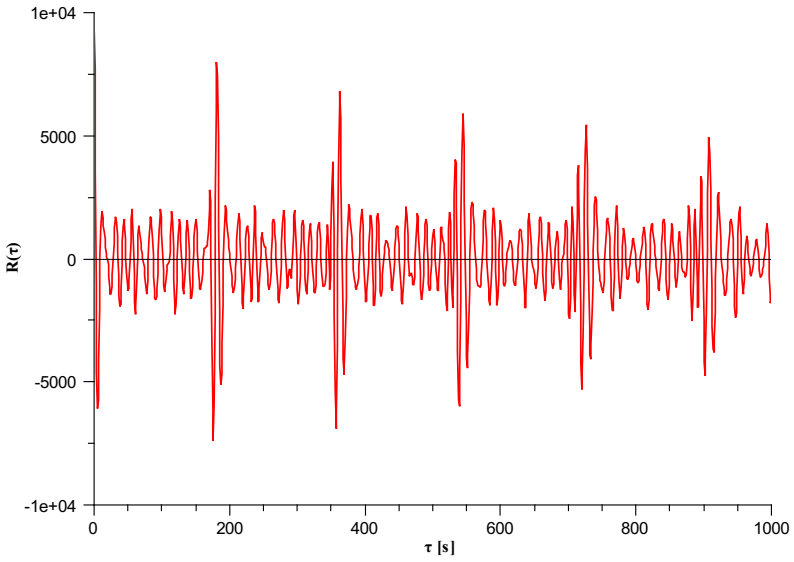

Figure 4.6: Autocorrelation function for a sequence of superposed wave components with regular frequency intervals

There are two ways to treat this problem. The straight forward way is to use a sufficiently large number of components, that is applicable for short time series. However, for our purposes this would result in a huge number of components. If we take again the example shown in Figure 4.3 with a frequency range of 1.9 rad/s and a desired simulation time of $t_{sim} = 10000$s, we obtain a maximum permissible interval-length of $\Delta\omega = 6.28 \cdot 10^{-4}$. This yields a required total number of components of 3026. This would result in unacceptably high performance requirements.

A second possibility is to choose the wave frequencies in such a way that they have surd frequency-ratios. This, for example, can be achieved by choosing the frequencies randomly from the respective frequency strip. The autocorrelation function then shows an irregular

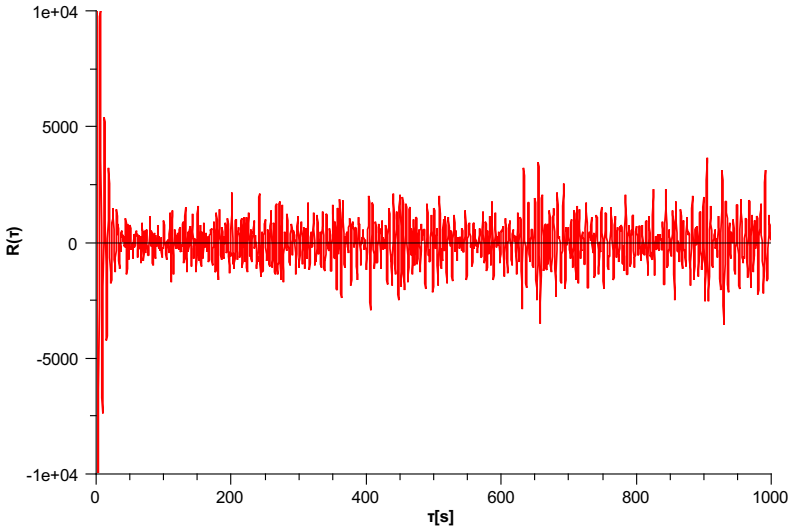

Figure 4.7: Autocorrelation function for a sequence of superposed wave components with randomly scattered, surd frequency intervals.

behaviour without any periodicity, but it does not descent to zero and varies between positive and negative values as shown by Jiang [35].

If the discretisation of the spectrum is done by using equienergetic intervals, which results in constant amplitudes for all components, the autocorrelation function descends after an initial peak to smaller values. Jiang [35] shows that the approach using constant amplitudes delivers the smallest possible variance of the autocorrelation function for all discrete solutions based on superposition. This means, that the solution comes closest to the real seaway. The autocorrelation function in this case descends very fast and shows no periodicity as shown in Figure 4.7.

4.2.4 Equivalent Wave according to Grim's Concept

The irregular seaway also causes non-regular elevations of the water surface along a ship's hull. This has significant influence on the instantaneous righting moments and therefore, has to be considered for the calculation of the ship responses according to our minimum requirements. The straight forward way to achieve this is to perform a pressure integration over the wetted surface in each time step. This delivers accurate results, but is very time consuming. A much faster way is to utilise hydrostatic lever arm curves, which are pre-calculated for a set of different drafts and trims in regular waves. The remaining problem is, how to map the irregular shape of the wavy surface along the water line to a regular

wave, which has approximately the same influence on the righting levers as the real water surface.

An approach for solving this problem was first published by Grim [23]. The concept of the "effective" wave maps the real water surface to a regular wave by applying a least squares method. The concept was later slightly amended and enhanced by Söding [67], now called the "equivalent" wave. This concept is presented briefly in the following, as it is one core component used in the numerical method *E4-ROLLS*.

The shape of the irregular wavy surface in the midship plane at $y = 0$ can be described by the following equation which is derived from Equation (4.1):

$$\zeta(x,t) = \sum_{N} \hat{\zeta}_j \cdot \cos(\omega_j t - k_j x \cos\mu_j + \varepsilon_j) \tag{4.7}$$

Söding approximates this irregular shape by the following ansatz:

$$\zeta_{eqv}(x,t) = a(t) + b(t)x + c(t)\cos\left(\frac{2\pi x}{\lambda}\right) \tag{4.8}$$

Equation (4.8) results in a regular wave with the wave length λ, whereas the wave crest and trough, respectively, are situated amidships ($x = 0$). The wave length usually is chosen equal to the ship length L. The time dependent shape of the equivalent wave is determined by the three parameters $a(t)$, $b(t)$ and $c(t)$, where the first parameter adjusts the actual still water level, the second parameter introduces a virtual trim and the last parameter, finally, determines the instantaneous wave height of the equivalent wave. Figure 4.8 illustrates the principle. The three parameters can be calculated as follows:

$$\begin{aligned} a(t) &= \sum_{N} Re\left(\hat{a}_j e^{i\omega_j t}\right) \\ b(t) &= \sum_{N} Re\left(\hat{b}_j e^{i\omega_j t}\right) \\ c(t) &= \sum_{N} Re\left(\hat{c}_j e^{i\omega_j t}\right) \end{aligned} \tag{4.9}$$

Here, ω_j is the encounter frequencies of the individual wave components used to create the irregular seaway, whilst $\hat{a}_j$, $\hat{b}_j$ and $\hat{c}_j$ are coefficients determined by applying a least squares method, which minimises the difference between the wave surfaces along the midship plane:

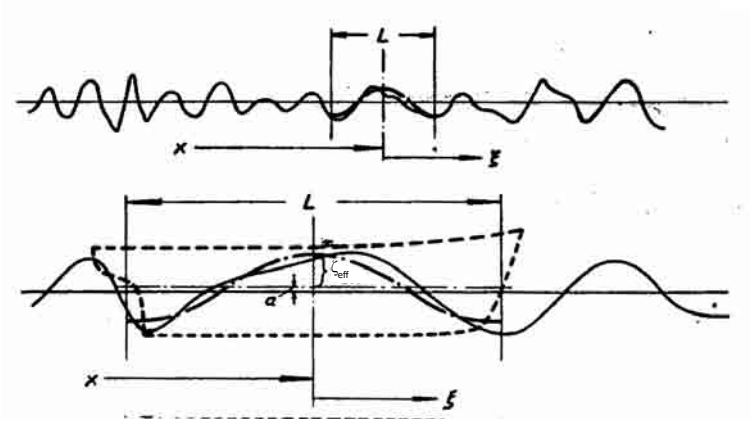

Figure 4.8: Principle of Grim's equivalent wave [23].

$$\int_{-L/2}^{L/2} \left[\zeta(x,t) - \zeta_{eqv}(x,t)\right]^2 dx \stackrel{!}{=} min. \tag{4.10}$$

L denotes the ship length. Each parameter $\hat{a}_j$, $\hat{b}_j$ and $\hat{c}_j$ then depends on the wave amplitude $\hat{\zeta}_j$, the encounter angle μ_j and the phase shift ϵ_j. In case the surge motion of the ship is not taken into account, the relative position of ship and waves is fixed. In this case, all three coefficients are constant for the entire simulation, which makes the determination of the equivalent wave very fast. If an additional surge motion shall be taken into account, the instantaneous relative movement between the waves and the ship results in additional terms for $\hat{a}_j$, $\hat{b}_j$ and $\hat{c}_j$, which contain the surge motion $\xi(t)$. In that case, the coefficients have to be determined for each time step. However, in connection with pre-calculated cross curves, it is still much faster than a full pressure integration.

4.3 Numerical Method E4-ROLLS

Methods assessing the ship motions in waves in the frequency domain based on strip theory are not able to account for roll motions induced by stability alterations. When the container vessel *E.L.M.A. Tres* capsized in heavy seas in the North Atlantic in November 1981 , Söding [66] first introduced a procedure for his investigations which made it possible to account for changing stability in waves and for its influence on the roll motion of ships. Using some ideas of Södings approach, Kroeger [39] in 1987 developed the first version of *ROLLS*. The code was enhanced later by Petey [56] to account for damaged ships as

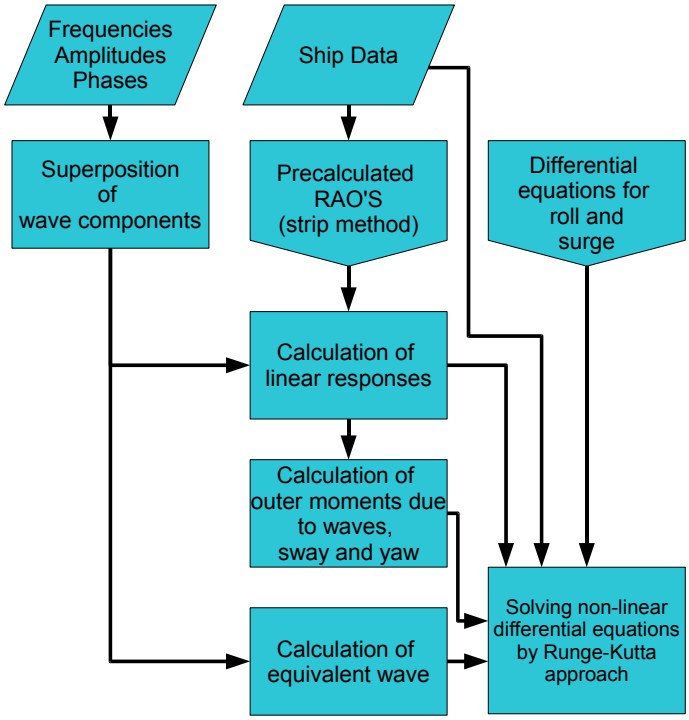

Figure 4.9: Principal architecture of the numerical method *E4-ROLLS*

well. Further improvement and extensive validation was performed within the framework of two research projects (see Billerbeck et al. [7], Krüger et al. [41], Clauss et al. [17] and Hennig et al. [26]), funded by the German Ministry of Education and Research (BMBF), which lead to the currently used version of *E4-ROLLS*. This version is fully implemented in the ship design system E4 (see Bühr et al. [16]) .

In order to account for the relevant couplings, the method considers all six degrees of freedom. These are split into two categories, which are treated differently. The first category contains the heave, pitch, sway and yaw motions. For these degrees of freedom it is assumed that the amplitudes remain moderate and therefore, a linearisation with respect to the wave amplitude is permissible. More important in this case is the correct treatment of the hydrodynamic forces, especially for sway and yaw motions. The second category consists of the remaining degrees of freedom, namely roll and surge. These two elements show a significantly non-linear behaviour with respect to the wave amplitude. The reason for this are large amplitudes concerning the roll motion on the one hand, and non-linear parameters, for example the restoring moments, on the other hand. Taking this into account, the category mentioned first is calculated by means of a strip method in the frequency domain before the time domain simulation itself is started. The second category consisting of roll and surge motions is simulated directly in the time domain

having regard to the relevant non-linearities.

The flowchart in Figure 4.9 shows the procedure realised in *ROLLS* to evaluate the ship motions. The irregular seaway is modelled from a set of regular wave components, defined by frequencies, amplitudes and phases by superposition as described in Section 4.2. From the transfer functions (RAOs) we obtain the responses for the four degrees of freedom treated linearly on the one hand and the exciting hydrodynamic forces and moments for the roll motion on the other hand. The latter depend on the transfer functions of the roll, sway and yaw motion.

In the second category of degrees of freedom the restoring forces of the roll motion are treated non-linearly, taking the true shape of the cross curve into account. In order to avoid the time-consuming calculation of the actual righting moments for each time step, the *ROLLS*-procedure works with pre-calculated cross curves. From these the actual righting arm is determined by interpolation. At this, the lever arm curves are pre-calculated for a set of different trims and drafts and for various amplitudes of a regular wave with a length equalling the ship length. For each wave the righting levers are determined for still water, wave trough and wave crest conditions. To make use of the pre-calculated lever arms the instantaneous water surface around the ship is replaced by a regular wave using the equivalent wave concept. At this point the environmental conditions, the linearised exciting moments and the non-linear restoring forces are known. Together with the information on the ship's weight distribution, they are used for the calculation of the roll motion in the time domain according to the following equation of motion:

$$\ddot{\varphi} = \frac{\sum M - M_d - \ m\ (g - \ddot{\zeta})\ h_s - \Theta_{xz}\left[\left(\ddot{\vartheta} + \vartheta\dot{\varphi}^2\right)\sin\varphi - \left(\ddot{\psi} + \psi\dot{\varphi}^2\right)\cos\varphi\right]}{\Theta_{xx} - \Theta_{xz}(\psi\sin\varphi + \vartheta\cos\varphi)} \tag{4.11}$$

Here, M represents the linearised exciting moments, consisting of the linear exciting moments obtained by RAOs and additional components due to wind, tanks and active roll damping devices like fin stabilizers and anti-roll tanks. M_d represents the total damping moment as introduced in Section 4.4. The mass moments of inertia around the ship's longitudinal axis are given by Θ_{xx} and the mass product of inertia in the x-z-plane is denoted as Θ_{xz}. The restoring moments are calculated from the ship's mass m, the righting lever h_s of the equivalent wave and the relative acceleration in the earth fixed ζ-direction.

The second degree of freedom which is simulated directly in the time domain, is the surge motion, calculated according to the following approach:

$$\ddot{\xi} = -\left[\frac{2R(v_0)}{v_0 m^*}\dot{\xi} + \frac{R(v_0)}{v_0^2 m^*}\dot{\xi}^2 + \frac{\Delta R}{m^*}\right] \tag{4.12}$$

At this, R represents the resistance curve in still water conditions, while ΔR is the added resistance due to waves. The latter resistance component is calculated by integration over the horizontal force components resulting from the submerged frame areas at a location x. Further, v_0 denotes the ship's mean forward speed, while $\dot{\xi}$ is the instantaneous speed component induced by the seaway. Finally, m^* represents the ship's mass including hydrodynamic components. The Equations 4.11 and 4.12 are solved in the time domain applying a Runge-Kutta approach.

Figure 4.10 shows an example for a sequence of pictures, comparing the ship reactions in a defined seaway. The left hand side shows the simulation with *E4-ROLLS* and the right hand side shows the same situation during the model test. Many of these parallel runs were carried out by Billerbeck et al. [7] within the framework of the research project SINSEE for validation purposes. The present sequence shows a very good agreement between model test and simulation.

4.4 Influence of Roll Damping

The roll damping moments are caused by forces due to radiation of waves, due to lift forces caused by transverse flows at forward speed and, finally, by viscous forces mainly due to vortex separation. Usually, the last component represents the dominant part in the overall roll damping. The method *E4-ROLLS* utilizes hydrodynamic forces from strip theory calculations, which assumes potential flows. While radiation forces as well as lift forces could be calculated directly by potential flow methods, it is not possible to account for any viscous forces. Consequently, the influence of roll damping on the ship response has to be modelled by using external data. These data can be either obtained from full scale measurements, model tests, or computational methods which enable to assess viscous forces. Today, the common way is still to perform model tests.

At this, the model is either tested in a free roll decay test, or the test is performed with externally excited models. In case of the latter method a predefined heeling moment is applied to the ship, which oscillates at frequencies close to the roll-resonance. The resulting maximum roll angle is registered as a measure for the roll damping of the vessel. The tests are usually performed for various exciting moments and for a selection of forward speeds. The result is a dimensionless coefficient of effective roll damping as introduced by Blume [9] which represents the relationship $\varphi_{stat}/\varphi_{res}$. Here, φ_{stat} denotes the heeling angle caused by the exciting heeling moment under static conditions. φ_{res} in turn is the

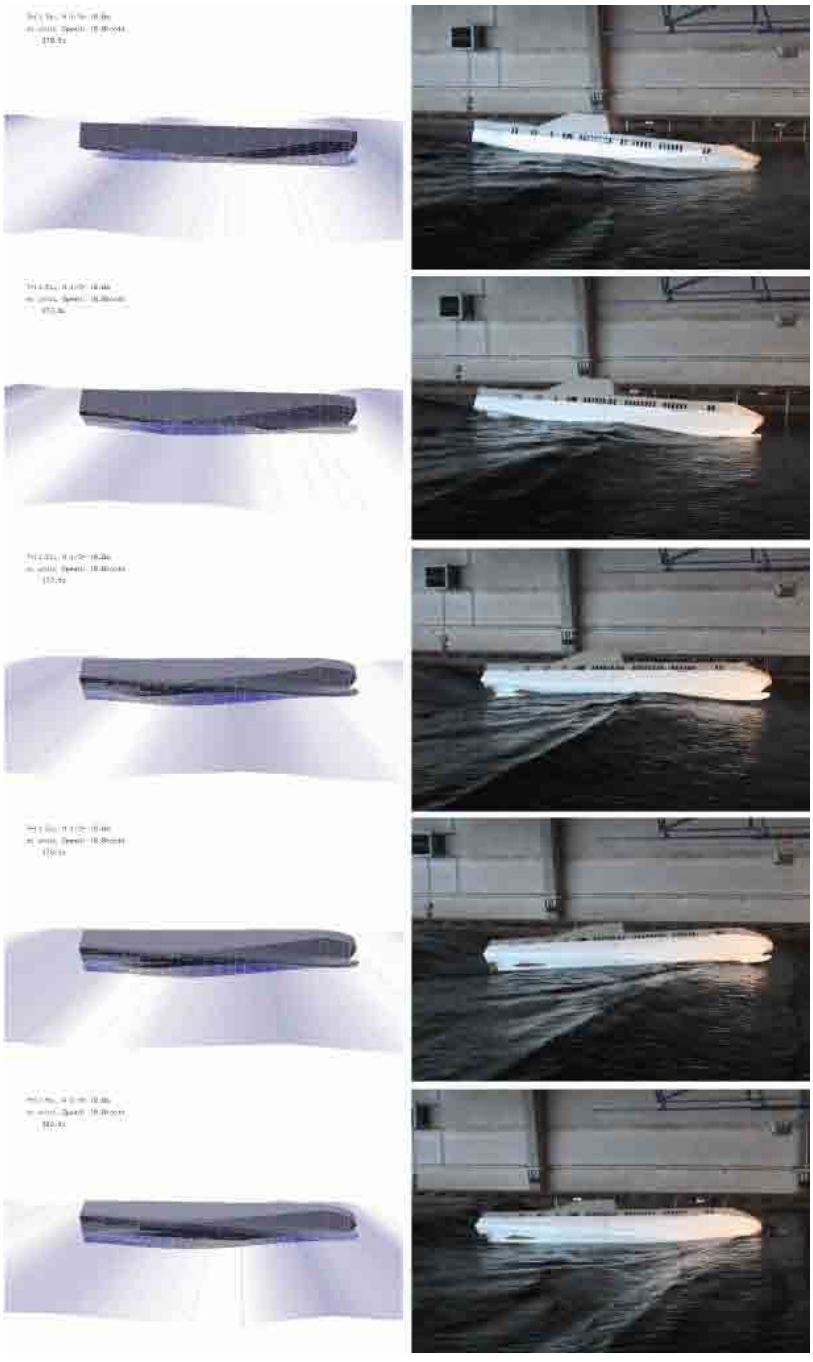

Figure 4.10: Visualisation of results calculated by *E4-ROLLS* in comparison to a model test. Validation project within the framework of the research project SINSEE (see Billerbeck et al. [7])

resulting, dynamic roll angle observed in resonance conditions. Figure 4.11 shows a set of curves for the dimensionless damping coefficient for different Froude numbers and for different resonance roll angles φ_{res}, obtained from the model tests performed by Blume.

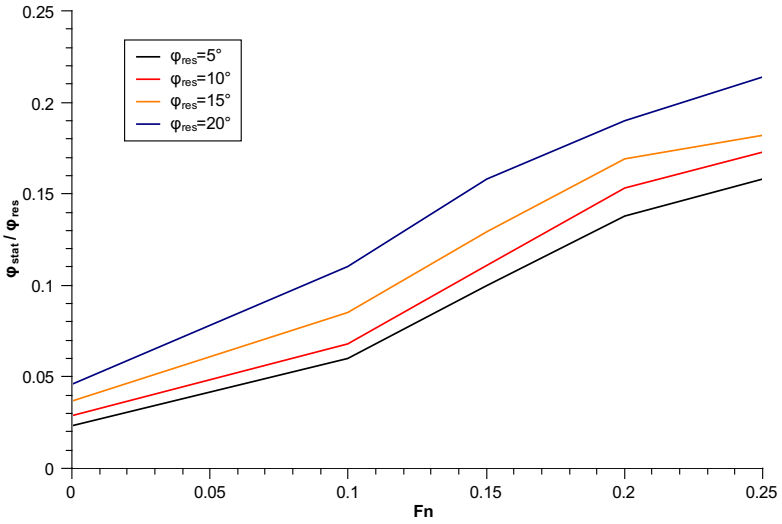

Figure 4.11: Damping coefficients obtained from model test for a ship with B/T = 3.460 and C_B = 0.503 according to Blume [9]

The method *E4-ROLLS* accounts for roll damping by a linear (d_L) as well as a quadratic (d_Q) roll damping coefficient:

$$M_d = d_L\dot{\varphi} + d_Q\dot{\varphi}|\dot{\varphi}| \tag{4.13}$$

The linear coefficient can be calculated from the effective roll damping coefficient as follows:

$$d_L = \frac{mg\overline{GM}}{\omega_\varphi}\left(\frac{\varphi_{stat}}{\varphi_{res}}\right)_0 \tag{4.14}$$

At this, ω_φ is the natural roll frequency of the vessel under consideration. The index 0 for the effective roll damping coefficient indicates that the extrapolated value for a theoretical resonance angle $\varphi_{res} = 0°$ is used here. The quadratic coefficient is obtained from similar considerations, resulting in the following relationship:

$$d_Q = \frac{3\pi}{8\omega_\varphi\varphi_{res}} \cdot \left[\frac{mg\overline{GM}}{\omega_\varphi}\left(\frac{\varphi_{stat}}{\varphi_{res}}\right)_{20} - d_L\right] + d_{QBK} \tag{4.15}$$

Here, the effective roll damping coefficient for a resonance angle of 20 degrees is used. From the total roll damping coefficient we have to substract the linear share d_L to obtain

the non-linear part only. Finally, the quadratic coefficient is enhanced by the influence of bilge keels (d_{QBK}), which is calculated by following an approach introduced by Gadd [21].

5 Selected Failure Criteria

Once the ship reactions in waves are known, either determined by model tests or by numerical simulations as shown before, they can be used to evaluate the ship safety in waves. For this purpose, procedures and criteria have to be available which judge the safety level of a ship. This can be realised either by quantifying the ship safety via characteristic numbers along with the definition of related threshold values, or by formulating prescriptive criteria, which have to be met in order to achieve a sufficient safety level. The following sections give a brief introduction into selected failure criteria addressing large amplitude roll motions and capsizing. These criteria were published by various researchers and document the development of capsizing criteria during the last decades in Germany.

5.1 The Kastner/Roden Criterion for the Extrapolation to minimum GM values

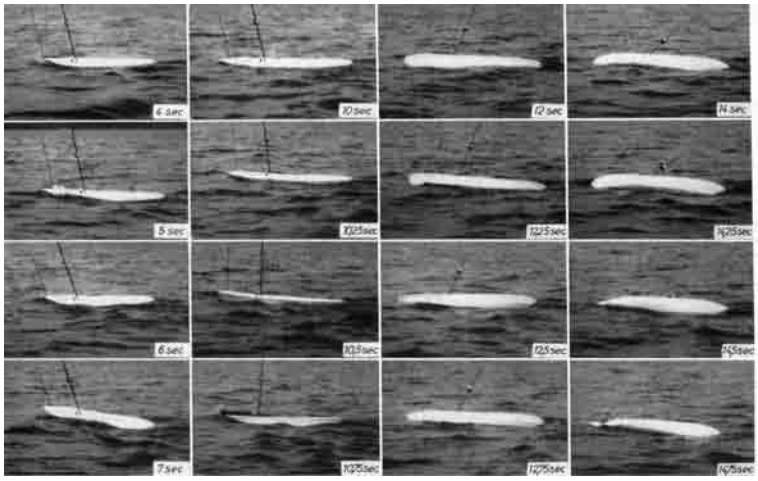

Figure 5.1: Model test in a natural seaway to determine the capsizing of a model according to Kastner and Roden, [59].

As a consequence of some capsizing accidents in stern quartering seas which were discussed in Germany since the early 50s, Kastner and Roden [37], [38], [60], [59], performed model tests with radio controlled models in a natural seaway on the large inland Lake Ploen. From these model tests , Kastner [37] developed a method to determine a minimum threshold value for the metacentric height (GM), in order to prevent a vessel from capsizing in rough weather due to insufficient stability. Therefore, the following criterion can be regarded as a criterion to prevent a pure loss on the crest accident, and it can be applied to those cases where actually this pure loss situation leads to a failure.

The authors observed the very interesting phenomenon that there seems to exist a clear limiting metacentric height, or small bandwidth of GMs, which distinguish a ship from being safe or unsafe (see [2], [3], [38], [60]). In case a model was operated below this limit, it was obviously unsafe as it capsized definitively, and if the model was operated beyond this limit, a capsize could not be observed, even if the model was exposed to the situation for a relatively long time. The histogram on the left hand side in Figure 5.2 shows the statistical distribution of the time after which capsizing did occur during the individual model tests.

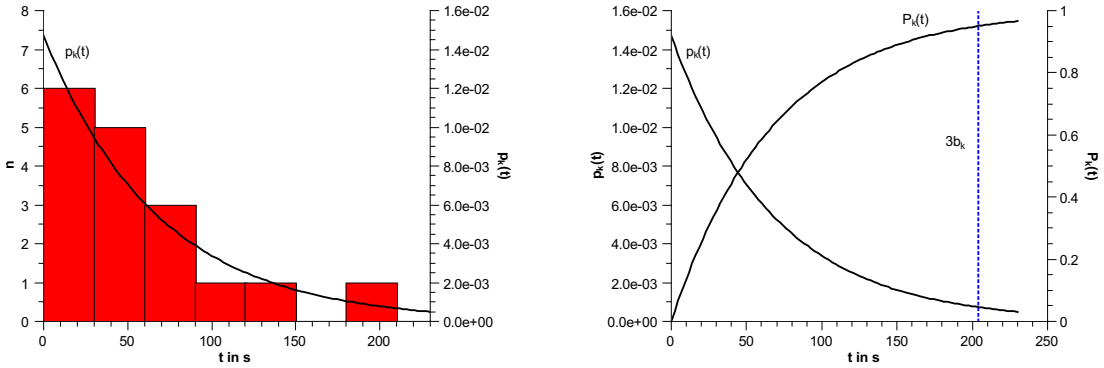

Figure 5.2: Statistical distribution of the capsizing times as results of the model tests by Kastner and Roden on the Lake Ploen and the definition of the expected capsizing period [59].

Kastner and Roden chose an exponential probability distribution to approximate the probability density function from the experimental results. The resulting probability density function (PDF) as well as the integrated cumulative density function (CDF) are shown in Figure 5.2 on the right hand side. The probability density function then yields to:

$$p_k(t) = e^{-\frac{1}{b_k}t} \tag{5.1}$$

Here, b_k denotes the expectancy value (weighted mean value) of the time to capsize, which in practise can be considered as the capsizing period. This means that the vessel

needs to travel b_k seconds in average in a specific seaway to experience a capsizing event. Integrating Equation 5.1 delivers the CDF for capsizing in the given conditions:

$$P_k(t) = 1 - e^{\left(-\frac{1}{b_k} \cdot t\right)} \tag{5.2}$$

The authors then determine the 95% -confidence intervall for capsizing within the respective time-interval. This value equals two times the standard deviation of the Gaussian normal distribution. For the chosen exponential probability distribution this time period containing 95% of all capsizing events yields:

$$T_k = 3b_k \tag{5.3}$$

Having defined the time interval of capsizing for an unsafe ship, the authors in turn require for a "safe" ship that only 5% of all capsizing events occur during T_k, assuming again an exponential distribution of capsizing events:

$$P_{nk}(T_k) = 0.05 = 1 - e^{\left(-\frac{1}{b_{nk}} \cdot T_k\right)} \tag{5.4}$$

This delivers a constant relationship between the parameters b_k and b_{nk}, which can be used to determine b_{nk}. The ratio amounts to:

$$\frac{b_{nk}}{b_k} = 58.4 \tag{5.5}$$

The authors then make the assumption that the vessel capsizes when the wave height exceeds a certain limit. For a given time interval, this wave height can be determined, whereas the time interval is given by the expected time to capsize b_k. From this and from the encounter period T_e between the waves and the ship, it is possible to calculate the mean probability of occurrence $\bar{p}_k$ for the extreme wave which leads to capsizing:

$$\bar{p}_k = \frac{T_e}{b_k} \tag{5.6}$$

The same relationship holds for b_{nk} and $\bar{p}_{nk}$ in the same way. For the mean probability of occurrence $\bar{p}_k$ it is possible to determine the wave amplitude $\hat{\zeta}_k^p$ expected to be exceeded in the given seaway, based on the considerations published by Bartsch [6] and Longuet-Higgins [47]. They calculate the expected value for the p-highest wave amplitudes, assuming that the wave amplitudes are Rayleigh distributed:

$$\hat{\zeta}_k^p = \frac{1}{p} \int_{\hat{\zeta}_1}^{\infty} \frac{2\hat{\zeta}^2}{m_0} e^{(-\hat{\zeta}^2/2m_0)} d\hat{\zeta} \tag{5.7}$$

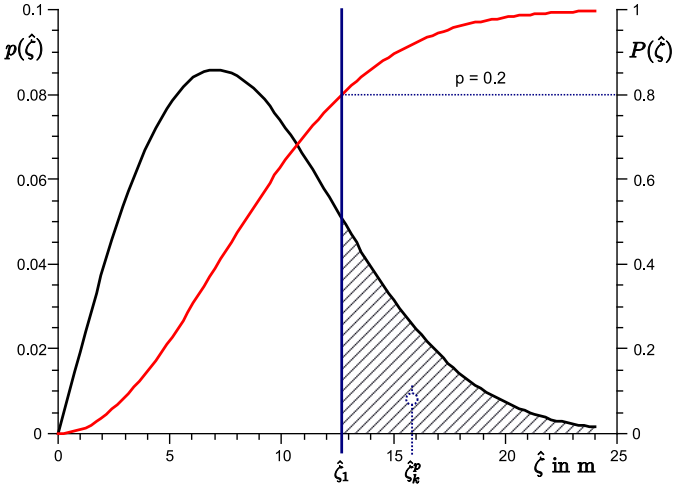

Figure 5.3: Expected amplitude $\hat{\zeta}_k^p$ for the p-highest amplitudes of a seaway, whereas the example is shown for $p = 0.2$.

At this, the lower boundary for the integration is calculated from the prescribed probability level p by:

$$\hat{\zeta}_1 = \sqrt{2m_0 \ln(\frac{1}{p})} \tag{5.8}$$

Here, m_0 is the integral over the wave spectrum S, which represents the variance of the wave amplitudes. Figure 5.3 illustrates the procedure for the case $p = 0.2$. Setting $\bar{p}_k$ for p, the related amplitude $\hat{\zeta}_k^p$ is obtained. The same procedure can be applied to $\bar{p}_{nk}$, resulting in the amplitude $\hat{\zeta}_{nk}^p$ in the safe condition. From these two wave heights the authors calculate the wave steepness by using the characteristic wave length of the seaway λ_1:

$$\frac{H}{\lambda_1} = \frac{2\hat{\zeta}^p}{\lambda_1} \tag{5.9}$$

The authors then assume that the wave steepness at which the vessel capsizes and the related GM-values are directly proportional. Then it is possible to establish a relationship between the wave heights and the GM values for both cases. This again is used to estimate a GM-value at which the operation of the ship is considered to be safe under the given environmental conditions:

$$\frac{GM_k}{GM_{nk}} = \frac{H_k}{H_{nk}} \tag{5.10}$$

This means that the GM of the ship present at the time of capsize has to be increased by the factor H_k/H_{nk} to obtain a sufficient safety level. Consequently, the capsizing criterion

of Kastner and Roden leads to the determination of a required minimum metacentric height GM_{nk} under the assumption that the actual GM value is insufficient.

5.2 Soeding's Concept of Amplified Waves

The accident of the container ship E.L.M.A. Tres [66] in the year 1981 undoubtedly was one of the major initiating factors which lead to the development of new methods for the assessment of large amplitude ship motions in waves based on numerical computations. Although it then was possible to assess the ship motions sufficiently accurate one problem remained. In principle it is very easy to determine capsizing probabilities or capsizing rates directly from the simulations. Assuming that capsizing is a rare event, the best estimate for the mean capsizing probability yields:

$$P_R = \frac{N_C}{t_{sim}} \cdot T_R \tag{5.11}$$

Here, N_C denotes the number of capsizings registered during t_{sim}, which is the period of real time simulated. T_R represents the average roll period of the vessel. The problem occurring is the rareness of large amplitude roll motions and capsizing at tolerable safety levels. This is especially true when simulating ships in realistic operating conditions in order to assess minimum permissible capsizing probabilities.

To obtain significant and realistic results it is necessary to register a sufficient number of capsizing events during the simulation. Söding [69], for example, recommends to exploit at least 5 events. Given an average capsizing rate of $R_C \approx 1/\text{a}$, the simulation has to cover at least 5 years real time. Despite the capacity of modern computer systems this is still not feasible, especially not for the statistical assessment of many different situations. Therefore, Söding and Tonguc [72] propose an extrapolation concept to reduce the computational effort. The idea of this concept is to perform simulations in a seaway which has the same parameters as the seaway for which the capsizing probability is wanted, but with an increased significant wave height. For this amplified seastate, the capsizing frequency is much higher than in the original seaway and thus, reliable results can be obtained within a reasonable simulation time.

In the initial form of the extrapolation concept, Söding and Tonguc make the basic assumption that the ship capsizes whenever a certain wave height H_C is exceeded. The capsizing frequency f_c then equals the frequency of exceedance of this particular wave height:

$$f_C(H_{1/3}) = f(H_C, H_{1/3}) \tag{5.12}$$

Here, $H_{1/3}$ denotes the significant wave height of the present seastate. The statistical distribution of the wave heights occurring in a irregular seaway equals the Rayleigh distribution, as long as the seaway itself can be considered as a Gaussian process. This condition is fulfilled with sufficient accuracy for the linear wave models used in our simulations. Then, the capsizing frequency depends on the mean up-crossing period of the waves T_0 and the significant wave height:

$$f_C(H_C, H_{1/3}) = \frac{1}{T_0} \cdot e^{\left(-\frac{2H_C^2}{H_{1/3}^2}\right)} \tag{5.13}$$

Söding and Tonguc now introduce the probability P_R that the ship capsizes at least once in a particular roll period of the duration T_R:

$$P_R = 1 - e^{(-f_C \cdot T_R)} \tag{5.14}$$

For small values of P_R this can be simplified to:

$$P_R = f_C \cdot T_R \tag{5.15}$$

Replacing f_C in Equation 5.13 by the relationship given in Equation 5.15, the following relationship can be established between the capsizing probabilities obtained when the ship is travelling in the desired wave height $H_{1/3}$ or when it is travelling in the increased wave height used for the simulation $H_{1/3}^{(s)}$:

$$\frac{H_{1/3}^2}{H_{1/3}^{(s)\ 2}} = \frac{\ln(P_R(H_{1/3}^{(s)}))}{\ln(P_R(H_{1/3}))} \tag{5.16}$$

Based on this first solution, Söding and Tonguc generalise their concept by assuming that the ship capsizes with a certain probability P if n successive waves all exceed the critical wave height H_C. As shown by Söding [68] the following relationship exists without specifying P, n and H_C in detail:

$$-\ln P_R = A + \frac{B}{H_{1/3}}^2 \tag{5.17}$$

Here, A and B are constants introduced during the development of the concept. Söding and Tonguc [72] show that A is almost constant for all investigated cases, with values varying between 1.0 and 1.25 according to Söding [71]. Taking $A = 1.25$ as constant value, Equation 5.17 leads to a relationship between the real capsizing probability and

the one obtained in amplified waves, which enhances the original formulation in Equation 5.16 by the constant factor A:

$$\frac{H_{1/3}^2}{H_{1/3}^{(s)\,2}} = \frac{\ln(P_R(H_{1/3})) + 1.25}{\ln(P_R(H_{1/3}^{(s)})) + 1.25} = (\delta C^2) \tag{5.18}$$

The original sources do not provide any procedure to determine the extrapolation factor δC, but the authors recommend to choose the factor in such a way that a sufficient number of capsizings can be observed during the simulation. As already mentioned earlier, Söding [69] recommends at least 5 registrations to obtain reliable results. Further, the concept does not provide any threshold values for the capsizing probability, above which ships can be regarded as safe. By selecting predefined scenarios, the methodology further disregards the probability of the scenario as such and the fact that also other scenarios may be critical. Our tests show further, that the results present some scatter depending on the extrapolation factor selected. For some cases, it appeared that the scatter of the results introduced by different extrapolation factors is sometimes of the same order of magnitude as the influence of governing stability parameters. Taking all this into account, the methodology as such does not directly deliver a capsizing criterion, but it is suitable to serve as an evaluation method for a given pre-defined scenario. Due to the reasons mentioned above, the concept should be applied only to small capsizing probabilities and moderate extrapolation factors.

5.3 Blume's Concept of Defining Sufficient Safety against Capsizing from Model Tests

In the early 1980's, Blume and Hattendorff [11] were performing systematic series of model tests at the Hamburg Ship Model Basin (HSVA). The main aim of these tests was to evaluate the behaviour of new hull forms, which first of all meant the new container vessels at that time, in following and stern quartering seas. Based on the results of these model tests, Blume later developed new minimum intact stability requirements for containerships, which are also known as "C-factor concept". Today, these requirements are part of the IMO Res. A749 for the alternative assessment of intact stability of container ships. More details on this concept can be found in Section 3.1.

For the development of the new criterion, it was necessary to categorise the individual model tests into safe and unsafe ones. Here, runs where the ship capsized were obviously unsafe, but it was unclear how to treat those ones where the ship did not capsize, but in which it developed large roll angles. To resolve this question, Blume developed a criterion based on the maximum roll angle detected during a test run and the residual area under

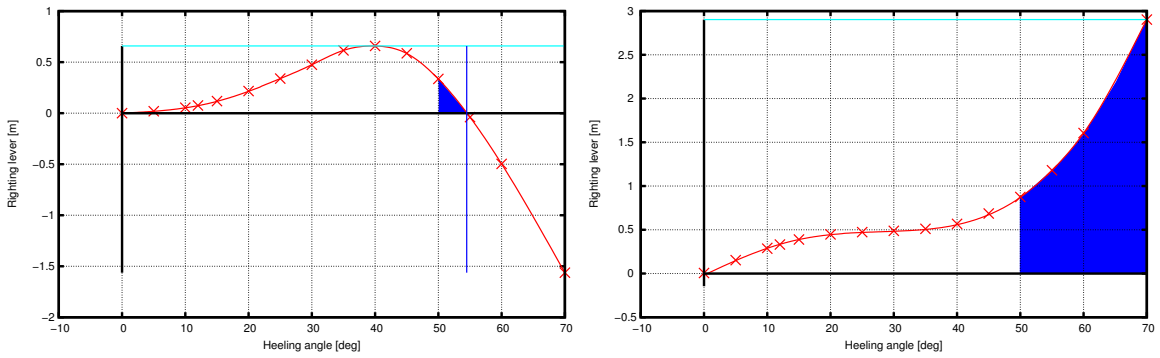

Figure 5.4: Lever arm curves for two different types of ships. Left side: Medium size container vessel. Right hand side: Car carrier

the still water lever arm curve beyond this angle. This criterion today is widely known as *Blume-criterion*. Its application is not limited to model tests, but any calculation method which delivers time series of roll angles, for example numerical simulations in the time domain, can be evaluated by the criterion.

The basic input, needed to apply the criterion, is a set of time series. For this, the test runs have to be repeated several times for the same loadcase and for the same environmental conditions. From each time series the maximum roll angle in the respective run is determined. Subsequently, the residual area below the still water lever arm curve between the maximum roll angle and the angle of vanishing stability is calculated. From this set of residual areas, it is possible to obtain the mean residual area $\overline{E}_R$ and the related standard deviation σ. Blume now assumes that the residual areas obtained from the different time series are approximately normal distributed. Consequently, reducing the mean value $\overline{E}_R$ by three times the standard deviation 3σ, results in a residual area E_R^*. The values for the residual area do not fall below this level with a probability of 99.87% according to the 6σ-confidence level of the normal distribution. As long as the residual area E_R^* is larger than zero the vessel does not capsize. Consequently, the criterion requires that E_R^* has to be larger or equal to zero in order to consider the ship as safe in the given conditions:

$$E_R^* = \overline{E}_R - 3\sigma > 0 \tag{5.19}$$

The approach neglects lever arm alterations in waves, as it addresses the still water lever arm curve, only. Nevertheless, for most ships the Blume-criterion was found to work very reliable, because it assures a sufficiently large safety margin between the largest permissible roll angle and the angle of capsize. For certain ship types, however, the Blume-criterion fails. This becomes clear when comparing the two lever arm curves shown in Figure 5.4. Both curves represent the intact stability limit according to the present regulations in the IMO Res. A.749. The chart on the left hand side shows a lever arm curve which

is typical for container vessels with a low initial metacentre and positive added stability of form. The angle of vanishing stability lies between 50 and 60 degrees. In such cases, our experiences show that the largest permissible heeling angle delivered by the Blume-criterion approximately lies between 45 and 50 degrees. Heeling angles of this order of magnitude seem to be barely acceptable for a minimum stability criterion which mainly targets the prevention of capsizing and total losses, although one has to expect certain damages to the equipment as well as to the cargo. The situation is somewhat different for the lever arm curve shown on the right hand side in Figure 5.4. Such type of lever arm curve is typical for ships with large weathertight superstructures, for example car carriers. The large superstructures result in a very large range of positive righting levers up to angles of 70 to 80 degrees until the submergence of non-weathertight openings. In this case, the Blume-criterion would deliver threshold angles of 70 degrees and beyond. This is not acceptable, even for a minimum stability criterion, because such large heeling angles inevitably must lead to severe damages to ship and cargo, as well as they most likely lead to severe injuries to crew and, in case of passenger ships, also to passengers.

6 The Insufficient Stability Event Index (ISEI)

In Chapter 2 the most relevant failure modes which endanger ships in waves, as well as the requirements towards possible future intact stability criteria are discussed. Chapter 4 shows how to assess ship motions by means of numerical simulations. We now join these findings in order to derive a procedure which is suitable to assess the ship safety in waves.

6.1 Concept

The idea behind the concept presented in the following is to evaluate the overall safety of a ship with a given loading condition against excessive roll angles and against capsizing by assessing all possible and relevant operating conditions. Operating conditions in this context are defined by two categories of data, which are environmental data and ship specific operating data. The environmental component is determined by the characteristic wave period T_1 of the irregular, short crested seaway in which the ship travels and by the significant wave height $H_{1/3}$. Operating data in this context are the actual ship speed v_s and the course of the vessel relative to the main encounter direction of the waves, in the following denominated by μ.

Each component contained in the definition of the operating conditions has a certain probability of occurrence. Consequently, the probability of occurrence of a specific operating condition is the product of the individual component probabilities. Assuming further that a ship faces extreme roll angles in the given conditions with a certain frequency of occurrence, we can calculate the overall rate of occurence of dangerous situations in a given loading condition as follows:

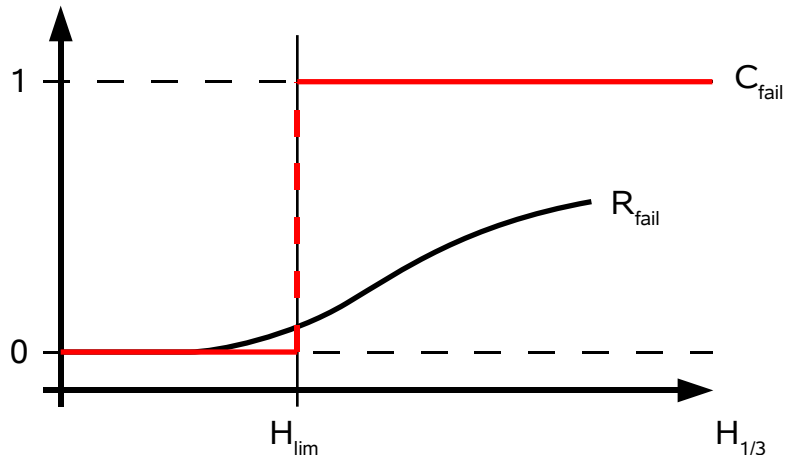

Figure 6.1: Basic concept of the failure coefficient C_{fail}

$$R_{accident} = \int_{T_1=0}^{\infty} \int_{H_{1/3}=0}^{\infty} \int_{\mu=-\pi}^{\pi} \int_{v_s=0}^{v_{max}} p_{sea}(H_{1/3}, T_1) \cdot p_\mu(\mu) \cdot p_v(v_s \mid H_{1/3}, T_1, \mu) \cdot r_{fail}(H_{1/3}, T_1, \mu, v_s) \cdot dv_s \cdot d\mu \cdot dH_{1/3} \cdot dT_1 \tag{6.1}$$

Here, the overall probability is obtained by integration over the probability density functions (PDF) of all components. p_{sea} denotes the probability density of the seastate, depending on significant wave height $H_{1/3}$ and characteristic period T_1. Then, p_μ is the probability density for the encounter direction of the waves relative to the ship. In contrast to the latter, the probability density for the ship's speed is conditional as it depends on the maximum possible speed in waves (v_{max}). This, in turn, depends on the actual seastate as well as on the encounter direction. v_{max} is obtained from the maximum possible power delivered by the propulsion train by balancing it against the total resistance of the vessel, including the added resistance due to waves and wind. For details see Section 6.4. Finally, r_{fail} represents the distribution function of the ship's failure rates over the different operating conditions which are characterised by seastate, course and speed. r_{fail} is called "relative failure rate" in the following, whereas the integral value is the failure rate R_{fail}. Usually the failure rate is given in the form of failures per roll cycle. In this case, Equation 6.1 delivers the overall accident rate $R_{accident}$ relative to one roll cycle. The fourfold integration is performed over the whole domain of possible values, whereas the boundaries of the integral over all speeds depend on the other variables $H_{1/3}, T_1$ and μ.

For the practical use of Equation 6.1 the problem remains that the true failure rate of a

ship in a certain situation r_{fail} is difficult to calculate, mainly due to the long simulation time required to obtain reliable results for this value. For the purpose of a minimum stability criterion, however, it seems to be of minor importance to know the exact amount of capsizings to be expected within a certain period of time, but to know rather whether a ship is unsafe in a certain operating condition. In order to simplify the procedure and to reduce the calculation effort, the actual failure rate r_{fail} is replaced by a so called failure coefficient C_{fail}.

This failure coefficient represents a binary function with the value 0 for all situations in which the ship is considered to be sufficiently safe and 1 for all situations considered to be unsafe. The idea behind this approach and the relationship between the failure rate r_{fail} and the failure coefficient is illustrated by Figure 6.1.

$$C_{fail}(H_{1/3}, H_{lim} \,|\, T_1, \mu, v_s) = \begin{cases} 0 & \text{if} \quad H_{1/3} < H_{lim} \\ 1 & \text{if} \quad H_{1/3} \geqq H_{lim} \end{cases} \tag{6.2}$$

The actual value of the failure coefficient C_{fail} depends on the ship speed v_s, the course μ, the characteristic wave period T_1 and a limiting wave height H_{lim}. The last component is determined by numerical simulations following a deterministic approach based on the Blume-criterion and a maximum limiting roll angle. The implementation of the decision criterion is described in detail in Section 6.2.

The calculation of C_{fail} by means of numerical simulations is carried out for discrete points in the overall domain. These situations are denoted as "operational cells" in the following. Each operational cell is defined by the characteristic wave period T_1, the ship speed v_s and the relative encounter direction between ship and mean wave direction μ. For each possible combination of parameters, one operational cell is created:

$$N_{cells} = N_{T_1} \cdot N_{\mu} \cdot N_v \tag{6.3}$$

In consequence, Equation 6.1 is transformed into a discrete form by replacing the integrals by sums over all possible operational cells. As it contains the deterministic component of C_{fail} the result is no longer called accident rate, but Insufficient Stability Event Index (ISEI):

$$ISEI = \sum_{i=1}^{N_T} \sum_{j=1}^{N_H} \sum_{k=1}^{N_\mu} \sum_{l=1}^{N_v} \delta P_{sea}(H_{1/3}^{(j)}, T_1^{(i)}) \cdot \delta P_\mu(\mu^{(k)}) \cdot \delta P_v(v_s^{(l)} \mid H_{1/3}^{(j)}, T_1^{(i)}, \mu^{(k)}) \cdot C_{fail}(H_{1/3}^{(j)}, H_{lim} \mid T_1^{(i)}, \mu^{(k)}, v_s^{(l)}) \tag{6.4}$$

Here, the δP denote the cumulated probabilities for a discrete range of values. These values are obtained from the probability density functions p as used in Equation 6.1 by integration over the desired range of values. The number of elements in each summation depends on the individual granularity chosen for the parameters.

As already pointed out in Section 2, the failure modes leading to large roll angles and subsequent capsizing differ, depending on the wave encounter relative to the ship. Whereas the ship is excited directly by wave induced heeling moments in beam seas, the roll motion in head, head-quartering, following and stern-quartering seas is mainly driven by dynamic lever arm alterations. To get more detailed information on when and where a ship is considered safe or unsafe, respectively, it is helpful to split the index into three sub-indices, quantifying the ship safety in three sectors, namely head, beam and following seas as indicated in Figure 6.2:

$$ISEI = ISEI_h + ISEI_b + ISEI_f = \sum_{h,b,f} \left\{ \sum_{i=1}^{N_T} \sum_{j=1}^{N_H} \sum_{k=1}^{N_\mu} \sum_{l=1}^{N_v} \delta P_{sea}(H_{1/3}^{(j)}, T_1^{(i)}) \cdot \delta P_\mu(\mu^{(k)}) \cdot \delta P_v(v_s^{(l)} \mid H_{1/3}^{(j)}, T_1^{(i)}, \mu^{(k)}) \cdot C_{fail}(H_{1/3}^{(j)}, H_{lim} \mid T_1^{(i)}, \mu^{(k)}, v_s^{(l)}) \right\} \tag{6.5}$$

The indices h, b and f denote head, beam and following seas, respectively. The three sectors are distributed over the full range of possible encounter angles as demonstrated in Figure 6.2. The $ISEI_f$, quantifying the hazard for ships travelling in following seas, contains the range of encounter angles from 0 degrees to 60 degrees. Consequently the

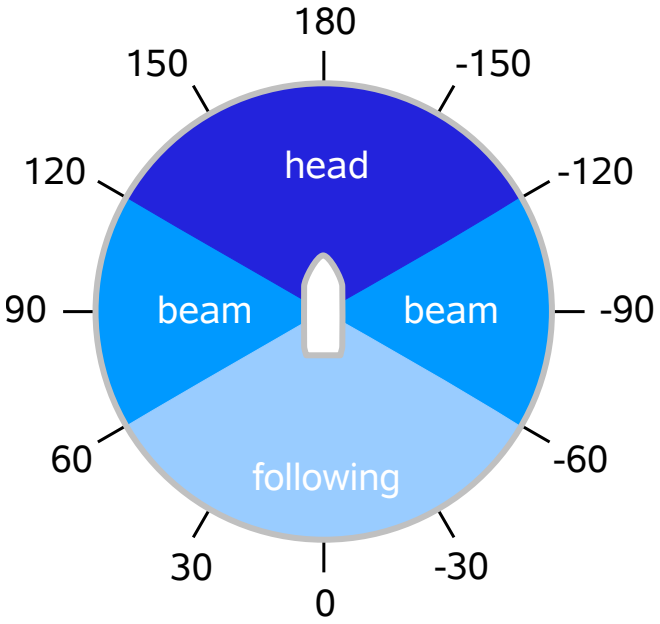

Figure 6.2: Wave encounter directions and related sectors

index for beam seas covers the range from 60 to 120 degrees. The remaining sector up to 180 degrees is represented by $ISEI_h$, the index for all head sea cases.

The overall Insufficient Stability Event Index in its final form given in Equation 6.5 can be interpreted as the basic probability for a ship with a specific loading condition being in a not safe operating condition, whereas "not safe" is determined by a quasi-deterministic decision criterion. As such the ISEI itself is not directly related to a certain period of time and it is also not meant to be.

The overall ISEI coefficient is a measure for the ship saftey in waves with respect to large amplitude roll motions. However, this is not sufficient for a criterion targeting the minimum intact stability of ships. Such a criterion presumes that the underlying procedure delivers a monotonically increasing safety level with increasing GM. This is not the case for the overall Insufficient Stability Event Index. The reason for this is that increasing the stability in fact always improves the situation in following seas. Under certain circumstances the safety increase in following seas is compensated by a safety decrease in head and head-quartering seas, because higher stability values often shift the vessels' natural roll period to shorter, critical values. This might be illustrated by the polar diagrams in Figure 6.3. These are calculated for the small coaster *Marianne Wehr* with GM values of 0.985 and 1.215 metres. The significant wave period amounts 6 seconds. The diagrams clearly show that increasing the GM improves the situation in following seas

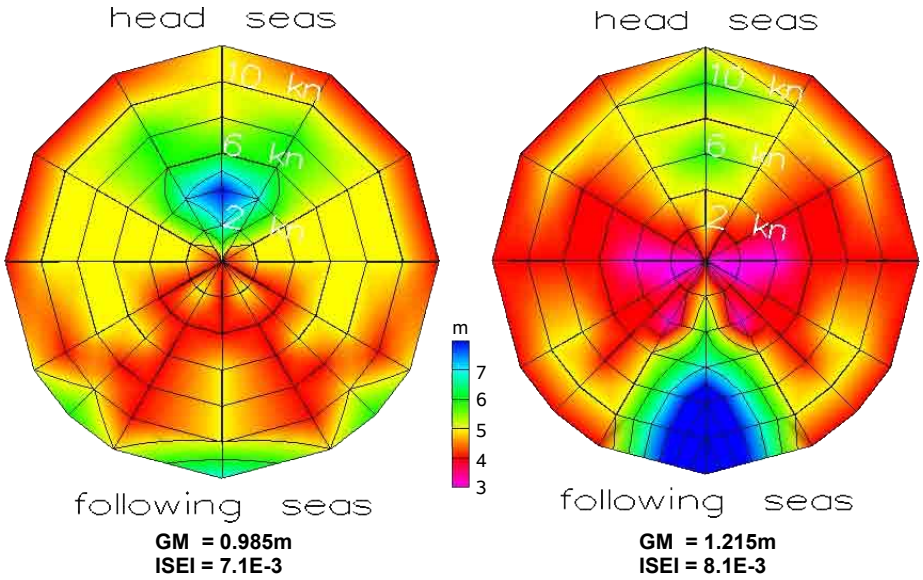

Figure 6.3: Limiting significant wave heights calculated for the small coaster MV Marianne Wehr ($L_{bp} = 55.0$m) with different GM values. Significant wave period is $T_1 = 6$s.

but leads to critical areas in head and head-quartering waves due to resonances, which is also expressed by the nearly constant values for the overall ISEI. Consequently, only the following seas part of the Insufficient Stability Event Index ($ISEI_f$) is taken into account for the determination of the required minimum intact stability.

6.2 Failure Coefficient C_{Fail}

As already introduced in Equation 6.2, the failure coefficient directly depends on the limiting wave H_{lim}. For all wave heights smaller than the limiting wave height, C_{fail} takes the value zero and for all values equal to, or larger than H_{lim} it becomes one. The limiting wave height is determined based on a deterministic decision criterion. This criterion contains two independent elements, namely the Blume-criterion and, secondly, the requirement that a maximum roll angle of 50 degrees is never exceeded during any simulation. The second requirement is introduced when the Blume-criterion fails for certain lever arm curves, especially for those with an very large range of positive levers (see also Section 5.3). The calculation rule for the limiting wave height H_{lim} then yields:

$$H_{lim} = \{H_i \in \{H_1, \cdots, H_n\} \mid E_R^*(H_{i+1}) \leqq 0 \ \vee \ \varphi_{max}(H_{i+1}) \geqq 50°\} \tag{6.6}$$

Where $\{H_1, \cdots, H_n\}$ represent the set of all wave heights investigated in the simulation and E_R^* denotes the value of the Blume-criterion. φ_{max} always represents the maximum roll angle detected in all time series calculated for a specific operational cell at a certain wave height. Then Equation 6.6 states that the limiting wave height is defined as the last wave height for which the Blume-criterion is just larger than zero **and** the maximum roll angle remains below 50 degrees.

The limiting wave height is determined individually for each operational cell from the numerical motion simulations. The polar diagram in Figure 6.4 shows an example for a complete set of limiting wave heights, used to determine the ISEI for one specific loading condition. Each polar diagram represents one significant wave period, for which a set of operational cells is evaluated each. The encounter angles are plotted in the angular direction, whilst the different speeds are shown in radial direction. All limiting wave heights together form surfaces which are represented by the colour-code in the diagrams. All wave heights below this surface are considered to be sufficiently safe, while all wave heights lying on, or above the limiting surface are considered to be dangerous for the ship in the related loading condition.

6.3 Seaway Probabilities

The discrete probability for the occurrence of a specific seastate $\delta P_{sea}(H_{1/3}^{(j)}, T_1^{(i)})$, directly depends on the two parameters significant wave height $H_{1/3}$ and characteristic period T_1, which are the integrated parameters characterising a seaway. These data can be obtained from long term measurements and observations, traditionally carried out with buoys, but nowadays also by satellite and wave-radar measurements. The results are commonly presented in form of scatter tables. These scatter tables deliver a two-dimensional, discrete probability distribution in dependency of the two parameters $H_{1/3}$ and T_1 as shown by example of the North Atlantic Ocean in Table 6.1. In this table, the given data represent the relative number of occurrences multiplied by 10^{-6}.

The data used for the Insufficient Stability Event Index are based on the values published in the *Global Seaway Statistics*, Söding [70]. This publication contains scatter tables for 126 locations, which form a regular grid distributed over the whole globe. The scatter tables given in this publication are based on raw data from two sources. One source is the commonly used scatter table as published by the *International Ship and Offshore Structures Congress* (ISSC [33]). These data cover only the North Atlantic Ocean. The second source used is the *Atlas of the oceans*, published by Young and Holland [84]. This source bases on satellite measurements and covers all sea areas in form of the 126 points also used in the Global Seaway Statistics, whereas the locations number 120, 125 and 126 approximately represent the area covered by the ISSC-scatter table. These data provide

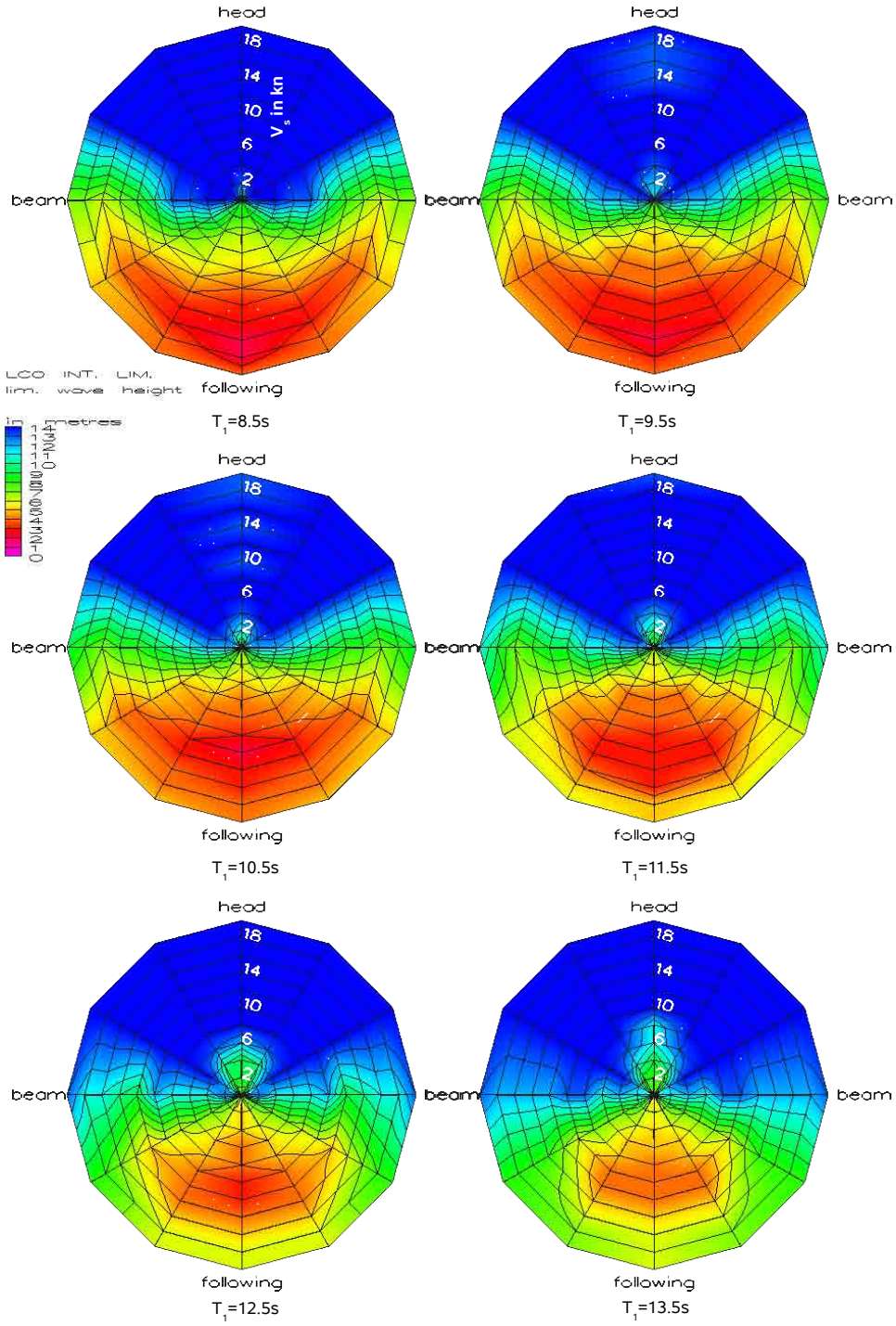

Figure 6.4: Limiting wave heights for one loading condition and the related operational cells. Calculated for a medium size container vessel ($L_{bp} = 276$m, abt. 4800 TEU)

Point 125; Latitude 54 degree, Longitude 314 degree

T_1 in s			$H_{1/3}$ in m																
from	to	FCUM	0.25	0.75	1.25	1.75	2.25	2.75	3.25	3.75	4.50	5.50	6.50	7.50	8.50	9.50	11.00	13.00	15.00
1.0	2.0	0.0	11	0	0	0	0	0	0	0	0	0	0	0	0	0	0	0	0
2.0	3.0	0.0	171	41	0	0	0	0	0	0	0	0	0	0	0	0	0	0	0
3.0	4.0	0.3	1259	1388	235	0	0	0	0	0	0	0	0	0	0	0	0	0	0
4.0	5.0	2.9	5303	8280	8956	4288	0	0	0	0	0	0	0	0	0	0	0	0	0
5.0	6.0	11.6	8058	14387	24301	25364	11936	2045	0	0	0	0	0	0	0	0	0	0	0
6.0	7.0	25.8	8276	14055	21646	27995	31247	26813	10639	1913	0	0	0	0	0	0	0	0	0
7.0	8.0	44.2	5360	9777	15335	21869	28438	31620	30234	25510	15886	76	0	0	0	0	0	0	0
8.0	9.0	59.4	2978	5557	8793	12343	16134	20005	23104	22880	30452	8811	599	0	0	0	0	0	0
9.0	10.0	72.6	1549	3047	4966	7079	9371	11755	14020	15448	30458	22686	10015	1566	0	0	0	0	0
10.0	11.0	82.8	976	1873	3014	4301	5691	6982	8096	9011	19484	18307	13922	7997	2249	173	0	0	0
11.0	12.0	89.7	592	1099	1701	2372	3104	3762	4321	4817	10690	11182	10893	8366	4222	1661	443	0	0
12.0	13.0	94.0	319	579	875	1194	1535	1859	2165	2439	5519	6093	6314	5760	4164	2422	1533	88	0
13.0	14.0	96.6	166	296	445	599	756	907	1055	1192	2725	3093	3373	3438	3132	2283	1897	346	23
14.0	15.0	98.1	85	154	231	309	383	451	515	574	1308	1501	1683	1831	1831	1559	1761	551	100
15.0	16.0	98.9	46	83	122	161	198	229	258	285	644	736	825	914	944	888	1325	610	165
16.0	17.0	99.4	28	46	65	84	103	120	134	148	333	374	407	446	473	471	800	480	198
17.0	18.0	99.6	17	26	34	43	53	62	70	77	172	189	201	218	236	243	442	323	194
18.0	19.0	99.8	9	14	18	22	27	31	35	38	85	94	100	109	118	124	246	213	157
19.0	20.0	99.9	5	8	10	12	14	16	18	20	43	48	52	57	62	66	140	138	114
20.0	21.0	100.0	3	5	6	7	8	9	10	11	24	26	29	32	35	37	83	88	79
		FCUM	3.5	9.6	18.7	29.5	40.4	51.0	60.5	68.9	80.7	88.0	92.9	95.9	97.7	98.7	99.6	99.9	99.9

Table 6.1: Scatter table containing the probabilities for specific seastates according to Söding [70]

information on the wave heights, but information on the related periods is missing. Söding [70] now combines both sources and develops a procedure, which enables the mapping of the information on the relationship between wave height and period given by ISSC [33] to the the wave heights obtained from Young and Holland [84]. The results are scatter tables as shown in Table 6.1.

In its standard application the Insufficient Stability Event Index aims to be a minimum stability criterion for ships in unrestricted, worldwide operation. Therefore it is reasonable to use the area providing the worst and hardest environmental conditions for the evaluation of ship safety. Consequently, a North Atlantic Location, namely point No. 125, is used for the evaluation. This is also in line with the IMO recommendations, given within the framework of future Goal Based Standards. At this, the functional requirements in Tier II determine the North Atlantic as reference area to be used for the safety assessment (see Hoppe [27]). Figure 6.5 shows a graphical representation of the probability distribution in location No. 125 according to the Global Seaway Statistics.

Although formally the hardest environment, for some ships the scatter table of the North Atlantic might not be suitable to judge upon their safety. Given a small ferry of about 90 metres in length, exclusively operating in the North Sea, or the Baltic Sea. Such a vessel often suffers in particular from short waves, which, additionally, may become very steep. Such waves are nothing unusual in the sea areas mentioned above. However, the

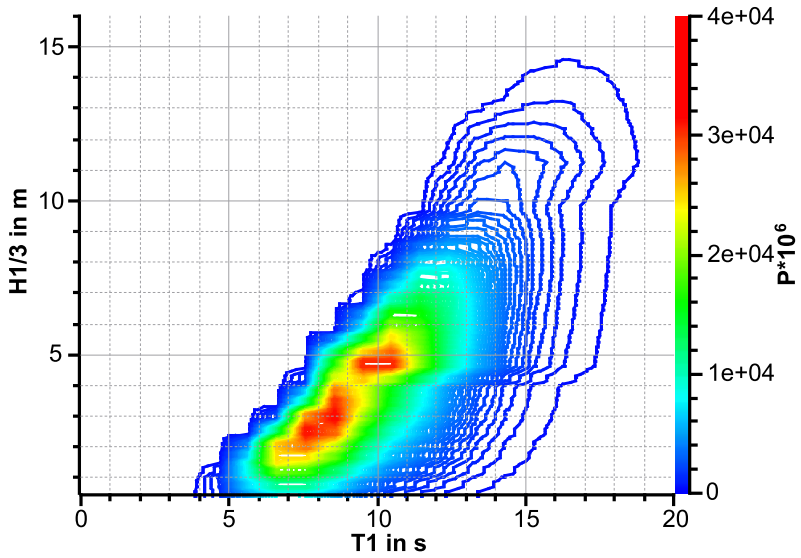

Figure 6.5: Probability of occurrence of waves in the North Atlantic Ocean according to Söding [70]

scatter table of area 125 shows that such short waves occur in the North Atlantic only at moderate wave heights up to 4.5 metres. As higher waves do not exist, they also do not deliver any contribution to the ISEI-value. Consequently the ship might be considered too safe. In such cases it is recommended to use appropriate statistics which cover the main area of operation.

6.4 Speed Probability Distribution

For the probability-distribution of the ship speed, no official statistics are available. Therefore, we have to make some assumptions at this point. First of all our criterion does not consider any time that the ship lays in the harbour, or any times of estuary trading with low speed. The actual speed travelled during a voyage in the open sea is influenced by a large number of parameters, partly due to physical constraints, but mainly due to the requirements made up by shippers and customers. Today, most ships are travelling in regular trades with fixed schedules which have to be maintained on a just-in-time basis. In order to attain a high reliability of these services the ship managers or charterers try to minimise delays by active guidance to the ships, provided by shore-based dispatchers. This includes voyage plans as well as weather routing. Currently, a trend towards lower ship speeds can be noticed, which is mainly influenced by the extremely high fuel prices.

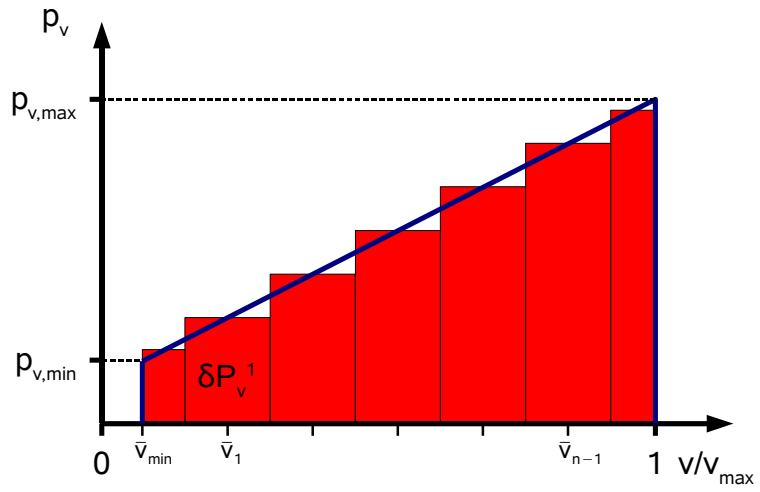

Figure 6.6: Conditional Probability density function (PDF) for the ship speed and discrete probabilities of occurrence for the ship speeds evaluated.

Nevertheless, ships are expected to operate close to their design speed in the majority of time and under normal operating conditions. Consequently, we assume that low speeds are less probable than higher speeds while being on the open sea.

Beside the operational aspects, physical constraints play a role with respect to the possible minimum and the maximum speeds in the given environmental conditions. A certain minimum speed always must be present in order to maintain the manoeuvrability of the ship. It is very improbable that the crew would actively choose speeds below this threshold value, but in case of a loss of propulsion, for example due to blackout, speeds down to zero are physically possible. However, in such cases, course keeping is no longer possible and in consequence most ships would yaw towards a beam sea position. Such an event is considered to have a low probability of occurrence. The present simulation method used to determine the ship responses treats the yaw motion by means of linear transfer functions. Thus, it does not account for broaching in case of very low speeds and in consequence the Insufficient Stability Event Index does not either. Taking all this into account, we assume a minimum speed of 2.0 knots for our probability assessment, assuming that speeds below this value are not possible under the operating conditions taken into consideration by the ISEI.

The maximum speed depends on the balance between the actual ship resistance on the one hand and the available propulsion-power on the other hand. At this, the ship resistance consists of the still water part and the added resistance components due to the influence of the waves and the wind. The calculation of the maximum speed is described in Section 6.4.1.

Keeping in mind all aspects discussed above, we choose a linearly increasing function to model the probability distribution of the ship speeds as illustrated in Figure 6.6:

$$p_v(\bar{v}) = a \cdot \bar{v} + b \tag{6.7}$$

Here, the speed v is brought into a dimensionless form by dividing by v_{max}, whereas a and b are the two parameters of the function. The function starts at $\bar{v}_{min} = v_{min}/v_{max}$ with a value of $0.2\ p_{v,max}$ and ends at 1 with a value of $p_{v,min}$. Depending on the relationship between the maximum and minimum speed, the two parameters a and b can be determined for each individual operating condition:

$$a = \frac{1}{\left(\frac{3}{4}\bar{v}_{min}^2 - \frac{3}{2}\bar{v}_{min} + \frac{3}{4}\right)} \tag{6.8}$$

$$b = \frac{5}{4}a \cdot \left(\frac{1}{5} - \bar{v}_{min}\right) \tag{6.9}$$

Once the function is known, the discrete probabilities for the individual speeds can be calculated by integration over the desired interval:

$$\delta P_v^i = \int_{\bar{v}_i - \delta\bar{v}/2}^{\bar{v}_i + \delta\bar{v}/2} a \cdot \bar{v} + b \; d\bar{v} = \left[\frac{a}{2}\bar{v}^2 + b\bar{v}\right]_{\bar{v}_i - \delta\bar{v}/2}^{\bar{v}_i + \delta\bar{v}/2} \tag{6.10}$$

Based on this equation all discrete speed probabilities can be calculated in all operating conditions, provided that the maximum possible speed is known.

6.4.1 Maximum Speed

The maximum speed achieved in a certain operating condition is the result of the balance between the overall resistance and the propulsive power provided by the ship's machinery. Here, three components are considered on the resistance side. The first component is the still water resistance of the vessel. This component is taken from the existing resistance curve at design draft. The two other components, the added resistance due to wind and waves is approximated by procedures described in Section 6.4.2.

On the other side, the provided propulsion-power depends on the maximum power of the machinery and on the characteristics of the propulsion train, including the propeller itself. The necessary information on the propeller is taken from the open water diagram, which

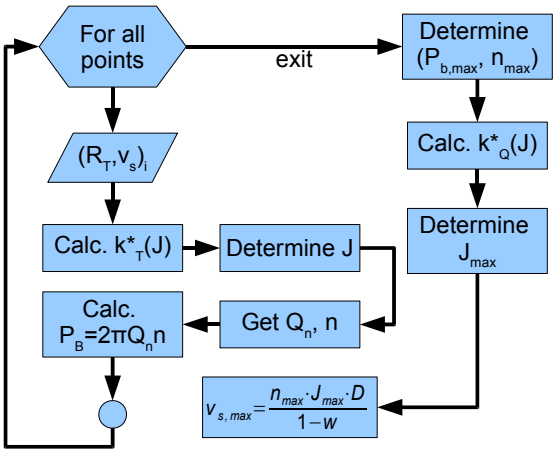

Figure 6.7: Calculation procedure for the determination of the maximum possible speed in a seaway.

contains the propeller efficiency and the dimensionless coefficients for thrust (k_T) and torque (k_Q) over the advance coefficient J, which is defined by:

$$J = \frac{v_s(1-w)}{nD} \tag{6.11}$$

Where n denotes the number of revolutions and D is the propeller diameter. Additionally, some information is necessary to account for the influence of the ship-propeller interaction when the propeller is operated in real conditions behind the ship. This is provided by the propulsive coefficients, namely the wake fraction w, the thrust deduction t and the relative rotative efficiency η_r. The characteristis of the engines is obtained from the engine map, stating the possible operating conditions and the respective power-output in dependency of the number of revolutions n. The engine map is limited by the maximum and minimum permissible number of revolutions and the torque limit together, with limitations regarding engine-surge, as upper boundaries of the power output (see Figure 6.9).

If all this information is available, the calculation procedure as sketched in Figure 6.7 can be applied in order to determine the maximum possible speed in a certain operating condition. The first step is to transform the overall resistance curve, consisting of all components mentioned above (Figure 6.8, left hand side), from its initial form, dependent on the speed v_s, into a power-consumption curve depending on the number of revolutions. The transformation is carried out for a discrete number of speeds. For this purpose, we determine the operating point of the propeller from the required thrust T given by:

$$T = \frac{R_T}{(1-t)} \tag{6.12}$$

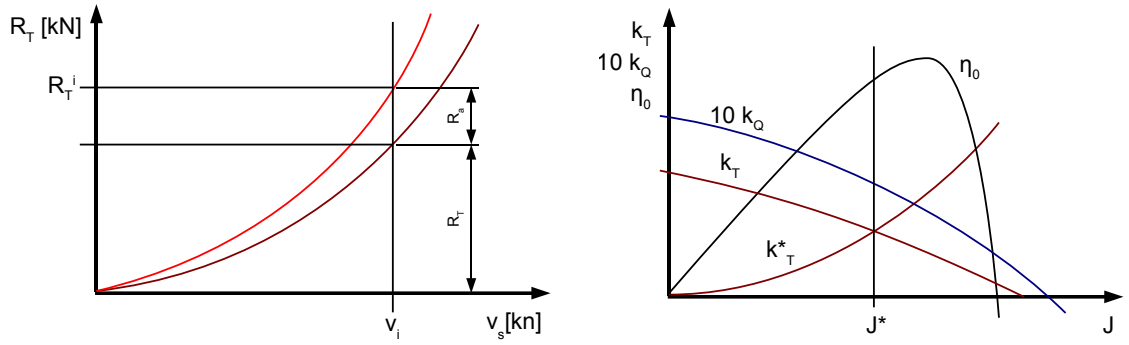

Figure 6.8: Left: Resistance Curves, Right: Open water diagram with propeller operating point

The thrust is used to calculate the propeller-demand curve k_T^* in dependency of the advance coefficient J.

$$k_T^*(J) = \frac{T}{\left[\rho \cdot D^2 \cdot (1-w)^2 \cdot v_s^2\right]} \cdot J^2 \tag{6.13}$$

In this equation, ρ denotes the density of sea water. The operating point of the propeller for the desired forward speed is given by the intersection of the propeller-demand curve k_T^* and the dimensionless curve of the thrust delivered by the propeller k_T in dependency of the advance coefficient as shown in Figure 6.8 on the righthand side. The advance coefficient of the operating point is denoted as J^*. From the coefficient $k_Q(J^*)$ we obtain the actual torque Q and from J^* we extract the corresponding number of revolutions n. Then, the delivered power of the propeller yields:

$$P_D = 2\pi Q n \tag{6.14}$$

This equals the power delivered by the engine, here denoted as brake power P_B, as far as we neglect any losses in the shaft line. In case a gearbox is placed between engine and propeller the related losses have to be taken into consideration and the number of revolutions has to be converted according to the transmission ratio. The resulting power-consumption curve is plotted into the engine map as shown in Figure 6.8.

In the next step we determine the upper intersection of the power-consumption curve with the boundaries of the possible and permissible operating conditions of the engine. This point represents the operating condition with the highest possible power output P_{max}, connected to a number of revolutions n_{max}. As shown in Figure 6.7, we then apply the reverse procedure to get the corresponding propulsion point. For this purpose, we

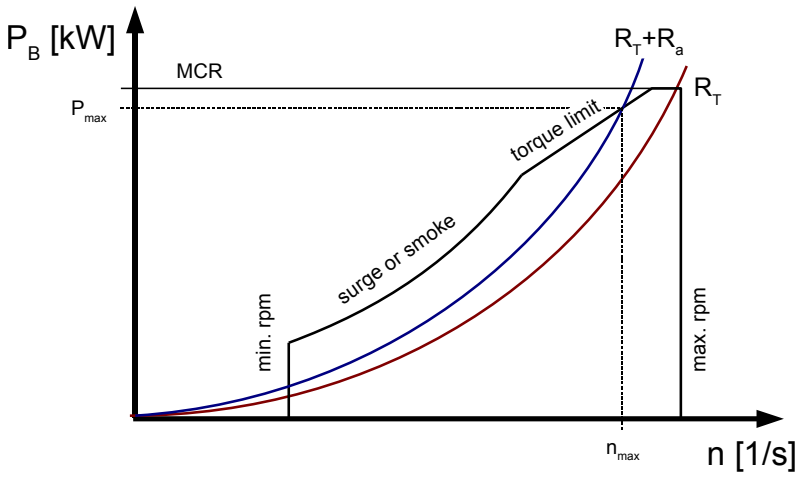

Figure 6.9: Engine map with power-consumption curve of the propeller.

calculate the dimensionless torque coefficient k_Q^* from Q_{max} and n_{max}:

$$k_Q^* = \frac{Q_{max}}{\rho n_{max}^2 D^4} \tag{6.15}$$

The intersection between the k_Q-curve of the propeller and the torque-coefficient k_Q^* marks the propulsion point which is met at the maximum attainable speed. From the associated advance coefficient J_{max}, we finally obtain the approach velocity v_a at the propeller, which can be converted into the maximum ship speed $v_{s,max}$ by dividing it by the wake fraction $(1 - w)$.

6.4.2 Added Resistance

The most important input, required for the calculation of the maximum speed of a vessel in a specific condition is the overall resistance force. In the present section, we present the procedures used to estimate the added resistance induced by the environmental influences, namely wind and waves:

$$R_A = R_{wind} + R_{waves}$$

Wind

The added resistance due to wind results primarily from the component of the wind acting in the direction of the longitudinal ship axis. The transverse component of the

wind in reality causes an additional resistance component by generating a yaw moment, which must be compensated by the rudder and a corresponding drift angle of the hull. This component is neglected in the present procedure. Taking the aforementioned into account, the wind resistance R_{wind} can be calculated by:

$$R_{wind} = \frac{\rho}{2} c_w v_{aw}^2 A_H \tag{6.16}$$

At this, A_H is the cross sectional area of the ship above the waterline, associated with a drag coefficient c_w, which is set to 0.85 by default. Additionally, ρ expresses the seawater density and v_{aw} denotes the resulting relative speed between the wind and the ship, which can be calculated as follows:

$$v_{aw} = v_w \cdot \cos\mu - v_s \tag{6.17}$$

Where v_w is the wind speed and v_s is the ship's forward speed. μ denotes the encounter angle between the wind and the ship's course. For the assessment of the wind resistance we assume that the wind approaches the ship always in the mean direction of the wave encounter.

The ISEI-concept does not account for wind directly. Therefore, the wind speed is not explicitely given as input parameter. To estimate the wind speed in a certain operating condition, we use the actual seastate given by $H_{1/3}$ and T_1. Assuming that the seaway exclusively consists of wind sea, it is possible to establish a connnection between the wave parameters and the related wind speed, based on the measurements carried out during the JONSWAP-project (see Hasselmann et al. [25]). According to Blendermann [8], the following relationship between the significant wave height $H_{1/3}$, the modal period of the related JONSWAP-spectrum T_m and the mean wind speed v_w exists:

$$\frac{gH_{1/3}}{v_w} = 9.4 \cdot 10^{-3} \cdot \left(\frac{gT_m}{v_w}\right)^{5/3} \tag{6.18}$$

We further take into account that the relationship between the characteristic wave length λ_1 and the modal period approximately reads:

$$T_m = 1.295\sqrt{\frac{2\pi\lambda_1}{g}} \tag{6.19}$$

Using Equation 6.19 in Equation 6.18 and applying some basic transformations, the mean wind speed yields:

$$v_w = \frac{H_{1/3}^3}{3.025 \cdot 10^{-6} \cdot g^2 \cdot \left(\frac{2\pi\lambda_1}{g}\right)^{5/2}} \tag{6.20}$$

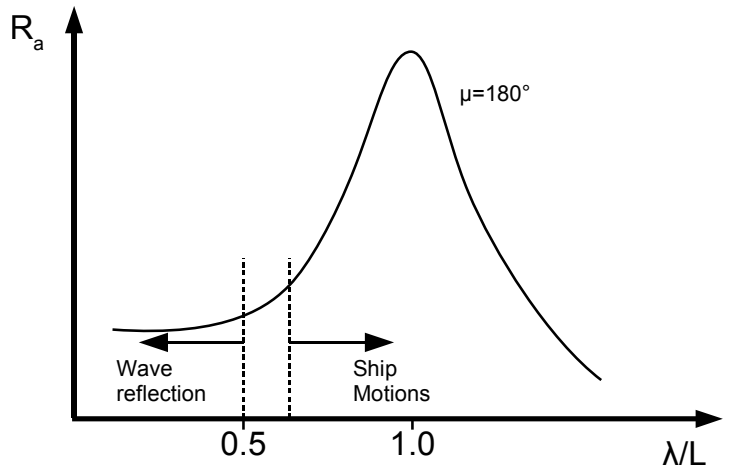

Figure 6.10: Added resistance due to waves in head seas. The sketch also shows the areas where the added resistance is dominated by forces caused by the ship motions and the areas where the main source is wave reflections at the bow.

Waves

The waves approaching the ship cause oscillatory forces on the hull surface. However, the averaged forces do not disappear completely, but there are remaining longitudinal forces which result in additional ship resistance. In accordance with the findings of Faltinsen et al. [20], we distinguish between short and long waves approaching the ship. Short waves in this context means waves with a length shorter than 0.5 times the ship length, and long waves are meant to be those with a wave length above 0.6 to 0.7 times the ship length. Figure 6.10 shows a principal sketch of the added resistance over the relative wave length λ/L_{bp}, indicating also the borders of short and long waves according to our definition. For the long wave case we use an approach developed by Boese [13], which delivers the added resistance as result of a second order longitudinal force. The short waves are considered by an asymptotic approach addressing bow wave reflections as presented in Faltinsen et al. [20]. Both approaches are based on potential flows and thus, neglect any viscous effects.

Long Waves All forces which depend linearly on the wave amplitude oscillate around the mean value of zero, which means that they cause no added resistance as such. This does not hold for higher order forces. However, Boese [13] restricts his method to second order terms, as they contribute the dominant part of the added resistance force. Moreover, this permits the extension of his approach to irregular waves. For a regular wave the mean

longitudinal force according to *Boese's* approach, extended by the contribution of the yaw motion (see Söding [65]), reads as follows:

$$\bar{F}_{\xi}^{L} = [\underbrace{\frac{m\omega_e^2}{2}\, Re(\hat{Y}_{\eta s}\hat{Y}_{\psi}^{*} - \hat{Y}_{\zeta s}\hat{Y}_{\vartheta}^{*})}_{A} + \frac{1}{2}\underbrace{\int_{L} \rho g \hat{Y}_{zR}\hat{Y}_{zR}^{*}\, \frac{dy}{dx} dx}_{B}] \cdot |\hat{\zeta}_w|^2 \tag{6.21}$$

Here, ω_e represents the encounter frequency of the waves and $\hat{\zeta}_w$ is the wave amplitude. $\hat{Y}_{\eta s}$ and $\hat{Y}_{\zeta s}$ are transfer functions, which deliver the displacement of the ship's centre of gravity in longitudinal and transverse direction, respectively. $\hat{Y}_{\psi}^{*}$ and $\hat{Y}_{\vartheta}^{*}$ are the complex conjugates of the transfer function for the yaw and the pitch angle. Finally, the third transfer function, denoted as $\hat{Y}_{zR}$ delivers the relative movement between the wave and the ship in dependency of the longitudinal location x.

Equation 6.21 consists of two components. The first part, marked as A, delivers the mean second order force due to the movement of the ship's centre of gravity, considering only the mean submerged hull. The second part B accounts for the parts of the hull surface, which emerge and submerge periodically when the wave passes along the ship. The mean longitudinal force $\bar{F}_{\xi}$ in irregular waves is obtained from simple superposition of the discrete wave components.

Short Waves In short waves ($\lambda < 0.5L$), the ship motions get small and thus, are no longer the main source of the added resistance. Faltinsen et al. [20] develop a method, which is based on the assumption that the dominating longitudinal force in short waves is induced by the reflection of the waves at the ship hull. At this, he neglects any wave-induced ship motions, why the approach is only valid in the asymptotic low wave length case. The longitudinal force of a regular wave resulting from this approach reads:

$$\bar{F}_{\xi}^{S} = \frac{1}{2}\rho g \hat{\zeta}_w^2 \left(1 + \frac{2\omega_0 v_s}{g}\right) \cdot \int_{L_1} \sin^2(\alpha - \mu + \pi) \cdot \sin(\alpha)\, dl \tag{6.22}$$

Here, $\hat{\zeta}_w$ represents the wave amplitude, ω_0 is the circular frequency of the wave and v_s denotes the ship speed. In the second part of the equation the integral runs over the whole non-shadow part L_1 of the waterline, which means the part directly hit by the approaching waves. Further, α is the waterline angle relative to the longitudinal axis of the ship and μ denotes the encounter angle between the ship and the wave encounter direction. In case of irregular waves, we again apply the superposition principle, taking into account all wave components.

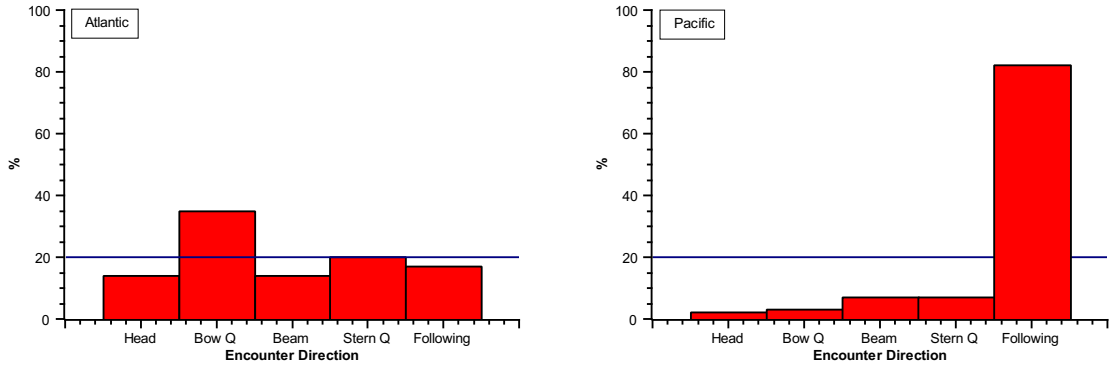

Figure 6.11: Course probabilities on the Atlantic-trade (left) and the Pacific-trade (right), based on full scale observations by Det Norske Veritas. By courtesy of DNV.

Then, the overall added resistance caused by an irregular seaway is calculated by:

$$R_{waves} = \begin{cases} \max\left(\sum_i \bar{F}_\xi^{L(i)},\ \sum_i \bar{F}_\xi^{S(i)}\right) & \text{if } \frac{\lambda}{L} \leqq 0.6 \\ \sum_i \bar{F}_\xi^{L(i)} & \text{else} \end{cases} \tag{6.23}$$

6.5 Course Probability Distribution

The course probability $\delta P_\mu(\mu^{(k)})$ references the probability of the relative encounter angle μ between the ship and the waves. Statistics on the relative encounter direction between ship and waves are sparsely available. The only data available for the present work are obtained from an measurement campaign carried out by the Norwegian classification society *Det Norske Veritas*. This investigation was made for two major trading routes, namely the Atlantic route connecting Europe and North America, as well as the Pacific route between North America and East Asia. The results are shown in Figure 6.11, where the wave encounter was coarsely categorised in following, stern quartering, beam, bow quartering and head seas.

The Atlantic route shows almost equally distributed wave encounter directions, with a slight dominance of the bow quartering directions. Thus, head, following and quartering encounter directions dominate here in comparison to beam sea situations, which in principle coincides with the expectations based on the main direction of wave propagation in eastbound direction. A quite different picture is found on the Pacific route. Here, the ships are travelling in stern quartering seas in almost 83% of the time. This observation is surprising, because normally one would expect a similar distribution as on the Atlantic.

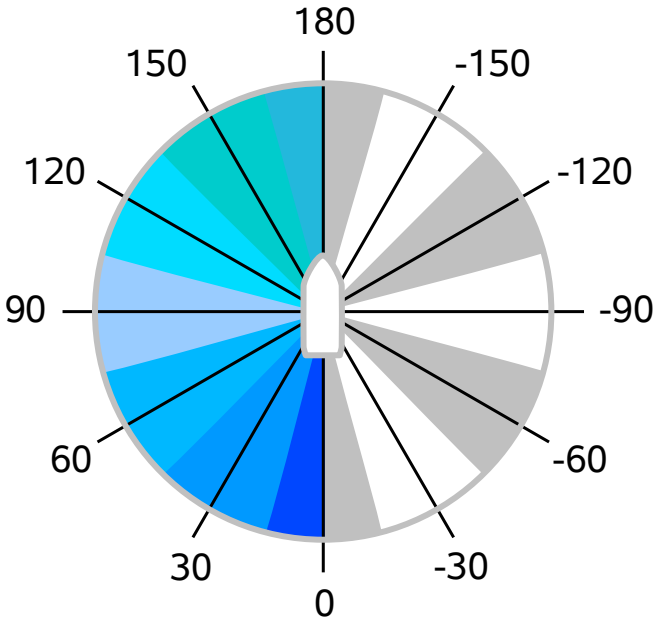

Figure 6.12: Discrete Sectors for Encounter Probabilities

However, this behaviour seems to be related to active weather routing, resulting in different routes chosen for the eastbound and the westbound trade, respectively. Further data, for example for the trade between Europe and East Asia are not available.

The ISEI criterion by default uses the seaway statisics of the North Atlantic Ocean. To maintain consistency also the course probabilities registered for this region are used by default. In case of significantly different operating profiles, other course probability distributions can be applied at any time. The probability distribution shows only small deviations between the different encounter sectors, why it can be assumed that the encounter angles are equally distributed in average. From this we get a constant probability density function:

$$p_\mu(\mu) = \frac{1}{2\pi}$$

According to Equation 6.5, the Insufficient Stability Event Index is evaluated for discrete operational cells. The calculation procedure considers seven encounter angles in the range between 0 and 180 degrees with an increment of 30 degrees. The resulting partitions are shown in Figure 6.12. From the sketch it becomes clear that the parts associated with 0 and 180 degrees have only half of the probability of occurrence than the other sectors. Taking this into account, the probability of occurrence amounts to:

$$\delta P_\mu(\mu) = \begin{cases} 1/12 & \text{if } \mu = 0° \vee \mu = 180° \\ 1/6 & \text{in all other cases} \end{cases} \tag{6.24}$$

As the ship reactions are considered to be fully symmetric, the encounter probability for the opposite values is already included and do not need to be considered separately. In order to take into account the subdivision of the ISEI into a following, beam and head seas index the probabilities for the sectors around 60 and 120 degrees, respectively, are further subdivided into two parts. One half is associated with the beam seas index and the other half with the following, or head seas index.

6.6 Influence of Roll Damping on the Capsizing Index

The Insufficient Stability Event Index aims to set minimum stability requirements. In connection with large amplitude roll motions, roll damping is often considered to be of equivalent importance as the stability of the ship (see for example Shin et al. [63]). This implies that it could be possible to grant some allowance to the ship stability, if the ship provides above-average roll damping. The following analysis (see also [42]) aims to show which influence roll damping has on the ISEI and whether the increase of roll damping beyond standard values has a comparable effect on ship safety like stability.

The reference ship used for the investigations is taken from a series of fast and very slender container feeders built in the years 1998 to 2000, which suffer from poor seakeeping characteristics due to insufficient roll damping.

The small roll damping is mainly caused by the very large bilge radius. Moreover, the ships were originally delivered without bilge keels, which were fitted later due to significant roll motions discovered during operation. The main particulars of the reference ship can be found in Table 6.2, Figure 6.13 shows the ship's frame plan.

L_{bp}	198,70	m
B	26,66	m
T	8,70	m

Table 6.2: Main particulars of the reference ship

Different sizes of bilge keels are added to the ship during the simulations, in order to investigate the relationship between roll damping and the maximum roll angles in a specific seaway.

The simulations are carried out for significant periods between $T_1 = 8.5$ and 13.5 seconds. For each wave length a full ISEI-calculation is performed, whereas speeds between 0 and 22 knots are investigated. The bilge keel height was varied between 0 metres and 0.60

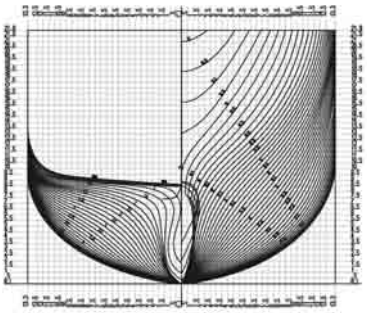

Figure 6.13: Frame plan of the reference ship

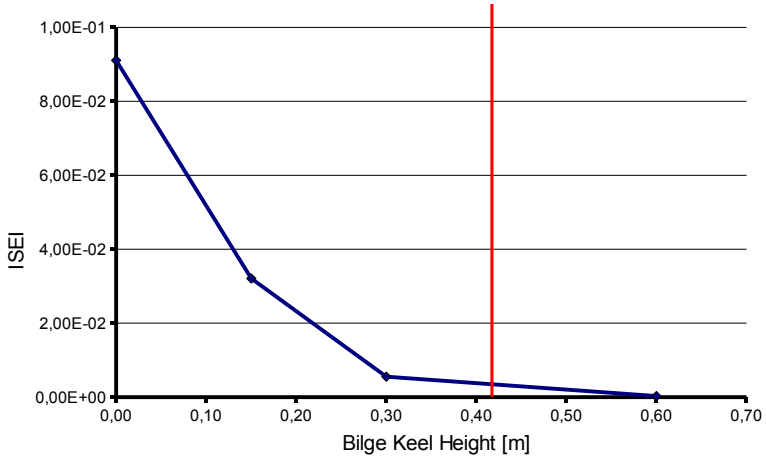

Figure 6.14: Capsizing Probability in dependency of bilge keel height

metres, at a constant length of 80 metres. The results of the calculations are shown in Figure 6.14.

The correlation between the roll damping, here represented by the bilge keel height and the Insufficient Stability Event Index, approximately shows a logarithmic characteristic. Consequently, the capsizing probability decreases rapidly for increasing roll damping on a low level. Opposite to that, bilge keels larger than commonly used sizes between 0.3 and 0.4 metres, do not have such a significant effect on the capsizing index. For example, the capsizing index decreases by about 2.7E-2 between the 0.15 metres and 0.30 metres bilge keel height. The decrease from 0.30 metres height to 0.60 metres height only adds up to 0.48E-2, which is about 17% of the increase in the low level region.

Bearing in mind that ships usually provide an average level of roll damping, it seems to be doubtful if a further increase in roll damping is a such powerful measure for improving the ship safety that it can compensate a reasonable stability allowance. For example an

increase of the bilge keel height from 0.30 metres to 0.60 metres, which doubles the area of the bilge keel, would allow to reduce the minimum GM only by about 0.015 metres according to our calculations. At this, a change of ship stability seems to be the more effective solution to decrease the Insufficient Stability Event Index.

7 Validation of the Concept

The validation aims to show that the Insufficient Stability Event Index is a reliable, quantitative measure for ship safety in respect to large amplitude roll motions and capsizing. To achieve this goal, the new criterion has to be tested whether it is able to identify all unsafe situations as well as safe situations by delivering clearly different index values. To assure a uniform safety level for all ships, the criterion shall additionally deliver similar index values for ships with similar main properties in similar situations. Finally, it has to be assured that the criterion is sufficiently conservative to assure that a tolerable safety level is guaranteed. On the other hand the criterion must not be too conservative as it then reduces the usability of safe ships unnecessarily.

For this purpose, the Insufficient Stability Event Index is benchmarked against other criteria in definitely unsafe situations and estimated safe situations. First, the main aim is to identify whether the new criterion reacts sufficiently sensitive on changes in the system. Secondly, this study is used to establish links between certain ISEI-values and the behaviour of ships in order to isolate possible threshold values. The most realistic benchmark-scenarios are real accidents as they always represent a clearly unsafe situation. A number of accidents which occurred in the years from 1950 up to the very recent past are investigated. At this, the focus is laid on ships which did capsize in heavy weather without any further damage by collision or grounding. A short introduction to the methodology behind these investigations is given in Section 7.1. Section 7.2 provides a sample accident investigation, dealing with the capsizing of the car carrier *MV Cougar Ace* in the year 2006. The results of all accidents investigated, according to the same scheme, is discussed in Section 7.3.

7.1 Analysis of Real Capsizing Accidents

Figure 7.1 shows a flowchart of the procedure used to validate the Insufficient Stability Event Index with capsizing accidents and to benchmark it with other capsizing criteria. The first step is to get as much information on the accident as possible in order to reconstruct the accident situation as close as possible to the reality. Especially the environmental conditions and the ship's loadcase and stability are of interest here. Our

main sources of information are usually the reports of the maritime safety investigation authorities, which are obtained from the official state archives.

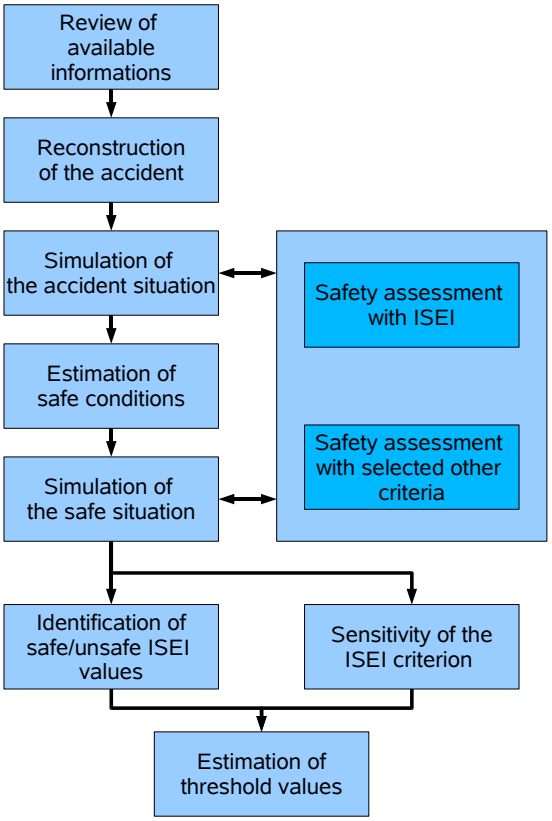

Figure 7.1: Investigation procedure for capsizing accidents used to validate the ISEI criterion.

The second step is to set up the numerical model and to perform the required simulations. The results are evaluated with selected capsizing criteria. The set of criteria includes those presented in Section 5 and additionally a set of empirical criteria, which are a side-result of the Lake-Ploen model tests in the 1960's performed by a German research group (see Kastner [37]). These criteria were never published officially, as they were only used to estimate safe conditions for the particular model used for the tests. However, these criteria are documented in related correspondence of Germanischer Lloyd [22]. According to this correspondence, the requirements are formulated as follows:

- The range of positive righting lever on the crest position should amount at least 15 degree.

- There should be a maximum righting lever (full scale) of 0.05 m or more in that range.

It must be taken into account that the actual ship sizes of the full scale reference vessels were in the range of 60 to 90 meters, therefore, one can not generalise these numbers for larger vessels. However, with respect to the size and type of the vessels at that time, the values might be taken as reference values, even though they seem to be very small. Additionally to this set of criteria, each accident condition is evaluated with the Insufficient Stability Event Index. A first assessment of ship safety follows, which analysis whether the set of criteria considers the ship as unsafe, or not. Using primarily the Kastner-Roden criterion, the attempt is made in the next step to estimate a safe operating condition for the ship, where the free parameter is the ship stability. Once a loadcase expected to be safe is found, the simulation is carried out again for the new situation. Again, all criteria are used to evaluate this second operating condition. This procedure is repeated until all applicable criteria consider the ship as safe.

This procedure delivers two values for the Insufficient Stability Event Index. One related to a clearly unsafe situation, represented by the accident condition and a second one, which represents the safe domain. Taking the values from all ships, a judgement on the sensitivity of the stability index can be made. Moreover, it becomes possible to determine a limiting value, splitting the overall domain into safe and unsafe sections.

7.2 Example: The Capsizing of MV COUGAR ACE

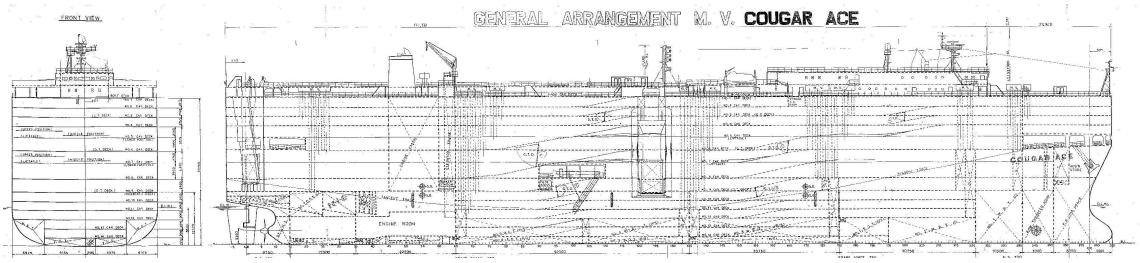

Figure 7.2: General Arrangement Plan of M.V. Cougar Ace

On July 24th, 2006 the Singapore flagged car carrier *M.V. Cougar Ace* was bound for Vancouver, Canada. The vessel was built in 1993 by Kanasashi Co., Ltd., Toyohashi, Japan. On late July 24th the ship suddenly heeled to about 60-80 degrees to port side and remained in this inclined position (see figure 7.3). The first message on the accident, issued by a crew member, was received by the United States Coast Guard at 11:09 p.m., see press release [78]. At that time, the ship's position was 230 miles south of the town Atka on the Aleutian Islands, approximately 48 degrees 14 minutes north and 174 degrees 26 minutes west according to Mitsui O.S.K. Lines Ltd. Public Relations Office [48]. It was further reported by various sources, for example newspaper articles in the Seattle Post [62] and a press release by Associated Press (AP) [5] that the crew was performing ballast water operations at the time of the accident. Furthermore, there were reports (see [62]) that the ship might have been hit by a large wave during the ballast water exchange. The ship remained afloat, as non-weather tight openings were not submerged, and was subsequently towed to Unalaska Island, where the ship arrived on 25th of August 2006 (see track in Figure 7.3, left hand side). The ship was up-righted again and transferred to Portland, Oregon for repair. The main particulars of the vessel are:

Length b. Perpendiculars :	190.00	m
Breadth, moulded :	32.26	m
Draft, (mld.) :	9.30	m
Depth :	33.46	m

The light ship weight of the vessel, obtained from the capacity plan published by US Coast Guard [81] amounts to 13768 tons. Information on the centre of gravity is not available.

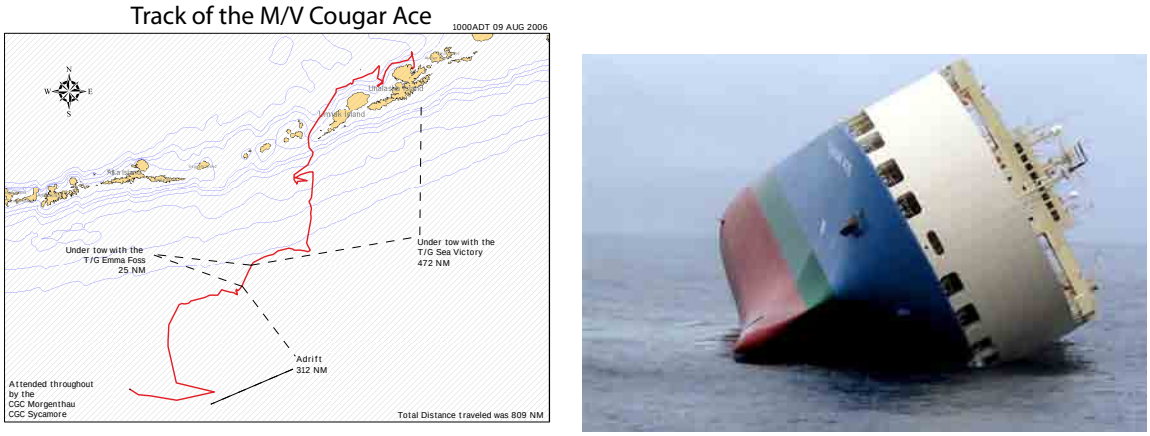

Figure 7.3: Left: Track of *M.V. Cougar Ace* after capsizing south of the Aleutian islands. Right: The vessel with a list of approximately 60 degrees after the accident (Map and Photo: US Coast Guard)

Type	Split	Weight [t]
Mazda 3	60 %	1.2
Mazda CX-7	30 %	1.8
Mazda RX-8, Mx-5	10 %	$\approx$ 1.5

Table 7.1: Mazda cars on board of *M.V. Cougar Ace*

On the voyage from Japan to Canada *M.V. Cougar Ace* was almost fully loaded with 4813 cars on board according to U.S. Coast Guard [80]. Details on the cargo split can be found in Table 7.1.

According to the US Coast Guard [78], the vessel carried 430 tons of Intermediate Fuel Oil (IFO380) and 112 tons of Marine Diesel Oil (MDO). More information on bunkers and stores has not been published so that some assumptions have to be made for the investigation, which, however, seems to be of minor importance in this context.

The information given on the environmental conditions by press releases and newspaper articles is rather vague. There are statements that the ship had been hit by a "large" wave during ballast water operations. The wave height and wave period are obtained from measurements with buoys by the US National Data Buoy Centre [50]. Additionally weather reports were obtained from the website of Oceanweather inc. [51] we can make the following statements on the sea state during the accident:

- The sea state was characterised by a pronounced swell-system, whereas wind sea was negliable.

- Waves were propagating mainly in north-easterly direction.
- The significant wave height can be estimated at $3 - 4$ metres.
- The wave spectra for the swell system obtained from the US National Data Buoy Centre [50] show peak periods between 9.1 and 10.8 seconds, equalling wave lengths from ca. 130 metres to ca. 180 metres.

7.2.1 Findings During the Accident Investigation

As the *M.V. Cougar Ace* is registered in Singapore, the accident has been investigated by the Maritime and Port Authority of Singapore. According to a statement submitted by the delegation of Singapore in IMO MSC 82 [32], the investigation of the accident has already been completed. However, no final investigation report has been published so far, so that some assumptions have to be considered for our investigations.

All known sources report that the crew were running ballast water operations at the time the ship started to list. According to the report that the delegation of Singapore submitted to the International Maritime Organisation (IMO) [32], these operations were carried out for the purpose of ballast water exchange which is required by the new IMO regulations on ballast water management. Based on these regulations, the crew had to carry out a complete ballast water exchange before entering Canadian waters.

According to the report mentioned above, the officer-in-charge sat up a plan for sequential exchange of ballast water. The report states that, "4 of its (n.b.: the vessel's) 9 ballast water tanks" had been empty at the time of the accident. Additionally, according to the report, ballast water has been pumped out for the adjustment of a steady list due to fuel oil consumption. In the vessel's capacity plan [36] eleven ballast water tanks are listed. This leads to the question which of the ballast water tanks are meant by the statement above.

No further information has been released on which of the ballast water tanks were empty at the time of the accident. However, the publications of the US Coast Guard (see US Coast Guard press release issued on August 2nd, 2006 [76] and the Situation Report No. 8, issued on August 16th, 2006 by the Alaska Department of Environmental Conservation [1]) on the incident give two hints on the ballasting condition, according to which the ballast water tanks number 4 and 5 on the starboard side must have been at least partly empty at the time of the accident.

The final floating condition of *M.V. Cougar Ace* is significantly influenced by the amount of ballast water on board, its distribution, cargo shift and water ingress. On these points the following information is available:

According to the US Coast Guard [80], only 41 cars were found to have shifted, whereas all other cars obviously had been properly lashed. Therefore, heeling moments due to cargo shift can be excluded to be relevant for the accident.

A second important factor is whether significant water ingress occurred and whether this happened before or after capsizing. An indication that at least no severe flooding took place is given by the fact that the vessel remained afloat in a stable position. The vessel was first investigated after the accident on July 30th by the salvage team. During this visit on board of *M.V. Cougar Ace* no water was found in the engine rooms according to the US Coast Guard [79]. Later reports contain information on water on car deck number 9, which is the main deck, accessible via three ramps. This information is contained in a US Coast Guard press release from August 2nd, 2006, in which plans are published on pumping the water on car deck number 9 to one of the ballast water tanks [76]. Two of the ramps are located amidships, one on starboard and one on port side. The third ramp is located at the stern on the starboard side. The port side ramp is fully submerged for a list of 60 degrees. The salvage team reports that the water entered the car deck "slowly seeping" [77] through this opening. It was further speculated, but never confirmed, that water from the port side ballast water tanks could have entered the number 9 car deck via air pipes. There is also no confirmed information available on the amount of water on the car deck, but according to various statements made by dock workers engaged in the off-loading of *M.V. Cougar Ace*, the damage to the cars on deck number 9 has been limited to the wheels. Finally, the US Coast Guard in its Public Affairs Release from September 1st reports that a "minor amount" of flooding was found in some of the vessels piping due to downflooding through vent piping.

7.2.2 Results of the Numerical Analysis of the Accident

Although no detailed information has been published on the loading condition, we can assume that the ship was travelling at the intact stability limit given by the IMO weather criterion. This is a typical operating condition for fully loaded car carriers that additionally have to take on ballast water in most cases, to meet the stability requirements. From the given weight information and from photos of the ship taken shortly after the accident, as well as from photos of previous voyages, we further estimate a mean draft of about 8.40 metres for the given loading condition.

In this floating condition the minimum metacentric height (GM_{min}) is limited to 2.05 metres by the weather criterion, equalling a maximum KG of 15.76 metres above baseline. Based on these findings the loadcase given in table 7.2 is generated.

Nevertheless, three scenarios are possible which all could have led to the intact stability failure:

Light Ship's Weight:	13767.999	t
long. centre of gravity of light ship:	87.100	m fr. AP
transv. centre of gravity of light ship:	0.000	m fr. CL
vertic. centre of gravity of light ship:	16.450	m fr. BL
Deadweight:	12879.455	t
long. centre of gravity of loadcase:	85.581	m fr. AP
transv. centre of gravity of loadcase:	-0.004	m fr. CL
vertic. centre of gravity of loadcase:	14.915	m fr. BL
Total Weight:	26647.453	t
result. long. centre of gravity:	86.366	m fr. AP
result. transv. centre of gravity:	-0.002	m fr. CL
result. vertic. centre of gravity:	15.708	m fr. BL
Equilibrium Floating Condition :		
Ships Weight :	26647.457	t
Longit. Centre of Gravity :	86.366	m.b.AP
Transv. Centre of Gravity :	-0.002	m.f.CL
Vertic. Centre of Gravity (Solid) :	15.708	m.a.BL
Free Surface Correction of V.C.G. :	0.050	m
Vertic. Centre of Gravity (Corrected) :	15.758	m.a.BL
Draft at A.P (moulded) :	8.458	m
Draft at LBP/2 (moulded) :	8.389	m
Draft at F.P (moulded) :	8.319	m
Trim (pos. fwd) :	-0.139	m
Heel (pos. stbd) :	0.061	Deg.
Volume (incl. Shell Plating) :	25997.516	m3
Longit. Centre of Buoyancy :	86.358	m.b.AP
Transv. Centre of Buoyancy :	-0.014	m.f.CL
Vertic. Centre of Buoyancy :	4.895	m.a.BL
Area of Waterline :	4564.322	m2
Longit. Centre of Waterline :	79.092	m.b.AP
Transv. Centre of Waterline :	-0.016	m.f.CL
Metacentric Height :	2.047	m

Table 7.2: Intact limit loadcase assumed for the time of the accident

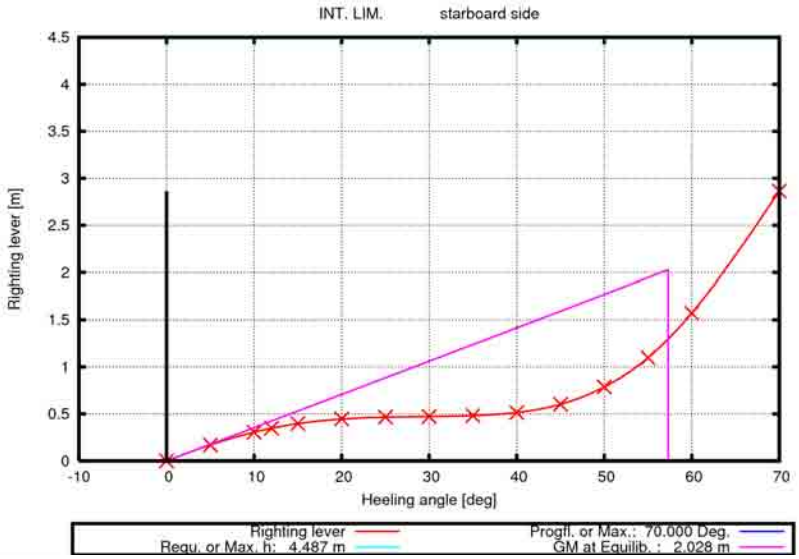

Figure 7.4: Lever arm curves for *M.V. Cougar Ace*. Lever arm curve for the intact stability limit according to the IMO weather criterion.

- **Pure loss of intact stability**
  In this scenario, ballast water exchange leads to a reduction of the total amount of ballast water in the lower double bottom tanks. This increases the vertical centre of gravity. Emptying two or more ballast water tanks, potentially leads to completely negative righting levers as the ship is travelling at the intact stability limit beforehand. Finally, this results in an equilibrium floating condition at about 60 degrees, where the ship is floating on its weathertight superstructures.

- **Capsizing due to heeling moments from asymmetric ballasting**
  In this scenario, the ship in principle has remaining positive stability, but asymmetric ballasting leads to heeling levers causing a large steady list. Normally, asymmetric ballasting is omitted by the crew members as far as possible. In this case, it might have occurred accidentally, for example due to malfunction of pumps or valves. Assuming that the ship had only very little stability left due to the ballast water exchange, even small heeling moments could lead to capsizing.

- **Reduced intact stability and wave induced roll moments**
  This scenario presumes that the ship has a small remaining stability without significant asymmetry in the ballast water distribution. If the stability is below certain limits, even small waves may lead to large roll amplitudes. In case the lever arm curve is of such type where two stable floating conditions exist, the ship might come to rest at a large heeling angle. This scenario is discussed in more detail below.

$KG_{initial}$ = 15.76 m All values are given for one tank			
Tank No.	Filling [%]	KG_{corr} [m]	δKG
3	50	15.92	0.16
3	0	16.08	0.32
4	50	15.88	0.12
4	0	16.01	0.25
5	50	15.96	0.20
5	0	16.13	0.37
APT	50	15.88	0.12
APT	0	15.88	0.12

Table 7.3: Shift of KG dependent on tank filling

To get an idea how emptying of several ballast water tanks affects the stability of *M.V. Cougar Ace*, we investigated the influence of the large double bottom tanks on the vertical centre of gravity.

The KGs in table 7.3 result from the shift of the solid centre of gravity and, additionally, from the free surface correction in case of partly filled tanks. The numbers in the table show that under normal operating conditions the crew had to expect a loss of GM not more than about 0.40 metres during the ballast water exchange of one tank. This shifts stability values down below the intact stability limit, set by the weather criterion in this case. However, all other intact stability criteria according to IMO A.749 are still fulfilled for this condition. In the case that two ballast water tanks are emptied at the same time, the GM is reduced by about 0.70 metres. In this case, the remaining GM amounts to 1.34 metres. In general, the lever arm curves of *M.V. Cougar Ace* are characterised by negative form stability, which is clearly visible in Figure 7.4. The ship has weathertight superstructures, leading to a strong increase of the righting levers at heeling angles beyond 50 degrees.

From the previous considerations, it seems to be very certain that *M.V. Cougar Ace* had no or only very small stability when she started to list. Beside the possibility that the ship simply capsized due to the absence of any uprighting levers, also external moments might have initiated the roll motion.

Based on the information given on the weather, we can conclude that M.V. Cougar Ace was travelling in following or stern quartering seas at the time of the accident. The waves were most probably long crested, which is typical for swell. Taking into account the ship's

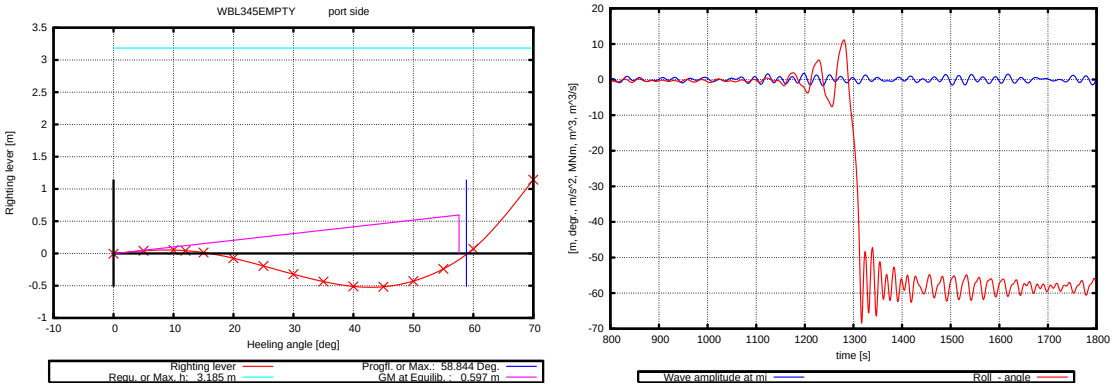

Figure 7.5: Left: Lever arm curve for ballast water tanks no. 2 and APT filled only. Right: Roll angle and wave amplitude amidships for the numerical simulation ($H_{1/3} = 3.0$m, $T_S = 10.0$s, long crested waves)

length between perpendiculars of 190 metres, the wave lengths present at the time of the accident lead to significant, periodic lever arm alterations.

At the time of the accident the significant wave height was reported at 3-4 metres. The numerical simulation was carried out in long crested, irregular waves with characteristic periods in the range from 9.1 to 10.8 seconds and a significant wave height of $H_{1/3} = 3.0$m. The encounter angle for the waves is chosen at 10 degrees.

The loading condition equals the one given in table 7.2, excluding the amount of ballast water. The ballast tanks are all empty now, except for number 2 and the aft peak tank (APT), assuming that the ballast water exchange is under progress for the remaining tanks. Therefore, an amount of about 1140 tons of ballast water remains on board. The resulting lever arm curve is shown in figure 7.5 on the left hand side. It becomes clear that the ship effectively has nearly no stability in this ballasting condition, even though the remaining GM amounts to about 0.60 metres.

The time series obtained from the simulation ($T_S = 10.0$s, $H_{1/3} = 3.0$m), shown in figure 7.5 on the right hand side, shows that the roll amplitudes are small before the accident. Then, suddenly the ship starts to roll, leading to the capsizing within a few roll cycles. Afterwards, the ship remains in a stable floating condition at about 60 degrees.

The numerical model has a floating condition which is very close to that of the real ship, with respect to draft as well as to heel and trim (see figure 7.6). This indicates that the chosen loading condition must be close to the real conditions on board of M.V. Cougar Ace. Thus, a dynamic capsizing event occurring in conjunction with very low intact stability is one scenario being able to explain the accident of M.V. Cougar Ace.

Figure 7.6: Floating condition of *M.V. Cougar Ace* after the accident in the stable condition with a list of 60 degrees. Left: Photo taken the day after the accident by the US Coast Guard (Photo: US Coast Guard). Right: Snapshot taken from the simulation shortly after capsizing.

The linear estimation of the ship's natural period for small roll angles and for the loading condition used in the simulation, delivers $T_e = 36.5$s. Assuming further a significant period of $T_S = 10.0$s and an encounter angle of $\mu = 10.0°$, neither a 2:1, nor a 1:1 resonance can be found close to the service speed of 18.6 knots. This, however, is just a rough estimation as the non-linearity of the lever arm curve, especially in the present case, strongly influences the natural roll period of the ship.

Still, resonant rolling is most likely not the primary source for the large roll angles detected during the simulation. Due to the very small righting levers, a pure loss of stability in waves seems to be the dominating cause in the present case. This is also supported by the lever arm curves shown in figure 7.7. Here, the ship's stability is calculated for the minimum and maximum wave lengths reported for the time of the accident. The wave height is chosen as 3 metres with the wave crest, or trough situated amidships, respectively. It can be seen very clearly that the ship has almost no stability at all, when resting on the wave crest within the range of observed wave lengths.

Concluded, it can be stated that the capsizing of *M.V. Cougar Ace* is clearly related to an almost complete loss of intact stability due to the massive reduction of ballast water during ballast water exchange operations. It is unclear which circumstances in detail led to this situation; the official statement of the flag state authority of Singapore, made at the IMO, does not contain any information on this.

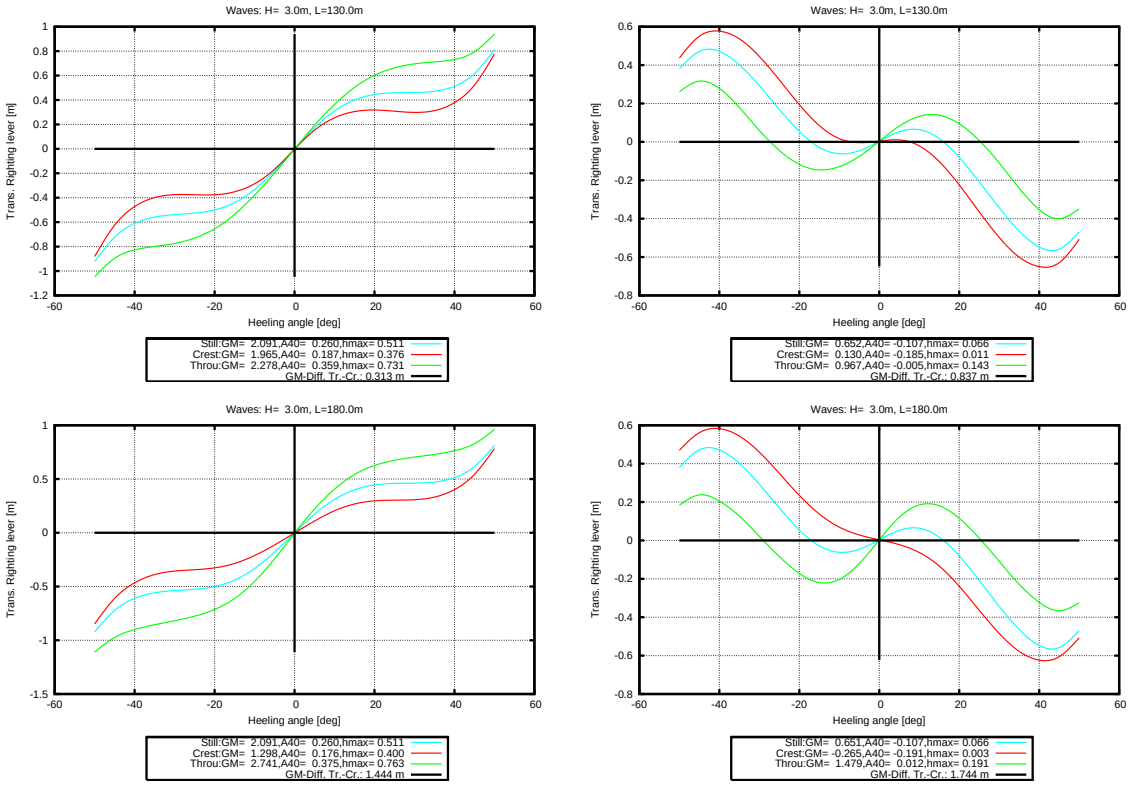

Figure 7.7: Lever arm alterations in waves (H = 3.0m) for wave lengths of $\lambda = 130$m (first row) and $\lambda = 180$m (second row). The left side shows the vessel's lever arms for a GM of 2.05 metres (intact stability limit), the right column shows the levers for the same waves with a GM of 0.60 metres.

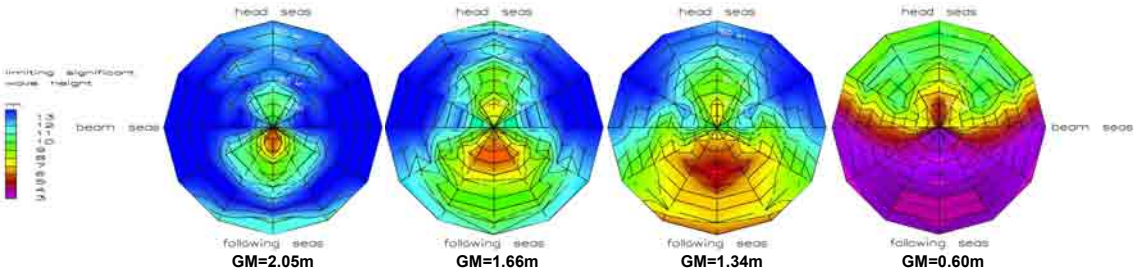

Figure 7.8: Polar diagrams showing limiting wave heights for different KGs; significant wave length 172 metres

7.2.3 Comparison of Different Capsizing Criteria for the Cougar Ace Accident

Finally, the question shall be discussed at which stability level *M.V. Cougar Ace* can be regarded as safe with respect to dynamic capsizing in waves and whether this stability level can be achieved by fulfilling the present intact stability regulations. In the present case, the limiting intact stability criterion according to IMO 749 is the weather criterion. The limiting KG according to this criterion amounts to 15.76 metres, equalling a metacentric height of GM = 2.05m. Figure 7.8 shows four polar diagrams, each presenting limiting wave heights below which the ship is regarded as safe against capsizing. The limiting wave heights are calculated by the Blume criterion in connection with a maximum roll angle of 50 degrees. All four diagrams are calculated for a characteristic wave length of 172 metres in short crested seas using a JONSWAP spectrum. The leftmost diagram shows the situation for the intact stability limit according to the weather criterion. The two diagrams in the middle represent situations where one, respectively two ballast water tanks are empty. Obviously, the limiting wave heights decrease drastically with increasing KG. Nevertheless, the ship can be regarded as safe at all speeds and encounter angles even for two emptied ballast water tanks, taking into account that the wave height at the time of the accident was not more than 3 to 4 metres. The KG at which the ship was travelling most likely when it capsized, must be regarded as extremely unsafe, at least when travelling in following and stern quartering seas, which is clearly visible in the rightmost polardiagram.

For two loadcases different intact stability criteria have been calculated and compared to each other. The KG for the first loadcase to be investigated is GM = 2.05m, which represents the intact limit according to the IMO weather criterion. The second loadcase investigated is the one with GM = 0.60m, representing the situation in which the ship most likely was, when it capsized.

The Kastner-Roden Criterion

The Kastner-Roden criterion is based on the average time between subsequent capsizing events. In case of the weather criterion-limited loadcase, no capsizes could be detected within a total simulation time of 1.0e6 seconds at 3 meters wave height. Thus, the resulting capsizing time is infinite. The average time between capsizings for the low GM case is calculated at 1398 seconds. Based on these values the criterion estimates a safe GM at 2.246 metres. This is clearly too conservative, as the calculation results show that the ship can already be considered "safe" at the intact limit case with a GM of 2.05 metres.

Soeding's Concept of Amplified Waves

Due to the very low stability of the accident-loadcase, the vessel capsizes in all simulations performed in 3 metres wave height. Thus, there is no need for Soeding's extrapolation concept as capsizing is not a rare event in this case. The capsizing probability is simply counted from the time series. For the intact limit the capsizing probability, in turn, is very low. Even for an extrapolation rate of 2.0, equalling a simulation wave height of 6.0 metres, no capsizings can be found during $1.0\mathrm{E}6$ seconds real time. The estimated capsizing frequency of $1.53 \cdot 10^{-23}$ per year is extrapolated from a simulation performed with a significant wave height of $H_{1/3} = 9.0$m. It has not been investigated how good the extrapolation method works for such large extrapolation rates (3.0). Nevertheless, from the results we can conclude that the capsizing probability at this stability level is extremely low and thus the ship can be clearly considered safe in this situation.

The Directly Computed ISEI

For all four loadcases defined in 7.2.2, the insufficient stability event index (ISEI) is calculated. Figure 7.9 shows the results. The initial loadcase with the limiting KG according to the weather criterion (GM $= 2.05$m) delivers a low ISEI ($6.60\mathrm{E}{-}05$) which clearly represents a safe situation. The cases with one and two emptied ballast water tanks deliver larger ISEI-values. As expected, we calculate a very high ISEI-value ($2.70\mathrm{E}{-}01$) for the accident scenario, identifying this situation as clearly unsafe. In the present case the weather criterion proofs to be relatively conservative with respect to the intact stability, which can be explained by the extremely large lateral windage area that is typical for car carriers.

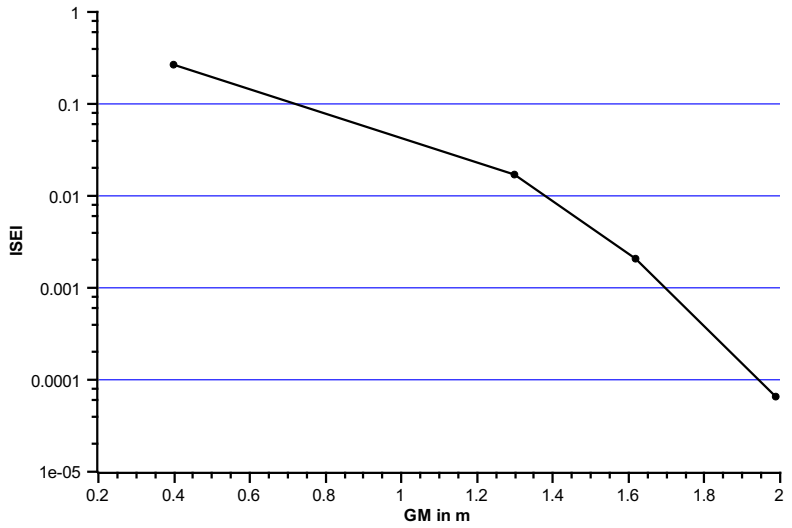

Figure 7.9: ISEI calculated from seakeeping simulations dependent on GM

Blume-Criterion

Due to the weathertight superstructures, the *M.V. Cougar Ace* has a range of positive righting levers of more than 70 degrees. Thus, the Blume criterion in its original formulation cannot be applied for the present ship as it addresses the residual area below the lever arm curve up to the point of vanishing stability, which here, does not exist within a reasonable range of heeling angles. Therefore, we use a modified form of the criterion limiting the maximum permissible roll angle to 50 degrees. The Blume criterion applied for 3m significant wave height is clearly fulfilled for the first case. The limiting wave height according to this criterion amounts to 12 metres. In the second situation the Blume criterion is not fulfilled, as the ship capsizes in all 100 simulations.

The Empirical Wave Crest Criteria from the Lake Ploen Tests

The righting levers in waves for the accident-loadcase (GM = 0.60m) are shown in figure 7.7. In the wave crest-condition the ship has no positive stability at all. Consequently, the range of positive lever arms also equals zero. In turn, the maximum righting lever for the intact stability loadcase amounts to 0.387 m, which is significantly above the limit of 0.05 m. The same applies for the range of positive stability, which amounts to more than 60 degrees due to the weathertight superstructures.

The Blume C-Factor

The C-factor concept was developed for container vessels. It is not applicable for ships with large depth, such as car carriers. The C-factor calculated for those ships takes unrealistic values and therefore, cannot be applied in this case.

7.2.4 Conclusions from the M.V. COUGAR ACE accident

Criterion	**GM=0.60m**	**GM=2.05m**
Kastner/Roden Capsizing time	1398 s	(inf)
Soeding Capsize Probability	22548 / year	$1.53\mathrm{E}{-23}$ / year
Blume (Modified) $E_R - 3s$	0.00 mmRad	222.62 mmRad
ISEI (direct)	$2.6 \cdot 10^{-1}$	$9.2 \cdot 10^{-4}$
Empirical Criteria Crest lever Crest range	 0.003 <0.05 0 <16 Deg	 >0.05 >16 Deg.
Blume c-factor	not applicable	not applicable

Table 7.4: Values of the different capsizing criteria for two loadcases. Left: Accident-loadcase with very low stability. Right: Loadcase defined by the IMO weather criterion which represents the intact stability limit for M.V. Cougar Ace.

The weather criterion provides a relatively conservative intact stability limit for this type of vessel, prescribing a minimum GM-value of about 2.05 metres. This is typical for car carriers as those ships have very large lateral areas leading to corresponding wind loads. Thus, this loadcase is regarded as clearly safe by all capsizing criteria applied. The corresponding ISEI amounts $6.60\mathrm{E}{-05}$, which represents a safe condition. The second loadcase with a GM of only 0.60 metres was determined according to the information available on the loading condition at the time of the accident. Although the GM is still positive, the lever arm curve shows very small maximum righting levers and only a small range of about 15 degrees. This situation is regarded as very unsafe by all applicable capsizing criteria. The ISEI is determined at $2.70\mathrm{E}{-01}$ for this situation, which shows that this condition is very unsafe.

7.3 Summary for Accident Investigations

Beside the *MV Cougar Ace* accident, in total ten accidents which occurred during the last fifty years were investigated, following the same scheme as in the given example. A complete documentation of the accidents investigations carried out at the *Institute of Ship Design and Ship Saftey* will be published separately.

Ship	**ISEI**	
	unsafe	estimated safe
Cougar Ace	$2.6 \cdot 10^{-1}$	$9.2 \cdot 10^{-4}$
Fidamus	$2.8 \cdot 10^{-1}$	$2.7 \cdot 10^{-3}$
Finnbirch	$6.7 \cdot 10^{-3}$	$4.1 \cdot 10^{-4}$
Halstenbek	$1.5 \cdot 10^{-2}$	$1.0 \cdot 10^{-3}$
Helga Matthiesen	$1.1 \cdot 10^{-2}$	$3.7 \cdot 10^{-3}$
Hoheneichen	$1.8 \cdot 10^{-1}$	$2.4 \cdot 10^{-2}$
Irene Oldendorff	$1.5 \cdot 10^{-1}$	$7.1 \cdot 10^{-3}$
Lohengrin	$1.5 \cdot 10^{-1}$	$2.8 \cdot 10^{-3}$
Marianne Wehr	$4.3 \cdot 10^{-3}$	$8.1 \cdot 10^{-3}$
Wilhelm (ex Arn IX)	$1.6 \cdot 10^{-1}$	$7.9 \cdot 10^{-4}$
Open Top Container	$1.5 \cdot 10^{-2}$	$1.0 \cdot 10^{-3}$
Aratere	$2.0 \cdot 10^{-2}$	$3.7 \cdot 10^{-5}$
ONR Tumble	$7.0 \cdot 10^{-3}$	$5.0 \cdot 10^{-4}$
ONR Flare	$4.7 \cdot 10^{-3}$	$1.8 \cdot 10^{-3}$
RoRo	$2.6 \cdot 10^{-1}$	$1.0 \cdot 10^{-3}$

Table 7.5: Ships for which detailed accident investigations were carried out. The last three ships do not represent real capsizing accidents, but are based on model test results.

The results of the investigations show that in almost all cases the stability criteria gives a common statement on whether a ship can be considered as safe or unsafe in a certain situation. All ships investigated and the ISEI-values obtained from the accident analysis are shown in Table 7.5. At this, the left column shows the index values calculated for the accident situation and thus, represents unsafe conditions. Most of the values lie in the region of 10^{-1}. The rightmost column in Table 7.5 contains those ISEI values which were obtained for the loadcases estimated to lie in the safe domain. For most of the ships the index delivers values between 10^{-4} and 10^{-2}. From this it can be concluded that

the border between safe and unsafe most likely lies in between the range from 10^{-3} to 10^{-2}, while a certain transitional area exists, where the ships are regarded as critical with respect to their intact safety.

Significant outliers are the *Marianne Wehr* and the *Hoheneichen*. Both ships are rather small old-fashioned coasters, built in the 1960's. In the first case we conclude that the accident can not have been caused by insufficient stability, but must have had other reasons. The stability was relatively large at the time of the accident. Following its basic principles, the Kastner-Roden criterion recommends to increase the stability further. Actually, this leads to an even worse index value, because the vessel then suffers from resonances in head seas. This is important to note, as just increasing the stability not always and not inevitably leads to an improvement of the overall ship safety. However, the accident investigations show that the risk of capsizing in following seas can always be reduced by increasing the stability. In case of the *Hoheneichen* the first loading condition clearly suffers from insufficient stability with high contributions to the index from following and stern quartering sea cases. Increasing the stability leads to a significant improvement in following seas, but leads to resonance conditions in head seas, which then feed the index. This explains the small overall improvements of the index in this case.

To conclude, the validation project shows that the ISEI delivers significant and consistent values and seems to be suitable to judge upon the ship safety related to large amplitude roll motions and capsizing. Furthermore, the analysis indicates that the approach is superior to those criteria which are not based on direct calculations or which take only one test-condition into account. In the next step, the findings made during the validation are used to find threshold values for the Insufficient Stability Event Index.

7.4 Threshold Values

The probabilistic assessment of safety-critical situations helps us to quantify safety and risk, respectively. However, this is of limited use for decision making, as long as no threshold values exist. Taking into account the findings obtained from the investigation of real capsizing accidents as presented in the previous section, the following statements can be made. The ISEI-values which are associated to clearly unsafe situations are exactly determined by the accident situation. In contrast, the exact boundary of the safe domain remains unknown. According to Table 7.5, the ISEI-values calculated for the accident loading conditions predominantly have the order of magnitude of 10^{-1}. For the estimated safe situation the ISEI-values typically lie well below 10^{-2}.

This result is also supported by a systematic investigation of a large number of different ships carried out at the *Institute for Ship Design and Ship Safety* (see [28],[43] and [42]).

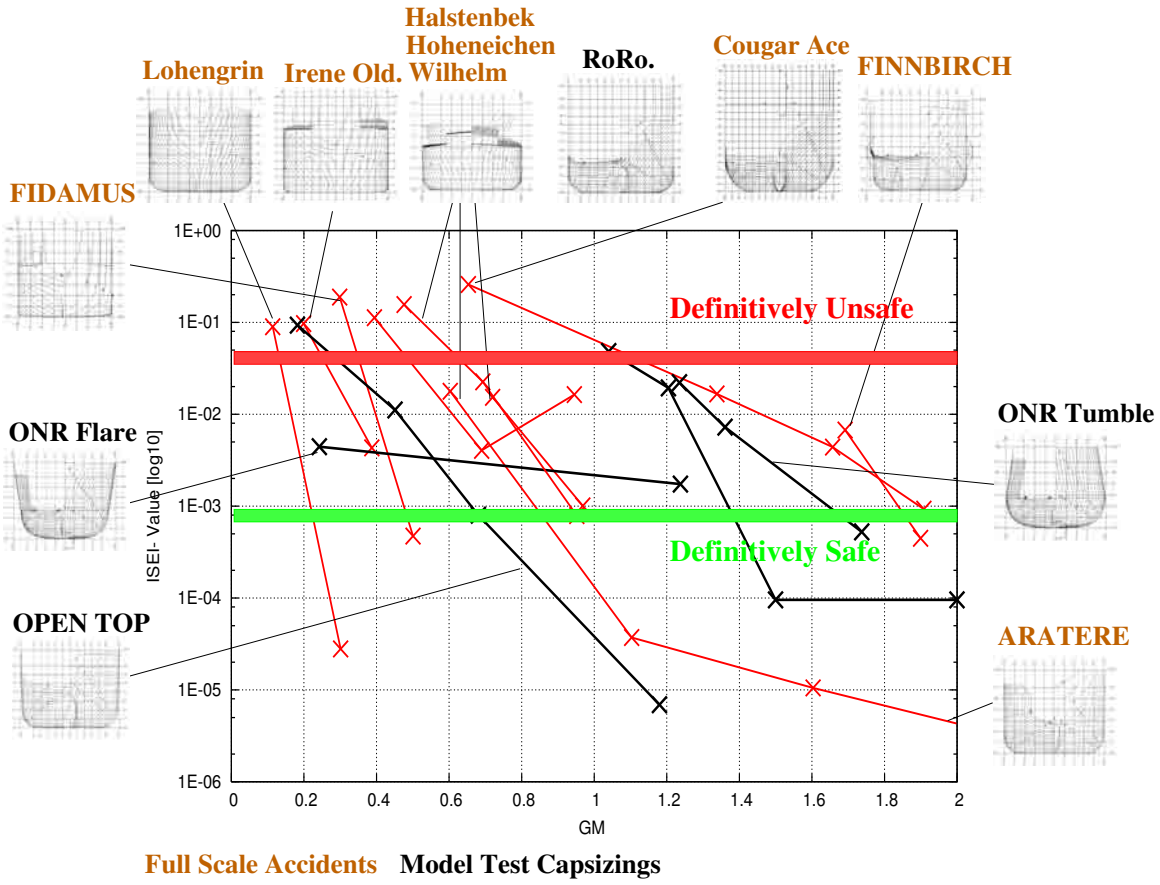

Figure 7.10: ISEI values in dependency of GM for a selection of investigated ships, each analysed with different loadcases.

Here, each ship is tested in three loading conditions, whereas the first equals the intact stability limit according to the IMO Res. A.749. The second and the third loadcase have larger GMs, increased by 0.5 metres and 1.0 metres, respectively. From this, it follows that the second loadcase roughly lies in the region where modern ships usually have their stability limit, determined by the damage stability requirements. Typically, the first loadcase delivers ISEI-values in the unsafe region (10^{-1}), while the second one delivers values in the range between 10^{-3} and 10^{-2}. The third one is mostly below 10^{-3}.

Figure 7.10 shows the ISEI-values calculated for a selection of the investigated ships in different loading conditions, also including the ships from the accident analysis. Accidents related to large amplitude roll motions with modern ships, travelling with permissible stability, are not very frequent, but they do occur more than once per year. On this basis we define the region around ISEI values of 10^{-2} as a "critical" region. Values below 10^{-3} are achieved for ships with sufficient stability and lever arm curves, which provide positive

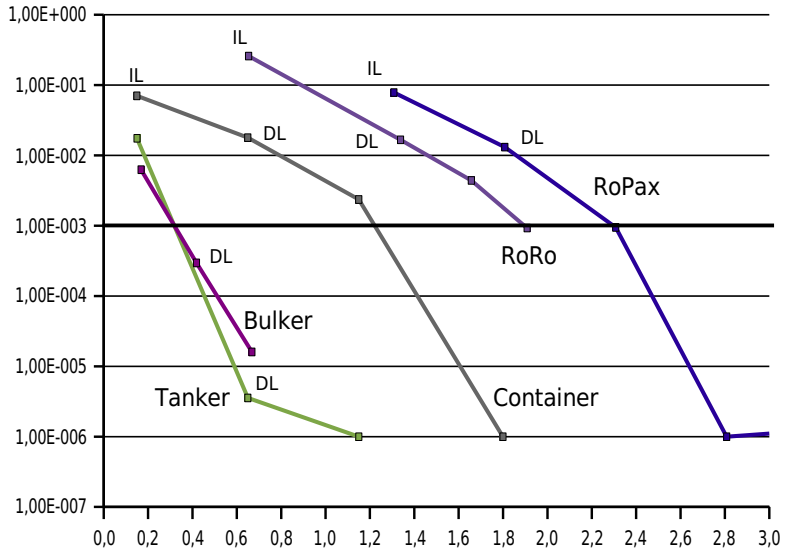

Figure 7.11: Typical examples of ISEI values over GM for four different ship types. IL indicates the intact stability limit according to present regulations, DL the corresponding damage stability limit. WC indicates the weather criterion.

righting arms even in the unfavourable wave crest condition. Taking this into account, the following threshold values for the ISEI are proposed:

- Values above $5.0\mathrm{E}{-2}$ are considered to be unsafe and not tolerable for all types of ships.
- Values between $1.0\mathrm{E}{-3}$ and $5.0\mathrm{E}{-2}$ are considered to be potentially dangerous. These values might be acceptable for small ships and for ships operating in restricted areas of operation.
- Values below $1.0\mathrm{E}{-3}$ are considered to be generally safe.

Compared to existing regulations currently in force, the new criterion requires a level of ship stability which is in average slightly above the current damage stability requirements. However, different ship types are affected differently. While the new criterion has almost no effect on the permissible intact stability of tankers and bulkers, which usually do not suffer from dynamic intact stability problems, RoRo-vessels as well as Containerships face slightly stricter limits compared to the existing intact limit. This is illustrated with four typical examples in Figure 7.11. Here, IL denotes the intact stability limit according to the currently relevant rules and DL is the corresponding damage stability limit. In case of the RoRo-ship, the general intact stability criteria and the weather criterion are presented separately, where the weather criterion has the index WC. Obviously, the Bulker as well as

the Tanker reach tolerable safety limits already at or close to the actual limiting stability. The Containership reaches at least the critical regions with help of the damage stability regulations. Nevertheless, an increase of further 0.60 meters of GM is required to bring the example vessel down to the recommended threshold value of 10^{-3}. The worst safety level in this example was found for the RoRo ship. This vessel is still regarded as highly unsafe when operated at its current damage stability limit, which is the strictest stability requirement currently in force. Again, the GM would have to be increased by about 0.60 meters to achieve a sufficient safety level according to ISEI. At this point it is also important to keep in mind that very large stability values increase the risk of damages due to large acceleration, which are not assessed directly by the ISEI-concept. At least for newbuildings the focus should not be laid purely on increasing the up-righting moments only, but advanced solutions can be more effective in such cases. Here, special attention should be paid on the optimisation of the lines design in order to minimise the lever arm alterations in waves by appropriate measures.

8 The Simplified Insufficient Stability Event Index (ISEIs)

The use of seakeeping simulations requires substantial, specialised knowledge in the field of numerical fluid dynamics. Significant effort is required for setting up, evaluating and validating the numerical simulations. Neither this special knowledge nor the required time-effort for the detailed analysis of ships by means of direct simulation can be presumed to be available for all institutions involved in determining and approving ships' intact stability. Especially shipyards producing mainly low-technology ship types and so far authorities in certain countries may have limited access to the required knowledge.

Beside these problems with the limited access to principally existing technology, there is another problem related to lacking standardisation of seakeeping simulations. Currently, there is no international standard to define the minimum requirements for numerical seakeeping codes which are employed for the assessment of dynamic ship stability. Nor is there a standardised procedure for the set up of environmental conditions to be used for the simulations. For the practical application of a simulation-based criterion this would mean that at first a basic standard for numerical seakeeping simulations needs to be established. This standard has to clearly define, what minimum requirements must be fulfilled by a code to be certified for intact stability assessment. This includes the definition of hazards that the code must be able to assess. The question needs to be asked, whether it is sufficient to predict the occurrence of parametric rolling as such, or if the code must be able to deliver a satisfactory estimation of the resulting roll-amplitude, which appears to often be a problem when the lever arm curve is linearised. Further, the standard would have to clarify various questions on model quality, for example, the number of degrees of freedom considered.

Currently, it is not visible that such an internationally accepted standard will be available in the near future, although increasing research activities in this field could be observed during the past few years. For example, the International Towing Tank Conference (ITTC) has incorporated a validation scheme for numerical seakeeping codes into their "Recommended Procedures and Guidelines" in 2002 [46]. Unfortunately, this procedure is limited to frequency domain codes and thus, not applicable to the codes addressing large amplitude roll motions in longitudinal waves. Another step towards a standardisation can

be benchmarking studies, although it often appears that the test cases themselves cause problems as the definition of details seems insufficient, which in turn leads to limited comparability of the results. The latest in a number of such studies ended recently. This study was carried out within the scope of the EU-funded project SAFEDOR [61] and targeted primarily the prediction of damage ship stability in waves (Papanikolaou and Spanos [52]). Additionally, a review of existing codes with their individual capabilities was compiled within the EU-project "Advanced Decision Support System for Ship Design, Operation and Training" (ADOPT) [73].

Taking all this into account, a regulation directly and solely depending on numerical seakeeping simulations today can hardly be accepted as a standard procedure for the assessment of the intact stability of ships. This results in the need for introducing an alternative approach in addition to the simulation based ISEI, which provides a simulation independent possibility to assess the ship safety in waves. At this, the simplified approach shall employ all experiences and findings made during the simulation based safety assessment. The following minimum requirements are made:

- The simplified approach has to be able to address the same phenomena as the simulation based approach.
- The simplified approach has to provide a comparable reliability with respect to sufficient minimum intact stability.
- Both calculations models have to be consistent as far as possible.
- First principle approaches shall be used wherever justifiable with respect to the required degree of simplicity.

The requirement for consistency implies that the index-values calculated by this "simplified" approach must come as close as possible to the simulated results, which then represent the benchmark for the quality of the simplified criterion. The following sections deal with the implementation of this simplified, simulation-independent criterion addressing the minimum stability of ships travelling in following and stern-quartering seas into the overall ISEI concept.

8.1 Concept

Following the requirement for compatibility and consistency between the simulation approach and the simplified criterion, the fundamental approach is kept identically. Again, the idea is to assess the ship response in several different operational cells, providing a comprehensive analysis of the ship's safety level. Each cell has a certain probability of

occurrence and contributes to the overall index with this value, in case the endangerment with respect to capsizing of the vessel exceeds a certain threshold value. As for the simulation-based approach, this threshold value is expressed in terms of a limiting wave height determined on the basis of a deterministic criterion, whereas the decision criterion is different in the case of the simplified approach.

In consequence we start with an approach which in principle equals Equation 6.5, leaving out the head and beam seas parts, because for the assessment of the required minimum intact stability of a vessel, the Insufficient Stability Event Index is evaluated in following and stern quartering sea situations only. Consequently, the simplified approach, specifically targeting the minimum intact stability assessment, is also limited to following and stern quartering seas in the range from $-\pi/3$ to $\pi/3$. An important difference to the simulation based approach is that we no longer refer to the significant wave height $H_{1/3}$ as property of an irregular seaway as before, but use the wave height H of an equivalent regular wave, on which the failure coefficient C^s_{fail} is now based. In the same way we do not refer to the significant wave period any more, but use the wave period T of the equivalent wave. The basic approach for the simplified Insufficient Stability Event Index ($ISEIs$) then reads:

$$ISEI_s = \sum_{i=1}^{N_T}\sum_{j=1}^{N_H}\sum_{k=1}^{N_\mu}\sum_{l=1}^{N_v} \delta P_{sea}(H^{(j)}, T^{(i)})\cdot \delta P_\mu(\mu^{(k)}) \cdot \delta P_v(v_s^{(l)} \mid H^{(j)}, T^{(i)}, \mu^{(k)})\cdot C^s_{fail}(H^{(j)}, H_{lim} \mid T^{(i)}, \mu^{(k)}, v_s^{(l)}) \tag{8.1}$$

The index s indicates that the simplified approach instead of a simulation is used to determine the limiting wave height. Here, δP_μ denotes the probability of occurrence of a certain course and δP_v is the probability that the ship travels at a certain speed. This component is treated with the same linear probability density function, as described in case of the simulated ISEI (see Section 6.4).

For the practical calculation of the simplified criterion, we introduce a further simplification to reduce calculation effort. An important fact discovered during the evaluation of a large number of polardiagrams, showing the individual limiting wave heights according to the *Blume-Criterion* , is that the relevant sector in the range between -60°and 60°shows little change in limiting wave heights over different encounter angles. A typical polarplot of a ship endangered in following seas is given in Figure 8.1. This behaviour could be observed in the majority of cases simulated in irregular, short-crested waves.

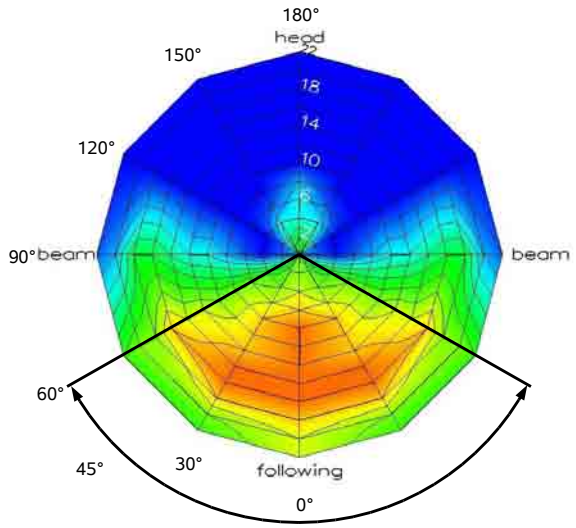

Figure 8.1: Typical distribution of limiting wave heights for a specific wave period T_1 for a ship travelling at the intact stability limit (Range: blue = 14.0 m, red = 3.0 m)

This justifies the treatment of the encounter angles in the sector from -60°to 60°not separately, but together, assuming that the limiting wave height does not change significantly within the selected range. Introducing this simplification instead of Equation 8.1 we can now write:

$$ISEI_s = \sum_{i=1}^{N_T} \sum_{j=1}^{N_H} \sum_{l=1}^{N_v} \frac{1}{3}\, \delta P_{sea}(H^{(j)}, T^{(i)}) \cdot \delta P_v(v_s^{(l)} \,|\, H^{(j)}, T^{(i)}) \cdot C^s_{fail}(H^{(j)}, H_{lim} \,|\, T^{(i)}, v_s^{(l)}) \tag{8.2}$$

To keep the commonality to the resulting values of the simulation based approach we introduce the factor $1/3$, taking into account the overall probability of the ship travelling in the following seas sector from -60 °to 60°. This is valid with the assumption that the encounter probability is equally distributed.

The calculation of the failure coefficient C^s_{fail}, which again takes only the two values 0 and 1 to indicate safe and un-safe situations, reads now:

$$C^s_{fail}(H, H_{lim} \,|\, T_1, \mu, v_s) = \begin{cases} 0 & \text{if} \quad H < H_{lim} \\ 1 & \text{if} \quad H \geqq H_{lim} \end{cases} \tag{8.3}$$

The related calculation procedure is explained in the following. The way the failure coefficient C^s_{fail} is determined represents the main difference between the simulation based $ISEI$ and the simplified criterion ($ISEI_s$).

8.2 Method to Calculate the Failure Coefficient C^s_{fail}

In accordance with the simulation based approach, the coefficient itself is only a binary operator (0, 1), whereas its value directly depends on the limiting equivalent wave height H_{lim}, dividing the overall domain into a safe and an unsafe region. For the simplified approach the limiting wave height is determined by employing characteristic values related to the dynamic stability of ships in waves. In this case, the wave crest and wave trough lever arm curves are used in combination with the encounter frequency which results from the combination of wave period, ship speed and encounter angle. This provides information on the absolute ship stability in waves as well as on its alterations and the related frequency of change. H_{lim} in this case does not refer to the significant wave height $H_{1/3}$, but to an equivalent, regular wave with the height H. This limiting wave height is calculated from the formula given in Equation 8.4, which consists of two parts. One part addresses the stability alterations of the ship itself, whereas the second part adjusts the limiting wave height according to the relationship between the ship's eigenfrequency of roll and the encounter frequency depending on the actual wave length.

$$H_{lim} = \mathrm{f}\ (\tfrac{\omega_e}{\omega_s}, C_i) \cdot C_{10}(\zeta'_{A0})^{C_{11}} \cdot \lambda \tag{8.4}$$

Figure 8.2 illustrates the fundamental work flow of the simulation independent calculation procedure. At first, we solve the term for the contribution related to the stability alterations in waves, which is represented by the maximum wave steepness factor ζ'_{A0}. C_{10}, C_{11} and C_i are correlation factors. The wave steepness factor is defined as follows:

$$\zeta'_{A0} = \frac{H_{A0}}{\lambda} \tag{8.5}$$

Here, λ denotes the actual wave length and H_{A0} is a mean limiting wave height, determined by a balance of areas under the lever arm curves, which is described in the following section.

In the next step, H_{A0} is corrected by the frequency dependent part, given by the function f in Equation 8.4. Details on this procedure are discussed in Section 8.2.2. Based on the resulting limiting wave height H_{lim}, C^s_{fail} is determined subsequently for all relevant wave heights. The procedure returns the simplified $ISEIs$ contribution for one operational cell.

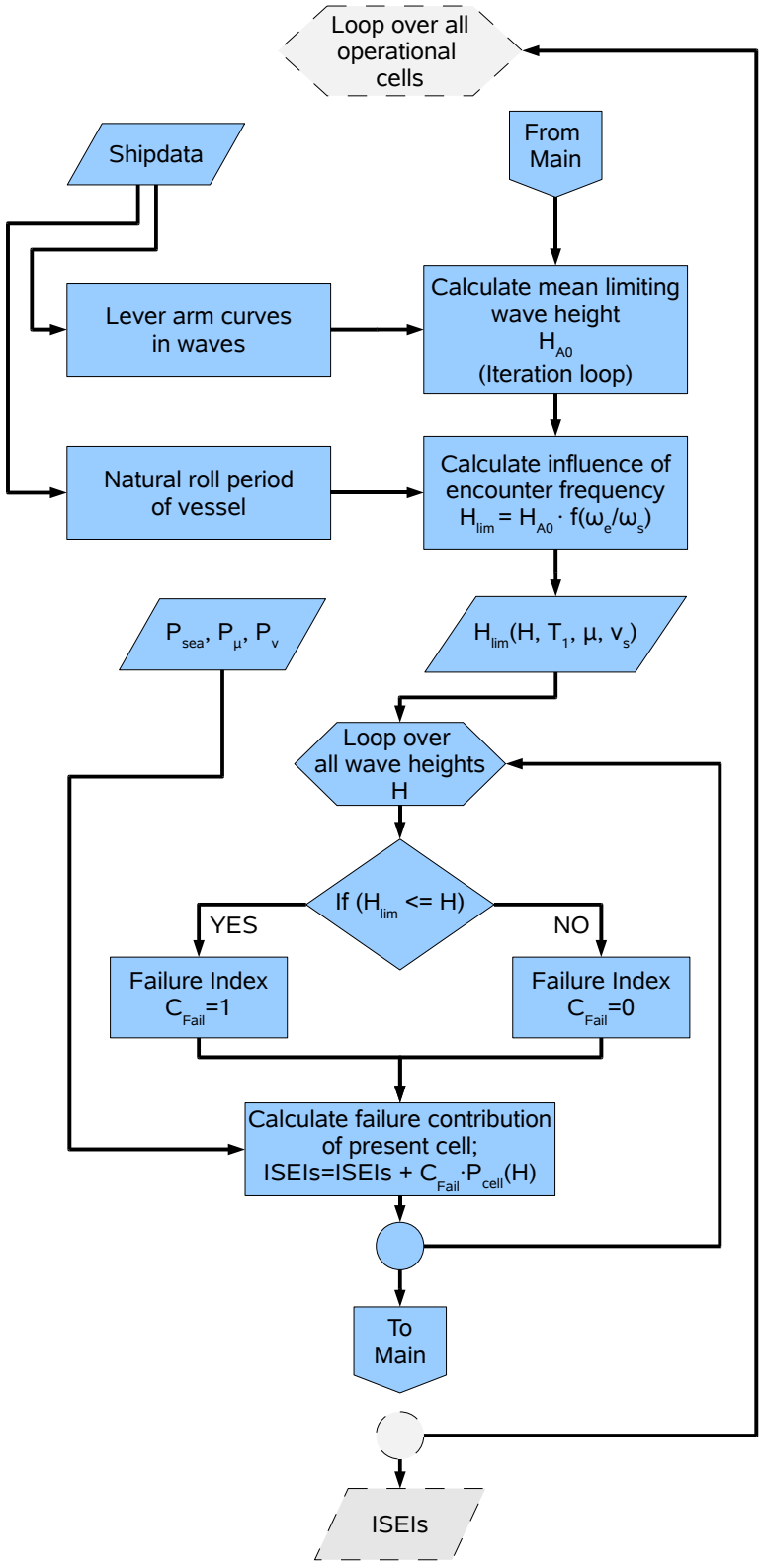

Figure 8.2: Generic concept principles for the simplified ISEIs

8.2.1 Calculating the Lever Arm Balance in Waves

The area under the lever arm curve is a measure for the potential energy stored in the system when the ship is inclined to a certain heeling angle. This can be easily proven by the relationship:

$$E_{pot}(\varphi_2 2) = \int_{\varphi_1}^{\varphi_2} \Delta \cdot g \cdot h(\varphi) d\varphi \tag{8.6}$$

For the lever arm balance we consider two different lever arm curves. These are the lever arm curves in wave trough and wave crest condition, whereas all levers are calculated in the equilibrium floating condition, including trim correction.

The instantaneous lever arm curve of a ship travelling in longitudinal waves changes dynamically between the two extreme situations "wave trough" and "wave crest". Depending on the wave length, the encounter frequency and the natural roll period of the ship, it usually leads to a positive energy balance. This means that due to the changing stability, caused by passing waves, a certain amount of net-energy is brought into the oscillating system during each period. These positive actions lead to the initiation of the roll motion and the growth of the amplitudes. If there is no further disturbance, the roll motion can grow until the ship finally capsizes. In a natural seaway this mechanism usually works only for a limited number of roll cycles, until wave components with different frequency, phase and encounter direction disturb the system. Nevertheless, if the net-energy contribution is large enough, even a small number of roll cycles suffices to capsize a ship.

A criterion targeting the minimum intact stability of a ship has to assure that the ship of interest is able to withstand this net-energy contribution, caused by the dynamic change of the righting levers, for a sufficient number of roll cycles. In the present case, we take the most unfavourable situation by assuming that the full difference-area between the maximum and the minimum righting arm curve is taken to calculate the net-energy introduced into the system. In order to survive the situation, this contribution then has to be absorbed completely by up-righting moments calculated from the smallest righting lever arm curve.

The first area used for the lever arm balance is calculated according to Equation 8.7 between the maximum and the minimum righting lever arm curve (h_{max}, h_{min}) in the given wave, up to an angle of 15 degrees (A_{15diff}) , as illustrated in Figure 8.3 on the left hand side. The second area to be considered is the area below the minimum of the two lever arm curves, which is integrated up to an angle of 40 degrees according to Equation 8.8 and as shown in Figure 8.3 on the right hand side.

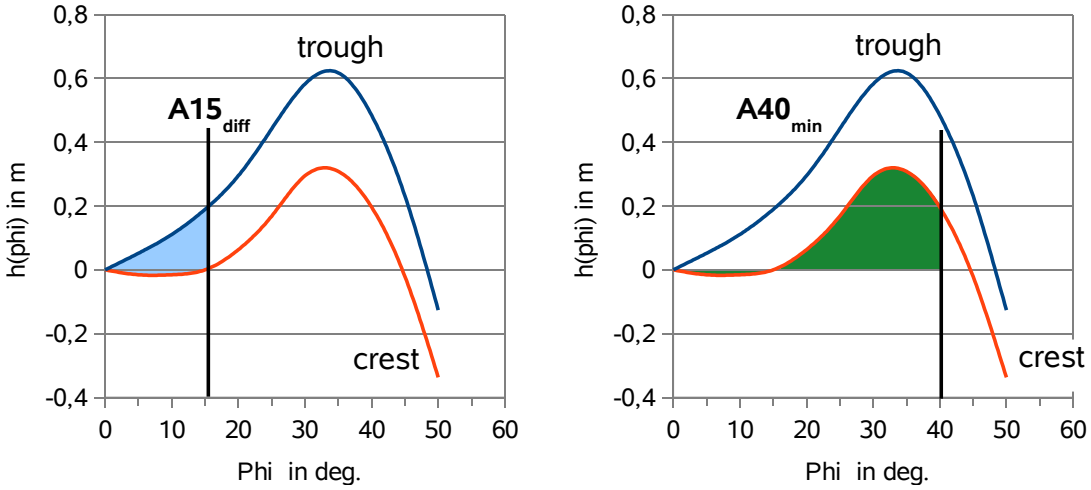

Figure 8.3: Concept of area balance under lever arm curve

$$A_{15diff} = \int_0^{15} h_{max}(\varphi) - h_{min}(\varphi)\ d\varphi \tag{8.7}$$

$$A_{40min} = \int_0^{40} h_{min}(\varphi)\ d\varphi \tag{8.8}$$

We now balance the two areas A_{15diff} and A_{40min} against each other. All wave heights in which the area up to 40 degrees is larger than the difference-area up to 15 degrees are considered to be acceptable, whereas all wave heights where A_{15diff} becomes larger than the area up to 40 degrees, are not acceptable. The decision criterion behind this criterion is that as long as the area A_{40min} is larger than A_{15diff}, the energy which triggers the roll motion is not sufficient to heel the ship beyond an angle of 40 degrees in the most unfavourable situation. Hence the mean limiting wave height H_{A0} yields:

$$H_{A0} := \left\{ H \in \mathbb{H} \;\middle|\; A_{40min} - A_{15diff} \stackrel{!}{=} 0 \right\} \tag{8.9}$$

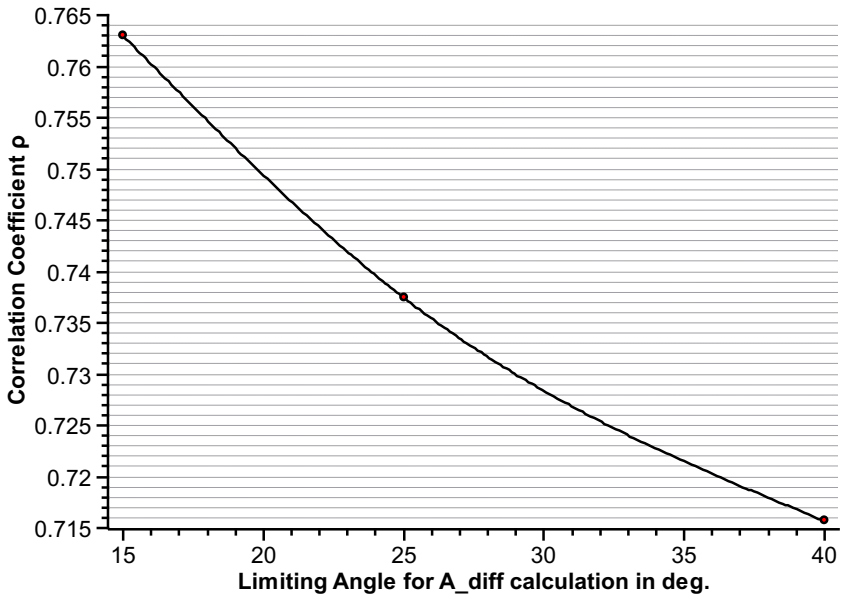

Figure 8.4: Correlation coefficients for the mean limiting wave heights calculated by simulation and simplified criterion. Variation of limiting angle for the calculation of the difference area A_{diff} between 15 and 40 degrees.

The upper limiting angle of 40 degrees is taken as the threshold value, because roll angles beyond this point lead to severe damage on board of ships and are therefore seen as unacceptable. The lower limit is set to 15 degrees. The reason for choosing this relatively small angle is, that parametrically excited roll motions are usually initiated by lever arm alterations at small angles. If the lever arm alterations in this region up to 10 to 15 degrees are sufficiently small, parametric roll motions can hardly develop. A number of limiting angles have been tested to achieve the optimum correlation between the simulation based criterion and the simplified approach. With this in mind, angles below 15 degrees are not taken into account as this leads to very small area differences, making the criterion less strict. Figure 8.4 shows the correlation coefficient for the mean limiting wave heights, obtained from the criterion and from simulation results. The limiting angle of 15 degrees is chosen as the best possible solution.

The balance as introduced in Equation 8.9 addresses ships where the roll motion is exclusively excited by the dynamic stability alterations. In waves significantly shorter than the ship's length, the magnitude of the lever arm alterations usually decreases and at a certain point becomes neglectable. Neither pure loss of stability nor parametric excited roll motions are likely to occur in such situations. If in these situations all waves approach the ship exclusively from 0°, which means exactly from abaft, theoretically there will be no

exciting moments. But assuming that ships are mostly travelling in short crested waves, some of the waves may also approach the ship from directions significantly different from the mean direction of wave propagation. If a ship is hit by a steep wave from quartering or even close to beam directions, this will cause a large heeling moment to the ship. To cope with this situation we introduce an additional component A_{ext}, accounting for the energy contribution introduced by this direct excitation component. Following this idea, Equation 8.10 can be extended by this extra contribution:

$$H_{A0} := \left\{ H \in \mathbb{H} \;\middle|\; A_{40min} - (A_{15diff} + A_{ext}) \stackrel{!}{=} 0 \right\} \tag{8.10}$$

The angle of wave slope causing the exciting moments to the ship can be calculated as:

$$\varphi_e = \arctan\left(\frac{2H_{lim}}{\lambda}\right) \tag{8.11}$$

The total energy introduced into the oscillating system then results from integrating the area under the lever arm curve up to the angle φ_e (Equation 8.12). Here, again, the most unfavourable situation is taken by using the largest righting levers h_{max}, which are usually observed in the wave trough condition.

$$A_{ext} = \int_0^{\varphi_e} h_{max}(\varphi)\; d\varphi \tag{8.12}$$

This addition increases the requirements made by the criterion in short and steep waves, whilst it only has minor influence in longer waves. A measure for the amount of energy contributed by this direct excitation component is the angle of the wave slope φ_e. Figure 8.5 shows the value for φ_e in dependency of the wave period (T) and the wave height (H). The maximum values are limited by the highest possible wave steepness ($\lambda/L \approx 1/7$).

Finally, the wave steepness factor resulting from the lever arm balance has to be adjusted in order to deliver consistent results compared to the simulation based approach. To achieve this goal we use two correlation factors, C_{10} and C_{11}, as introduced in Equation 8.4. These factors are determined from a set of ships by means of regression analysis. The sample ships are loaded at their intact limit determined according to the IMO regulations currently in force. In total, the available database contains 176 ships, whereas each of them is investigated for six different significant wave periods, which results in 1150 datapoints overall available for the regression. Table 8.1 lists the number of ships, sorted by ship type, which are contained in the regression database.

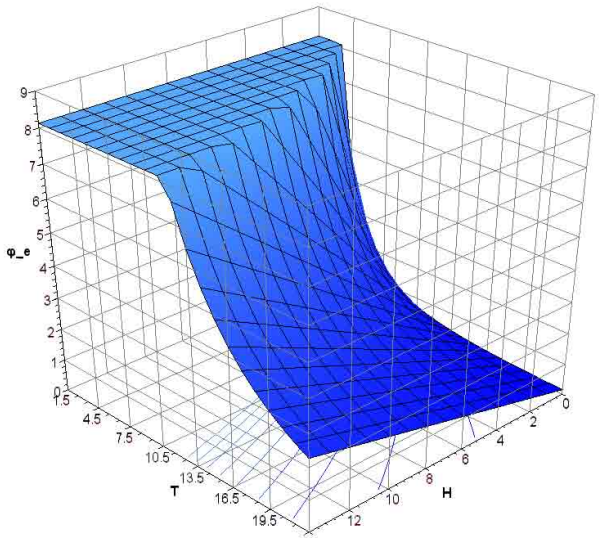

Figure 8.5: Illustration of the influence of the correction for short and steep waves: Graph shows virtual heeling angle depending on wave period and wave height

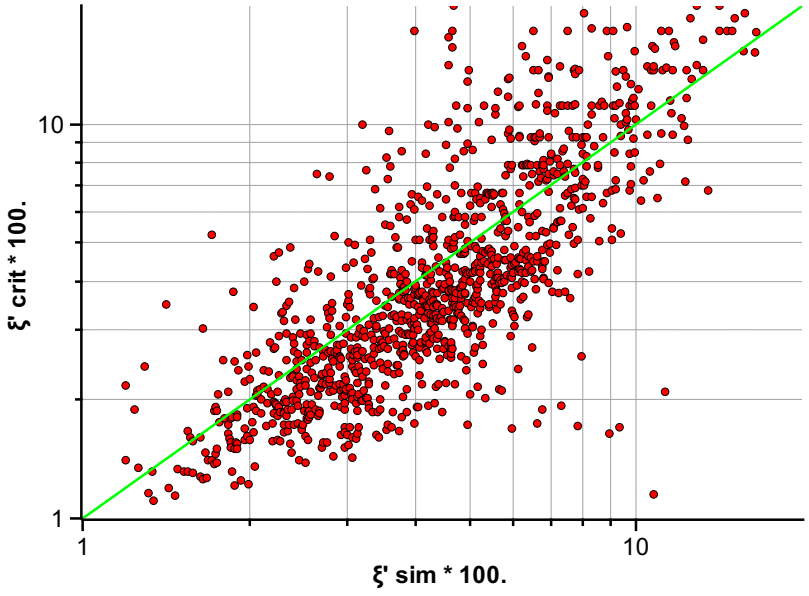

Figure 8.6: Scatter plot showing mean limiting wave steepness of simulation(abscissa values) and simplified criterion (ordinate values)

Ship type	Ships	Cases
RoRo	34	116
RoPax	48	164
Pax	18	55
Container	31	97
Bulker	14	42
Tanker	7	20
Multi-Purp	13	35
Navy	7	23
Other	4	10

Table 8.1: Number of ships and associated loadcases contained in the evaluation database. Sorted by ship type.

The regression delivers correlation factors of C_{10} = 0.94414 and C_{11} =0.9251. The resulting scatter diagram for the correlated values is shown in Figure 8.6. The correlation coefficient between the limiting wave heights is calculated at 0.764, which indicates a strong dependency of the limiting wave heights on the lever arm balance.

The correlated values also show a good agreement with moderate and mean wave steepnesses. For very steep waves the lever arm balance tends to be slightly less conservative than the simulation. This again shows the necessity to account for the directly excited moments in steep waves. The introduction of the A_{ext}-addition to the pure lever arm balance in longitudinal waves improves the situation significantly.

8.2.2 Frequency Dependency of the Limiting Wave Height

The first part in Equation 8.4 is introduced to account for the dependency of the limiting wave height, from the relationship between the encounter frequency of the waves relative to the ship and the eigenfrequency of the roll motion. Typically, there are three critical frequency ratios. The first one is given at ω_e/ω_s =0. This occurs when the speed of wave propagation equals the ship's forward speed. Generally, this situation is often related to the pure loss of stability scenario, as the ship rests on the wave crest for a long period. The other two situations that are critical for the ship, are the resonance conditions when the encounter frequency equals the ship's eigenfrequency of roll, or when the encounter frequency is twice the eigenfrequency. The latter mentioned is usually the more critical, as the ship faces a wave trough condition in one reversal point of the roll motion and a wave crest condition in the other. This maximises the net-energy introduced into the system.

In order to identify and quantify the relationship between the frequency ratio ω_e/ω_s and the limiting wave height, the results of the numerical simulations were analysed. For this purpose, a mean limiting wave height ($\overline{H}_{lim}$), averaged over all speeds is calculated for each case in the database. Then, the normalised difference between the limiting wave height (H_{lim}) and the mean wave height is determined according to Equation 8.13.

$$\delta H^1_{lim} = \frac{H_{lim}(v_s) - \overline{H}_{lim}}{\overline{H}_{lim}} \tag{8.13}$$

The results are plotted over the frequency ratio ($\frac{\omega_e}{\omega_s}$), whereas the frequencies were calculated according to Equations 8.14 and 8.15. In order to calculate the more complicated natural roll frequency of the ship in waves, some assumptions and simplifications need to be made. In particular, the approach has to account for the changing stability in waves, which is realized in this case by introducing an effective metacentric height GM_{eff}. The idea behind this approach and the underlying calculation procedure used for the determination of GM_{eff} can be found in Section 8.2.3.

$$\omega_e = \omega - \frac{\omega^2}{g} v_s \cos\mu \tag{8.14}$$

$$\omega_s = \sqrt{\frac{g\ GM_{eff}}{i'^2}} \tag{8.15}$$

The results are shown in Figure 8.7. The values are scattered over a relatively large area indicating that there are more influencing factors than covered by the present approach. Another reason for the widely scattered values may be the averaging of limiting wave heights over a range of encounter angles. Finally, the calculation of the ship's natural roll frequency contains uncertainties to some extent, due to the non-linearity of the lever arm curve and due to effects in waves. This problem is described in more detail below. Nevertheless, the trend of the overall dataset shows a clear imprint of the resonance conditions. Especially the 2:1-resonance is visible by a significant reduction of the mean value of the limiting wave height factor.

To account for this dependency between the limiting wave height and the frequency ratio of encounter frequency and natural roll frequency of the ship, the mean limiting wave height, as determined by the area balance described above, has to be corrected by the function $f(\omega_e/\omega_s)$. This function is obtained by means of regression from the simulated dataset as presented in Figure 8.7. The functional approach used for f is parted into two sections, one reaching between the frequency ratio of 0 and 2.8, the second formula covering all values above. This procedure was introduced, as one usually expects significant reductions in the limiting wave heights for frequency ratios 0, 1 and 2, but no significant influence of

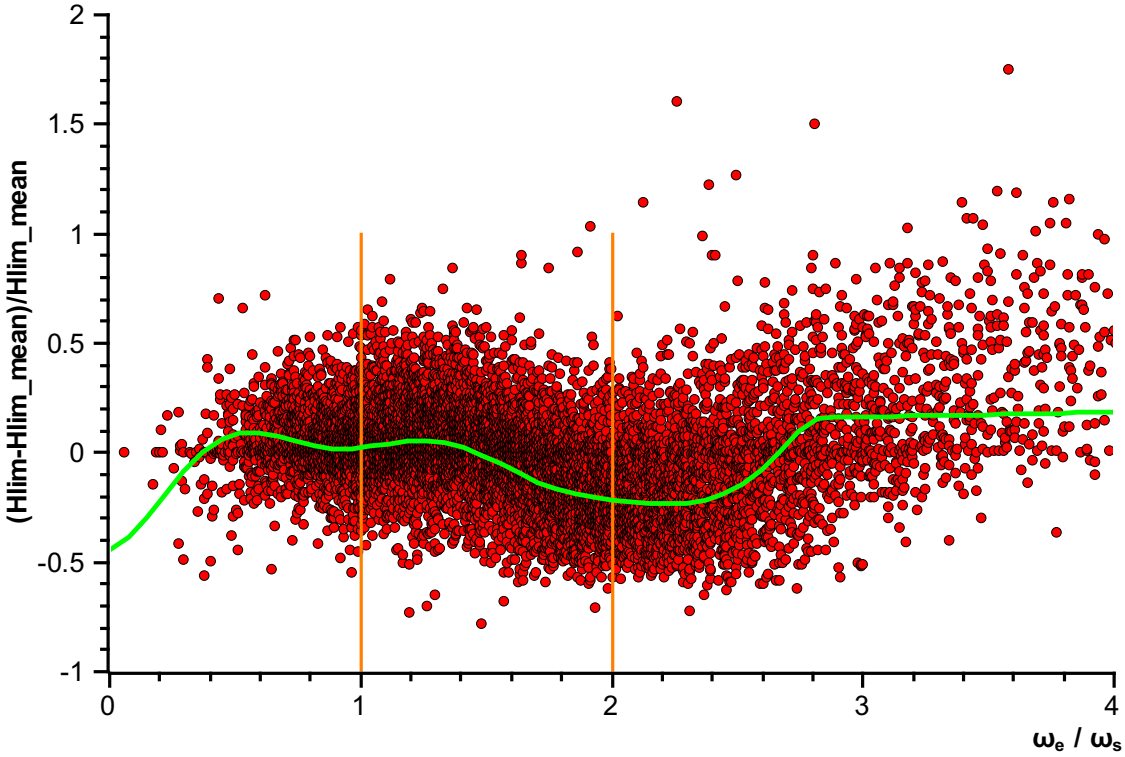

Figure 8.7: Deviation of limiting wave heights from mean limiting wave height over frequency ratio between encounter frequency and natural roll frequency of the ship

higher multiples of the resonance condition. Due to this, we need two different functional approaches as defined in Equation 8.16, whilst the overall function has to deliver consistent values at the connection point at ω_e/ω_s =2.8. Equation 8.16 fulfils this condition.

$$\mathrm{f}\ (\tfrac{\omega_e}{\omega_s}, C_i) = \begin{cases} \mathrm{f}_0\ (\tfrac{\omega_e}{\omega_s}, C_i) & \text{for} \quad \tfrac{\omega_e}{\omega_s} < 2.8 \\ \mathrm{f}_0\ (2.8, C_i) + C_9 \cdot \tfrac{\omega_e}{\omega_s} & \text{for} \quad \tfrac{\omega_e}{\omega_s} \geqq 2.8 \end{cases} \tag{8.16}$$

Here, f_0 is a function composed of three sine-functions with different frequencies and phase shift. The resulting function reads:

$$\begin{aligned} \mathrm{f}_0\ (\tfrac{\omega_e}{\omega_s}, C_i) \quad = \quad & C_1 \cdot \sin(2\pi \frac{\omega_e}{\omega_s} - C_2\pi) + \\ & C_3 \cdot \sin(\pi \frac{\omega_e}{\omega_s} - C_4\pi) + \\ & C_5 \cdot \sin(C_6\pi \frac{\omega_e}{\omega_s} - C_7\pi) + C_8 \end{aligned} \tag{8.17}$$

The first sine-component has its minimum values at exactly 0, 1, and 2 $\cdot\omega_e/\omega_s$. As we consider the 2:1-resonance as the more severe condition, which is also supported by the distribution of the values in Figure 8.7, the second sine-function counteracts the first with a 1:1-resonance condition. The amplitude and the phase shift are adjusted with correlation factors $C_1 \cdots C_4$. The third component is provided for further adjustment of the regression function to the given data-sample. C_5 to C_8 are also correlation factors. The non-linear regression procedure is performed by applying a scaled Levenberg-Marquardt algorithm. It delivers the following values:

C_1	$-4.257E-01$
C_2	$9.311E-01$
C_3	$-1.807E-01$
C_4	$1.511E+00$
C_5	$4.578E-01$
C_6	$1.912E+00$
C_7	$7.773E-01$
C_8	$-6.200E-02$
C_9	$2.318E-02$

Table 8.2: Correlation factors calculated for the regression function (Equation 8.17) from the data-sample as shown in Figure 8.7

The resulting function is plotted in Figure 8.7 as a green line. From the chart, it becomes obvious that the regression function is clearly able to assess the two desired resonance conditions and pure loss at zero speed. For higher ratios we assume that the almost constant value represents the behaviour sufficiently accurate. Therefore, the calculation procedure as well as the necessary formulae to assess the limiting wave height in waves is complete. The validation of the concept can be found in Section 8.3. In the following, the remaining problem of the calculation of the natural roll frequency of ships in waves shall be discussed.

8.2.3 Approximate Calculation of the Ship's Natural Roll Frequency in Waves

The ships natural roll frequency, also called eigenfrequency of roll, is required to estimate whether the ship sails close to a resonance condition or not. Generally, the eigenfrequency of an oscillating system can be determined from its mass moment of inertia (Θ_{xx}) and a constant stiffness coefficient (k), which delivers the restoring moment by multiplication with the heeling angle. The related formula reads as follows:

$$\omega = \sqrt{\frac{k}{\Theta_{xx}}} \tag{8.18}$$

This relationship is valid as long as the damping of the motion is low, which is the case for the ship's roll motion. In practise, this very simple relationship suffers from a series of difficulties when being applied to the roll motion. The major problem is the non-linearity and, if the ship is travelling in waves, the variability of the lever arm curve over time. The restoring moment is no longer constant in those cases, but it changes with the heeling angle as well as with the time. This means that even in still water conditions the amplitude of the roll motion influences the natural roll frequency. In cases of a positive added form stability, the frequency decreases with increasing amplitudes and vice versa for a negative added form stability. If the ship is travelling in waves, the lever arm is not only time dependent, but is then also dependent on the wave height and length. This is one fundamental condition for the possibility of parametric roll excitation. Hence, the natural roll frequency must not be considered as a fixed property of the ship, but it is classed as another variable of the oscillating system. Nevertheless, for our simplified approach it is necessary to obtain at least a rough estimation at which speed the ship is endangered by parametric resonance (see also Krüger and Kluwe [44]).

To avoid the afore mentioned problems, the roll eigenfrequency is usually estimated by simply setting the initial metacentric height (GM) as constant stiffness coefficient. This delivers a reasonable estimation for ships with an almost linear lever arm curve at small

roll angles. Modern ship forms often feature large bow flare and barge like transoms. These hull forms lead to highly non-linear lever arm curves, where the initial GM has only a very limited significance for the real stiffness of the system, as it can be easily observed from Figure 8.8.

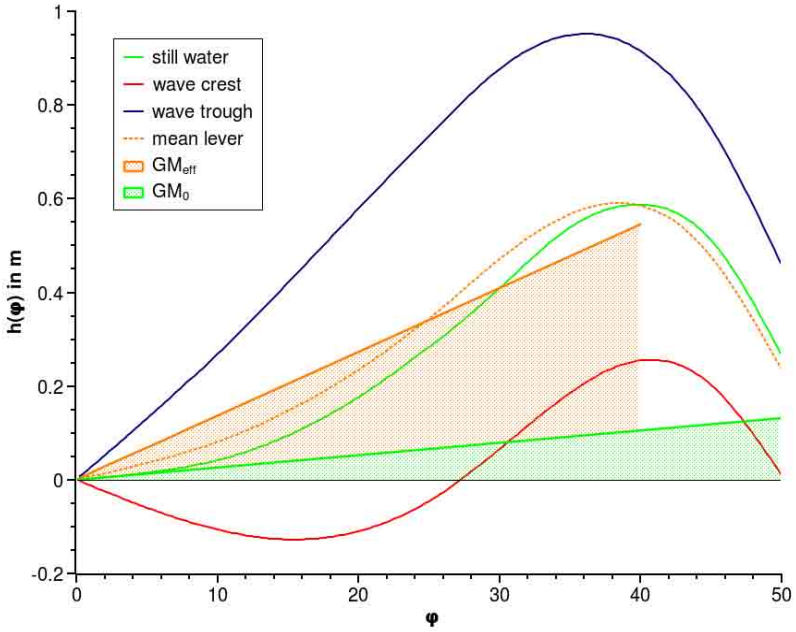

Figure 8.8: Lever arm curves for a container ship in waves (H=5.0m). Diagram shows the lever arm curves in still water conditions as well as wave trough and wave crest lever arms. GM is shown in wine colour, the effective linearised stability graph is printed in orange.

Therefore, we do not use the initial GM for our estimation, but a so called effective linearised stability coefficient, denoted as GM_{eff} in this context. Like the traditional GM it also represents a linearisation of the lever arm curve, but while the GM denotes the gradient at zero degrees heel, the effective coefficient is obtained from an approach based on energy conservation. For this purpose we calculate once more the area under the lever arm curve up to an angle of 40°and determine the GM_{eff}-value so that the area below this line up to 40°equals the real value. Then, the formula to calculate the GM_{eff}-values reads:

$$GM_{eff} = \frac{2}{\varphi_{40}^2} \int_0^{40} h_{eff}(\varphi, H)\ d\varphi \tag{8.19}$$

Here, φ_{40} denotes the angle of 40°expressed in radian. In order to take into account that

the ship travels in waves, we do not use the still water lever arm curve for the integration, but a mean lever arm curve h_{eff}. This curve, represented by the orange dotted line in Figure 8.8 is the average righting lever calculated from the extreme values in wave crest (h_c) and wave trough condition (h_t) and thus can be expressed as follows:

$$h_{eff}(\varphi, H) = \frac{h_c(\varphi, H) + h_t(\varphi, H)}{2} \tag{8.20}$$

This approach is based on the ideas of Wendel [83] which have lead to the development of the intact stability standard BV1033 of the Federal German Navy. It is important to note that the lever arm curves are dependent on the actual wave height. Consequently, the whole calculation of the frequency correction (Equation 8.16) for determining the limiting wave height H_{lim} has to be carried out iteratively, always using the latest value of H_{lim} for the lever arm calculation.

Beside the restoring forces, the acceleration dependent forces are the second main-influencing value for the eigenfrequency. For rotating systems, these are expressed by the mass moments of inertia (Θ_{xx}), here calculated around the ship's longitudinal axis. For use in Equation 8.15 they are transformed into the roll radius of gyration (i'), which can be calculated according to Equation 8.21. Here, Δ denotes the ship's displacement in tons.

$$i'^2 = \frac{\Theta_{xx}}{\Delta} \tag{8.21}$$

To obtain an exact solution, the mass moments of inertia would have to be calculated individually for the instantaneous centre of rotation, which is expected to be situated somewhere in between the longitudinal mid-axis of the waterplane area and a longitudinal axis passing through the centre of gravity. To simplify this calculation, the mass moments of inertia are calculated with a fixed origin situated in the ship's centre of gravity, which seems to be sufficiently accurate for the present purpose. The mass moment of inertia includes all weight items of a loading condition and the lightship weight, whereas all components are defined by their mass, their position and their extension in all three dimensions. Additionally, the roll-eigenfrequency is influenced by acceleration-dependent hydrodynamic forces. They are treated as added mass and therefore have to be considered for the Θ_{xx}. These forces are dependent on several parameters, first of all the hull form and the roll-frequency. As the exact determination is difficult and is beyond the effort acceptable for our simplified criterion and as, moreover, the contribution of these forces to Θ_{xx} is expected to be small, at least for common ship types, we consider them by a general 5% addition to the "dry" values.

Then, all input data and all calculation procedures are available to estimate the roll eigenfrequency according to 8.15. Figures 8.9 and 8.10 give an impression of how accurate the simplified approach detects the resonance conditions in following seas. The polardiagrams on the left hand side show the limiting wave heights obtained from the numerical simulation according to the Blume- and the 50°-max-criteria. In all examples, the resonance conditions can be easily identified by the lower limiting wave heights. The black circles indicate, where the simplified procedure predicts 1:1 and 2:1 resonances. For this investigation the mean wave height from both resonance conditions was used for the calculation. The charts on the right hand side show the individual lever arm curves calculated for the present wave length and wave height. Beside the still water curve, the wave crest and wave trough curves along with the mean lever arm curves are displayed. The purple straight line indicates the effective linearised stability. The first two examples show a medium size container vessel, the last one in Figure 8.9 and the first one in Figure 8.10 are calculated for a RoRo-ship and the last two examples represent a cruise ship and a RoPax-ferry, respectively. All ships were simulated at their intact stability limit according to the IMO A.749 [29].

The examples confirm the findings published in Krüger and Kluwe [44], that the effective linearized stability GM_{eff} provides the possibility to detect the dangerous resonance conditions with reasonable accuracy, whereas, in contrast, the use of the initial GM sometimes delivers wrong results, as shown in the third example. Here, the 2:1 resonance is detected at -0.57 knots using the initial GM, which means that this resonance is not met in following seas. However, the ship clearly shows a critical condition at about 2 knots, which is detected correctly when estimating the resonances using GM_{eff}.

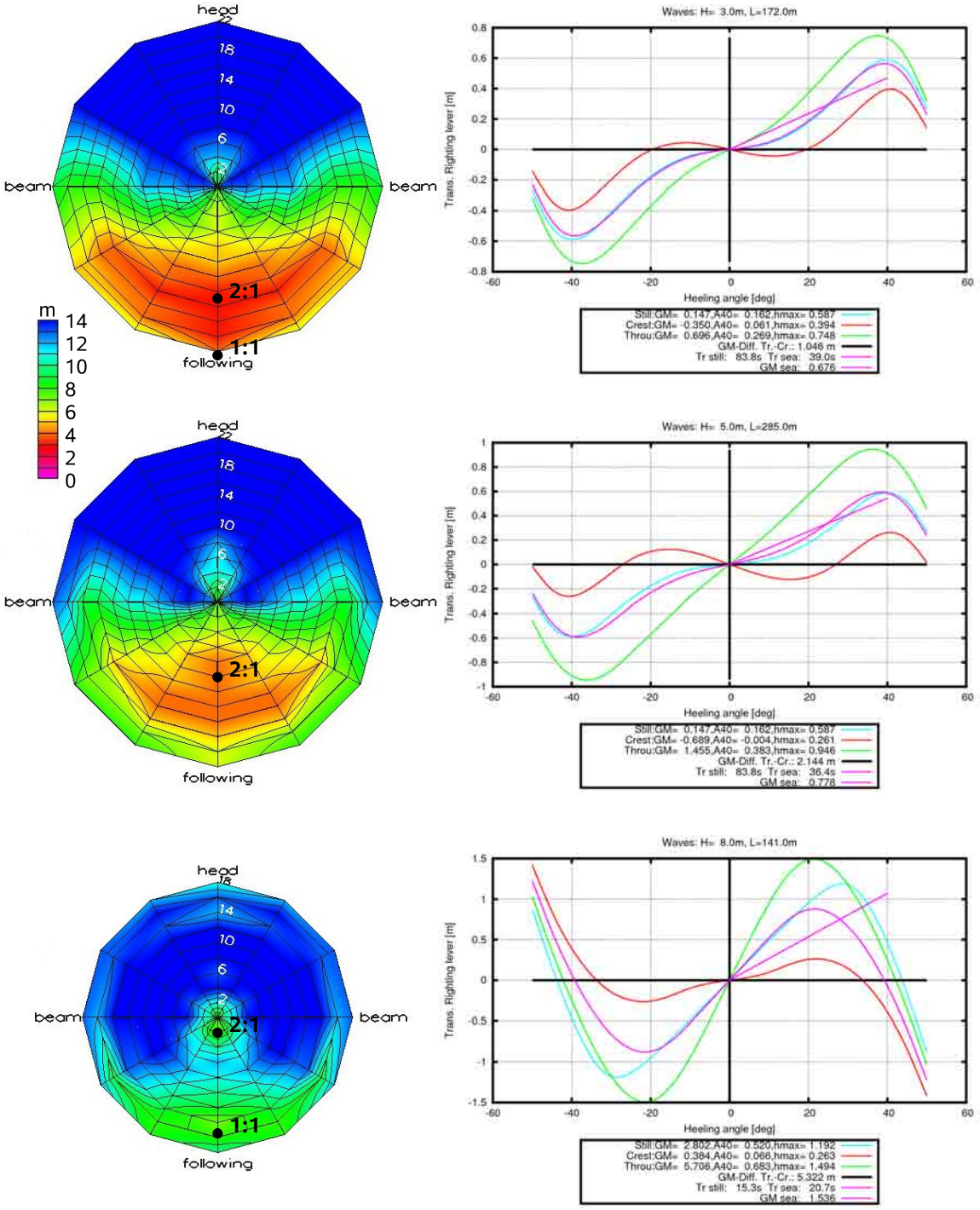

Figure 8.9: Resonance conditions for ships in following seas. Natural roll frequency determined according to the simplified approach using GM_{eff}. Right hand side curves show still water, wave crest and wave trough lever arm curves as well as the mean lever arm curve and the effective linearised stability line.

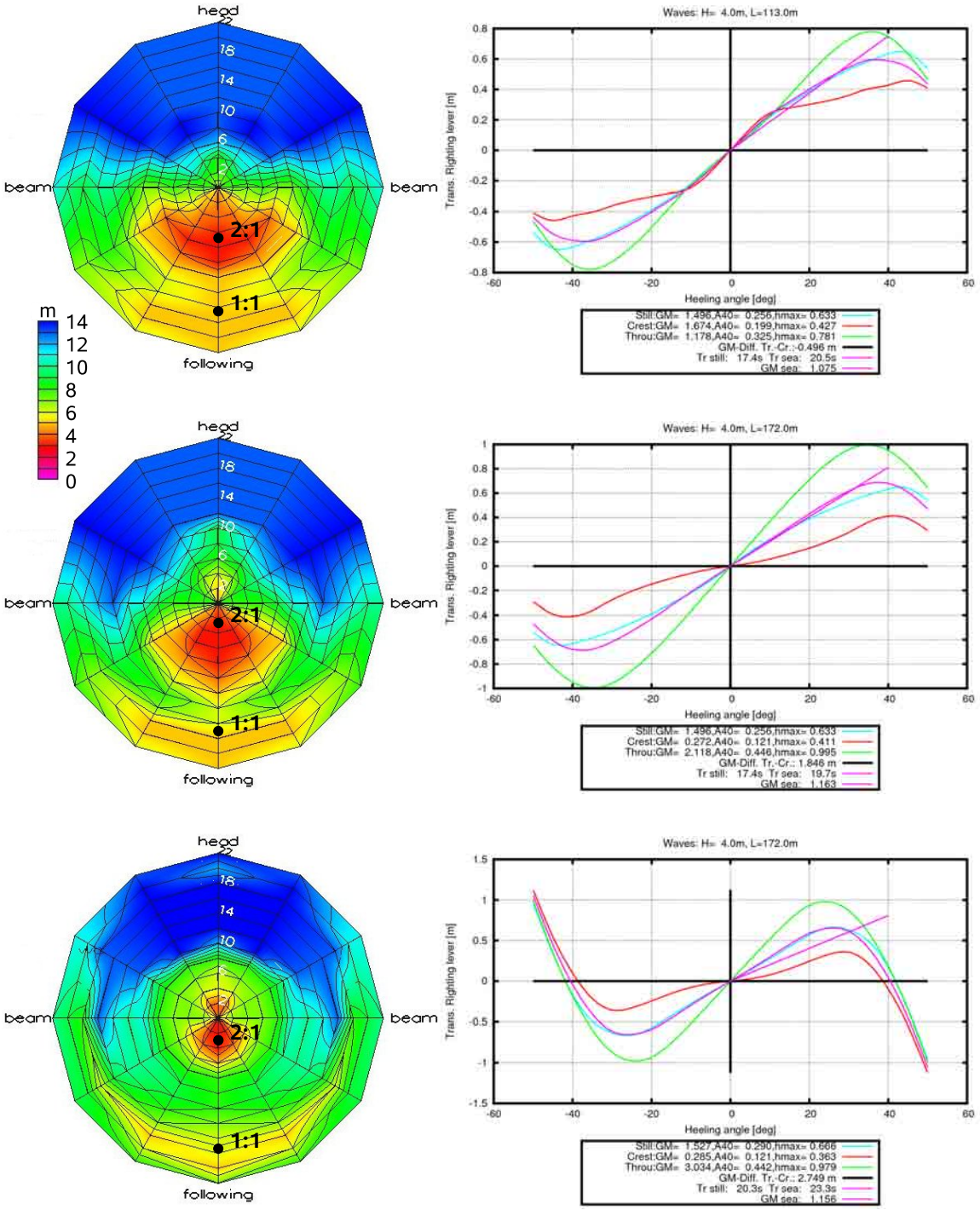

Figure 8.10: Resonance conditions for ships continued.

8.3 Evaluation and Validation of the Minimum Stability Criterion

This section analyses how precise and how reliable the simplified insufficient stability event index (ISEIs) predicts the safety level of a ship, compared to the simulation based approach. In the following, a number of indicators will be discussed to outline this comparison. It is not only important that the values obtained from the simplified criterion come close to those from the simulation, but it is also of interest how reliable a certain statement is. For example, how large the probability is that a ship is considered to be safe according to the simplified criterion, whereas the simulation shows that it is unsafe.

The following paragraphs analyse these questions statistically and by means of selected examples. The basis for the investigations is a database, consisting of 176 ships of different type and size. Some more information on the contents of this database can be found in Section 8.2.1 For each ship simulation results are available for at least three generic loading conditions. For the first loading condition the vertical centre of gravity is always adjusted in such a way that the ship is brought to its intact stability limit according to the present requirements in the IMO Res. A.749. All ships are investigated at their design draft without any initial trim. The mass and the longitudinal and transverse centres of gravity are chosen accordingly. For the second loading condition the VCG is decreased by 0.5 metres, while the displacement remains unchanged. This loading condition in average comes close to the damage stability limit to be fulfilled by the ships according to the current SOLAS [31] requirements. For the third loading condition the VCG is reduced by another 0.5 metres. This loading condition is considered to be the "safe"-condition with sufficient stability in all situations. For selected ships further loading conditions are available, which are also added to the overall dataset.

8.3.1 Comparison and analysis of the simulated ISEI and the simplified ISEIs

For the subsequent investigations the simulation based ISEI and the simplified approach ISEIs are calculated and compared with each other. Figure 8.11 shows the ISEI values for all ships in the database. The abscissa represents the results of the simulation based approach (ISEI), whereas the ordinate values are obtained from the simplified, simulation independent criterion. Every ship is represented by three different generic loading conditions, each marked by various colours. The red bullet points represent ISEI values calculated for loading conditions which equal the ship's individual intact stability limit, according to the present regulations in the IMO Resolution A.749. The yellow bullet points represent loading conditions where the GM was increased by 0.5 metres in comparison to

the intact limit case. In average, this approximately represents the stability level of ships which are operated at the damage stability limit according to SOLAS [31]. Finally, the green bullet points specify loading conditions with the GM-values increased by 1.0 metres relative to the intact limit.

Figure 8.11 clearly confirms that both approaches show the same trend. This is expressed by higher values for cases with low ship stability and smaller values for the loading conditions with increased stability, as the red bullet points are concentrated in the right upper section of the chart, and the majority of the green are located on the lower left hand side. Additionally, it should be noted that pronounced outliers are located almost only above the 45°-line.

In order to evaluate the statistical properties of the two ISEI-approaches the mean values are calculated for the three loading condition categories according to Equation 8.22 and shown in Figure 8.12 on the left hand side.

$$\overline{ISEI} = \frac{\sum_{i=1}^{n} ISEI_i}{n} \tag{8.22}$$

Here, n represents the overall number of samples in the actual category of loading conditions. The mean values confirm the statement made above that both approaches clearly deliver the same trend. The mean results of both approaches have the same order of magnitude in all loading condition categories, whereas the simplified criterion in average delivers more conservative results than the simulation based scheme. This is a volitional feature of the simplified criterion as it incorporates larger uncertainties due to the approach chosen for detection of the limiting wave heights. The aim of adjusting the simplified criterion to the conservative side is to ensure that it does not consider combinations of ship and loading conditions as being save while the simulation shows an unacceptable risk for this situation. Thus, a larger safety margin has to be maintained when assessing a ship with the simplified criterion. In case a specific, more critical design can not be realised on this basis, a detailed investigation including simulations is required to assess whether the seakeeping behaviour is sufficiently safe or not. The risk of a misjudgement in a certain operating condition by the simplified criterion with respect to given threshold values is evaluated in more detail below.

Assuming a threshold value of $1.0\mathrm{E}{-3}$ for both the simulation based approach and the simplified criterion, the overall domain in the scatter plot can be subdivided into four sectors as shown in Figure 8.13. For further information on the determination of the threshold value see Section 7.4. Sector 1 contains all values which are considered to be safe by the simulation, but being judged unsafe by the criterion. In all these cases the criterion delivers a too conservative decision relative to the threshold value of $1.0\mathrm{E}{-3}$. Sector 2 contains all cases which exceed the threshold value according to both approaches,

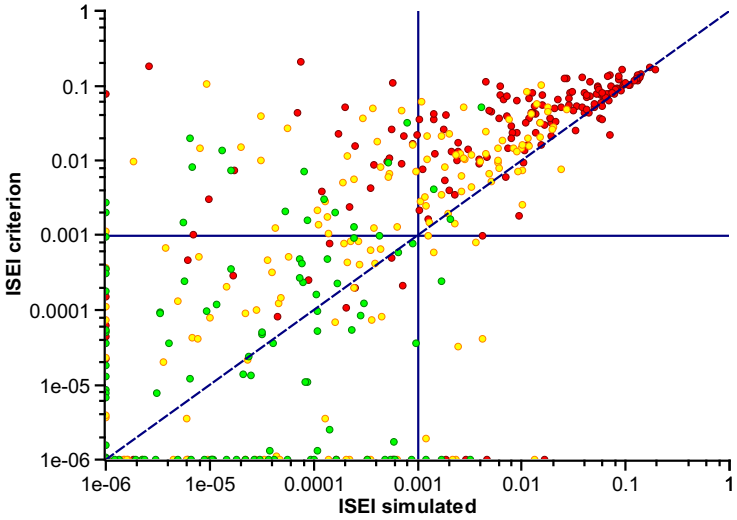

Figure 8.11: The chart shows all ships in the database. Every ship is represented with three loading conditions: Red marks indicate the intact stability limit according to the IMO regulations, yellow shows a loading condition with a GM increased by 0.5m relative to the intact stability limit and green marks indicate loading conditions where the GM was increased by 1.0m.

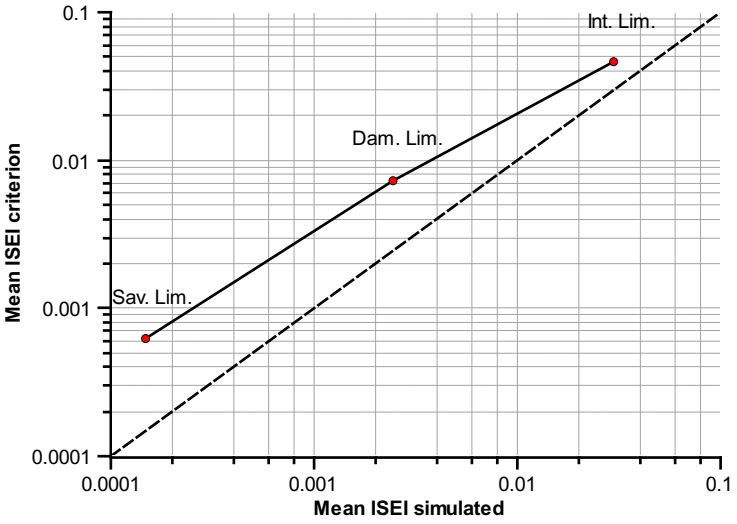

Figure 8.12: The chart shows the arithmetic mean value for each of the three types of loading conditions shown in Figure 8.11. The abscissa contains the mean values for the simulated approach and the ordinate shows the corresponding values for the simplified criterion.

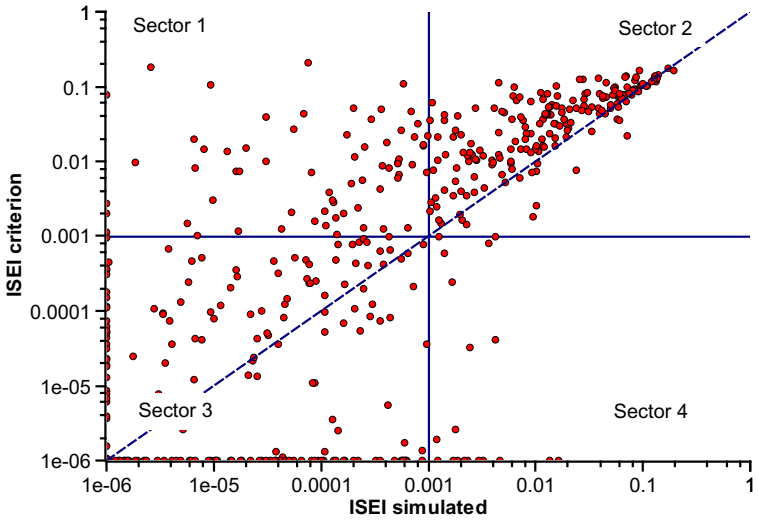

Figure 8.13: Sectored scatter diagram

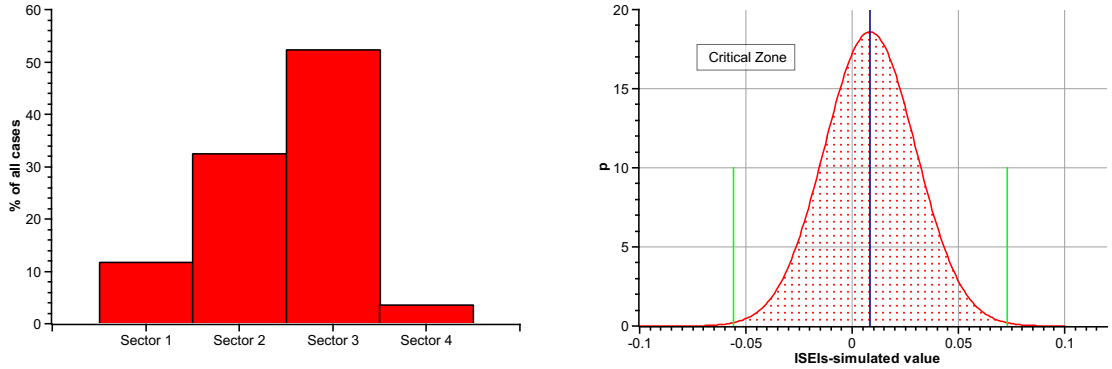

Figure 8.14: Left hand side: Distribution of cases after sectors as indicated in Figure 8.13. Right hand side: Statistical distribution of the difference between the simulated and the simplified ISEI values. The blue bar shows the expected value, the green lines indicate the borders of the 6σ-confidence interval

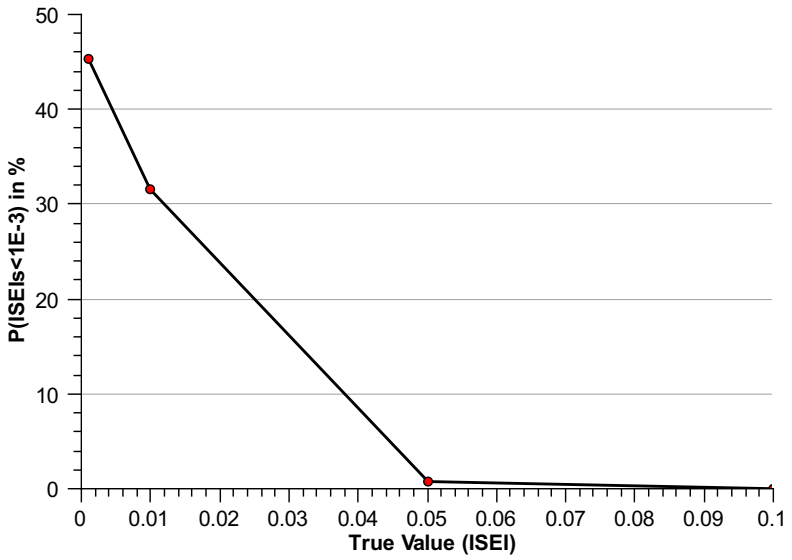

Figure 8.15: Probability in % that the simplified criterion (ISEIs) delivers values below the threshold value of 1.0E-3 in dependency of the "true" value obtained from the simulation (ISEI)

whereas the cases in sector 3 are considered safe by the simulated ISEI as well as by the simplified criterion. Finally, cases in Sector 4 represent the most unfavourable situation where the simplified criterion considers the ship as safe, while the simulation exceeds the given threshold value, which means that the criterion is less conservative than the simulation.

The next step is to analyse how the overall dataset is distributed over the four sectors and how many of the datapoints are located within the "unwanted" sectors 1 and 4. The bar plot in Figure 8.14 on the left hand side shows the distribution by sector, of the full data set containing all ships and all loading conditions. Obviously, most of the cases lie in the correct sectors 2 and 3, namely 84.74 %. The rest is split into the sectors 1 and 4, whereas 11.75 % are located in sector 1 and the remaining 3.5 % in sector 4. This shows again that the simplified approach tends to deliver slightly more conservative results than the simulation, which leads to the positive effect that the share of situations wrongly considered to be safe by the criterion is very low.

In this context, the statistical properties of the differences between the "true" values obtained by the simulation based approach (ISEI) and the simplified criterion (ISEIs) are of importance. For this investigation, the difference between both ISEI-values was

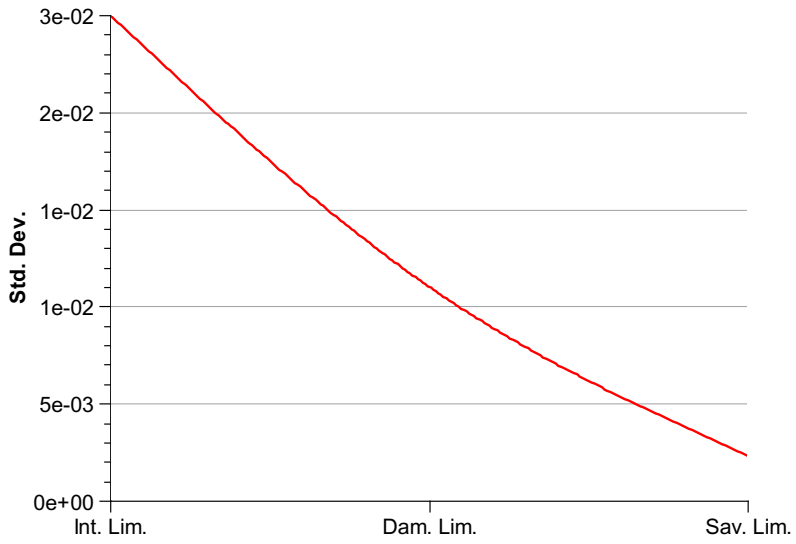

Figure 8.16: Standard deviations for the individual loading condition categories.

calculated for all cases by Equation 8.23.

$$\delta ISEI_i = ISEIs_i - ISEI_i \tag{8.23}$$

For this set of values we determine the arithmetic mean value ($\overline{\delta ISEI}$) as approximation for the statistical expected value. Based on this the standard deviation for the differences reads:

$$\sigma_{\delta ISEI} = \sqrt{\frac{1}{n-1} \cdot \sum_{i=1}^{n} \left(\delta ISEI_i - \overline{\delta ISEI}\right)} \tag{8.24}$$

Now we assume that the difference values $\delta ISEI_i$ are approximately normal distributed around the expected mean value, resulting in the graph shown on Figure 8.14, right hand side. The assumption of normal distribution is not fully correct, because this implies that negative ISEI values would be possible for small ISEI values, but for validation purposes the approximation is sufficiently accurate.

Based on this, it is possible to ask how large the risk is that the simplified criterion considers a certain ship with a specific loading condition as safe, although the simulation delivers values larger than the threshold value. Depending on the "true" value delivered by the simulation the failure probability of the simplified criterion is plotted in Figure 8.15. Obviously the failure probability decreases fast with increasing distance to the threshold

value of $1.0\mathrm{E}{-3}$. It is important to note that the probability of a real unsafe ship with simulated ISEI values above the critical threshold of $5.0\mathrm{E}{-2}$ (see Section 7.4) being considered safe by the simplified criterion is close to zero (0.0069).

When looking at the standard deviation another problem with respect to the quality assessment of the criterion becomes clear. The ISEI values reach over several orders of magnitude. Larger values usually tend to have also larger absolute deviations from the mean value. Putting all values together delivers a standard deviation which is too large for the smaller values. For example, a ISEIs value around 1.0E-4 never must have a standard deviation of 2.0E-2, which is 200 times its own value. In order to overcome this problem at least partly, the overall dataset is split into the three different loading condition categories once again. The same analysis as described beforehand, now is applied to the individual categories. The results are plotted in Figure 8.17. The topmost group of diagrams represents the cases according to the intact stability limit, the second group those according to the assumed damage stability limit and the third group contains all cases with high ship stability for which the GM was increased by one meter. As expected, the standard deviation decreases significantly with decreasing ISEI values, which may be observed also from Figure 8.16. The standard deviation for the loading conditions in category three, containing the cases with high ship stability, is reduced by the factor 10 compared to the category where the ships are operated at their intact stability limit. This is important to note as it ensures sufficient reliability of the criterion also for smaller values. Another important finding is that the criterion keeps its conservative tendency throughout all categories.

Not only the distribution of the differences between both approaches, but also the distribution of the individual loading condition categories over the four sectors is investigated. The related bar plots are shown in Figure 8.17 on the left hand side. As expected, the majority of the cases with low stability is located in sector 2, which means that these cases do not fulfil the requirements of the criterion. A share of about 12% is located in sector 1. Those cases are ships which typically suffer from large lever arm alterations, what makes them unsafe from the simplified criterion's point of view, but which, nevertheless, do not capsize in the simulation. This behaviour was observed for very slender vessels with relatively high stability, for example navy vessels. Blunt ships like tankers or bulkers can be found in this category as well. Here, the criterion may detect resonance conditions to which this type of ships does not react very sensitively. Thus, the results obtained from the simplified criterion are conservative in those cases. The intermediate loading condition shows the largest scatter over all four sectors as ships are operated close to the limit between safe and unsafe. Nevertheless the unwanted sector 4 remains below 6% of all cases. Finally, the loading condition category three, containing all ships with high stability shows more than 80% of all samples in sector 3, which means that simulation as well as the simplified approach consider these situations as sufficiently safe, whereas occurrences in the sectors 2 and 4 are almost neglectable.

Summing up all results, the statements made by the ISEIs with respect to the location of ships and loading conditions in the four sectors can be considered as sufficiently reliable. The conservative tendency of the simplified approach relative to the index values obtained from the simulation based criterion is wanted in order to avoid misjudgements close to the critical limit.

8.3.2 Application of the Simplified Criterion

As shown earlier, the Insufficient Stability Event Index can be used as a minimum stability criterion if the following sea cases are evaluated only. This is due to the reason that in following seas the loss of stability on the wave crest represents the dominating failure mode. Increasing the stability (GM) in such a case will always result in an improvement of the safety level. The simplified, simulation independent criterion exclusively addresses this failure mode. Consequently, the simplified criterion as well as the following sea part of the simulation based approach can be used to determine GM-required curves. These limiting curves are determined from interpolation between index values calculated for different GMs evaluated at each draft investigated. In the following the minimum GM curves obtained from both the ISEI-approaches are put side by side with the curves obtained from the existing regulations for intact and damage stability according to the International Maritime Organization.

RoRo Vessel		
Lpp	186.0	m
B	26.2	m
T	7.0	m
Speed	18.0	kn

Table 8.3: Main Data of the demonstration RoRo vessel

The application example chosen for the demonstration is a RoRo-vessel with main particulars as given in Table 8.3. The vessel represents a most recent design which has been optimised for good seakeeping behaviour during the design phase. This is clearly visible from the fact that the ISEI-limiting curves become the governing criterion only on large drafts close to full scantling conditions. For ships with poor seakeeping behaviour this is expected to occur at much smaller drafts already. In the present case the ISEI-criteria require a slightly higher GM than the existing criteria on full scantling draft, whereas the existing intact stability criteria, the general criteria as well as the weather criterion, are overruled by the ISEI for the displacements relevant in practice. This holds for this type of ship, but may be different for other types, like Tankers and Bulkers.

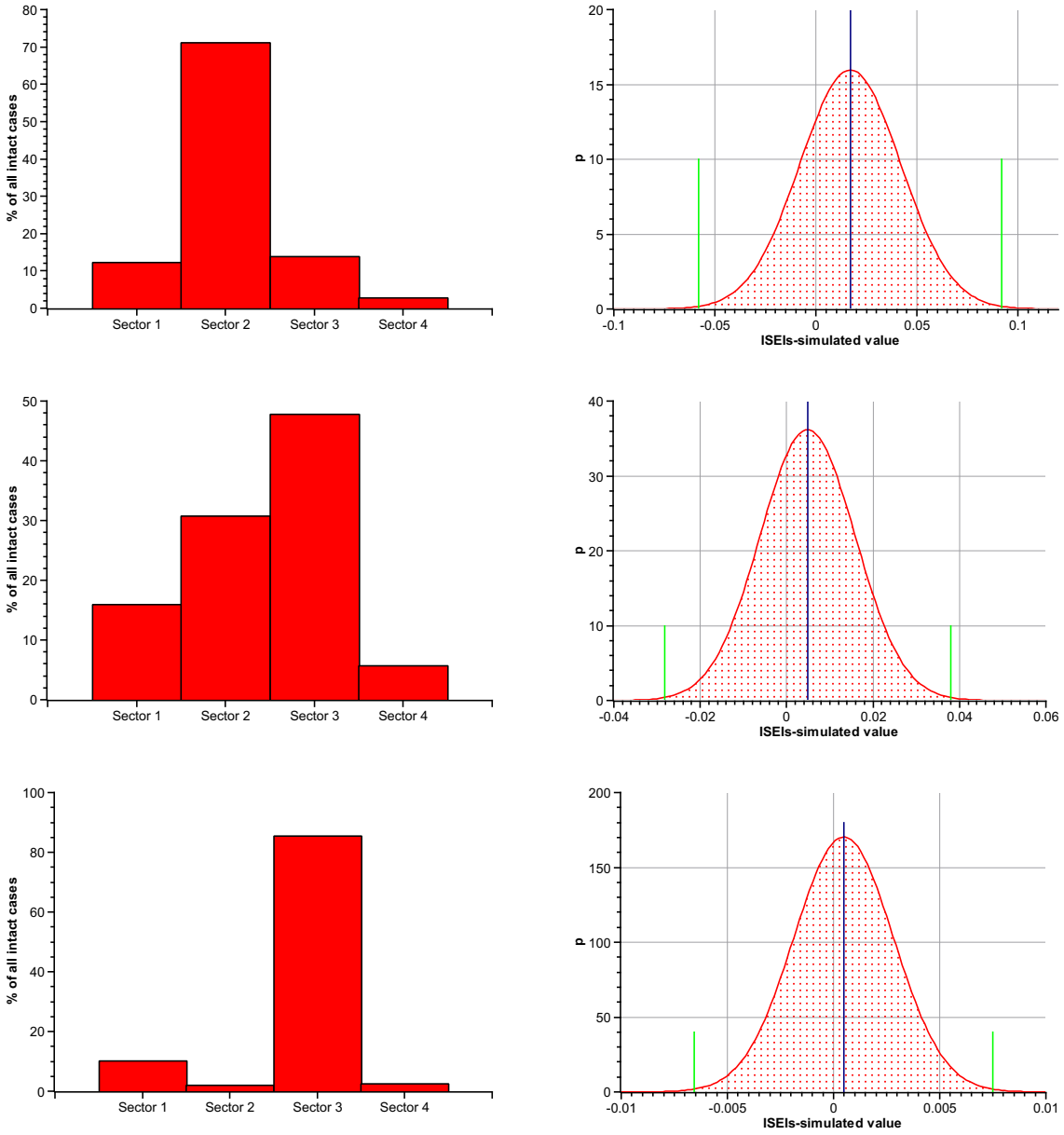

Figure 8.17: Left hand side: Distribution of cases after sectors as indicated on the left hand side in 8.14. Cases split by loading condition: The topmost chart shows the distribution for the loading conditions according to the intact stability limit, the second chart the distribution for the loading conditions with GM increased by 0.50 metres and the last one for those with an GM increased by 1.0m with respect to the intact stability limit of the individual ship. Right hand side: Statistical distribution of the deviation between ISEI and ISEIs for the individual loading conditions.

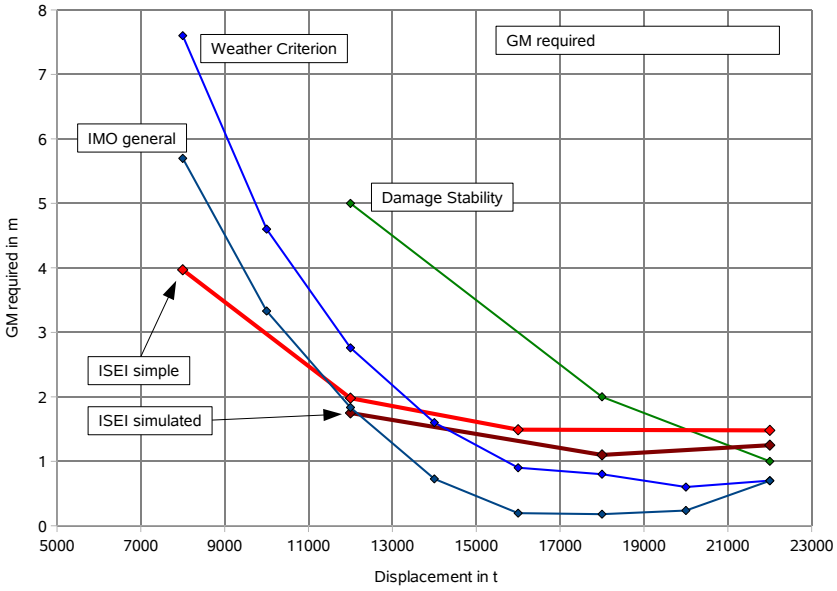

Figure 8.18: GM-required curves for a RoRo vessel, which was optimised with respect to seakeeping behaviour.

Both approaches, the simulation based as well as the simplified, deliver the same trend over the different drafts, whereas the simplified approach is slightly more conservative, as expected. The given example clearly demonstrates the applicability of the ISEI approach for the determination of GM-required curves, as far as we restrict ourselves to following sea scenarios.

9 Conclusions

On the way to a dynamic intact stability criterion the first part of the present work analyses the various failure modes endangering ships in waves. While directly excited roll motions in waves approaching the vessel from abeam usually do not lead to safety critical rolling, longitudinal waves prove to be much more dangerous. This results from the stability alterations caused by those waves, which in turn lead to the reduction of stability while the ship is resting on the wave crest. In extreme cases this phenomenon can lead to the total loss of stability. Additionally, the alteration of stability is a dynamic and periodic process, where the stability oscillates with the encounter frequency of the waves. If the relation between the encounter frequency and the natural roll frequency of the vessel comes close to 1 or 2, pronounced resonance can be observed, leading to fast growing roll amplitudes. The negative influence of the aforementioned phenomena is well demonstrated by a number of capsizing accidents which occurred during past decades.

This is reason enough to ask whether current rules and regulations cover these dynamic failure modes. The second part of the work therefore presents an overview on the intact stability criteria currently in force and analyses their backround. The criteria recommended by the International Maritime Organization (IMO) do not cover dynamic stability with respect to stability alterations at all. Moreover, the general intact stability criteria do neither provide a uniform nor a sufficient safety level for large merchant vessels as well as for modern hull forms. The most advanced stability standard is found in the BV1033, the stability regulations of the German Navy. This criterion directly balances righting and heeling arms against each other, where the lever arm curve is corrected for the stability reduction in waves. However, this criterion does not fully take into account the dynamic alteration of lever arms and hence, does not cover parametrically excited roll motions.

All this induces a compelling need for new intact stability criteria which cover the relevant dynamic failure modes and which provide a uniform and identifiable safety level for all ships. A framework for the development of future rules and regulations known as "Goal Based Standards" is under ongoing development at the IMO. This framework shall provide a clearly defined structure of future criteria by introducing a five tier system, where each tier represents a different depth of detail. The relevant parts are incorporated into the development principles of the dynamic intact stability criterion presented in this work.

Based on the findings made so far, Section 3.5 defines the requirements towards future intact stability criteria. At this, a set of different criteria is suggested to cover the full range of dynamic failure modes potentially leading to damages and total losses of vessels. Following these ideas, the present work concentrates on the subproblem of insufficient stability, mainly in following seas.

The most accurate way to assess the dynamic behaviour of ships is to analyse the ship responses directly. For decades this was only possible by making time and cost intensive model tests. The short duration of the individual test runs and the small number of variations possible, limits the possibilities of a probabilistic assessment of the problem in particular. But today, numerical motion simulation codes are available which have been tested and validated thoroughly. This comes along with a significantly increased speed and capacity of computers, enabling the simulation of long times series in a large number of different operating conditions. For the development of the new intact stability criterion presented in this work, the numerical code E4-ROLLS is used. This code is a tailor-made solution for assessing large roll motions by omitting capabilities not crucial with respect to rolling. The result is a very fast and efficient code, suitable for the probabilistic assessment of ship motions. The main characteristics of the code are presented in Chapter 4. In the same chapter the question is discussed how the natural environment must be modelled in order to obtain realistic results for the ship responses. The natural short crested seaway in E4-ROLLS is generated by superposition of regular wave components, following the energy distribution given by a spectrum. Standardly, a JONSWAP-spectrum is used in the present work, which is suitable to model fully developed wind sea.

Once the ship response is known, criteria must be available to deliver a statement on the ship's safety in a given situation. In case of model tests or time domain simulations, the response is usually given in form of time series. In principle, these can be analysed in two ways. One possibility is to generate statistical data from it, as for example the significant roll angle or a certain rate of exceedance of some value. The second way is to apply a deterministic criterion to the response data, which then delivers a passed/failed-statement. An overview on capsizing criteria of both types is presented in Chapter 5. The *Blume*-criterion combines the statistical evaluation of the time series with a deterministic statement. Our investigations show that this criterion delivers a reliable statement on the likelihood of the exceedance of the angle of vanishing stability.

Therefore, *Blume*-criterion is also used as one element for the Insufficient Stability Event Index (ISEI). The idea behind the index is to determine potentially unsafe operating conditions by means of numerical simulations and to evaluate these situations with respect to their probability of occurrence. Here, the first part is of deterministic nature, while the second part is probabilistic. The deterministic part delivers limiting wave heights for all situations investigated by applying the *Blume*-criterion. All wave heights above the limit are considered to be dangerous. Their overall probability of occurrence is calculated

by the product of the seastate probabilities and the probabilities for the current course and speed of the vessel. The sum over all investigated operational cells delivers the index value.

The North Atlantic Ocean is chosen as a reference area for the seastate probabilities as it is known to be the area with the hardest wave climate. This is in-line with the IMO requirements as settled in the Goal Based Standards. The course probability is assumed to be equally distributed, whilst for the speed probability a linear distribution is chosen.

Following the concept, an increasing index value indicates decreasing safety against capsizing. To enable the use as minimum stability criterion, a threshold value is made available. For this, the largest tolerable index value is determined on the basis of real capsizing accidents. A number of accidents is re-investigated and evaluated for this purpose, following a structured procedure. Starting point is always the loadcase and the environmental conditions which were most probably present at the time of the accident. This situation is always considered to be clearly unsafe and thus, all index values calculated for it represent insufficient safety levels. Then, the stability is increased until all of a defined set of criteria indicate sufficient safety. The result is a set of curves for the individual ships. Based on this set, clearly unsafe, critical and safe regions can be identified for the Insufficient Stability Event Index. From this procedure results that ISEI-values below $1.0 \cdot 10^{-3}$ can be accepted as sufficiently safe, whilst values above $5.0 \cdot 10^{-2}$ are considered to be highly unsafe. The region in between represents critical values, which might be acceptable if the ship is operated with special precautions in sheltered waters.

These threshold values, together with the simulation based index provide a comprehensive framework to evaluate the ship safety with respect to the dynamic seakeeping behaviour. At the current stage of implementation the procedure mainly targets the assessment of minimum stability with respect to pure loss scenarios. The reason for this limitation with respect to practical use is that only for this failure mode a minimum GM-required curve can be determined, whilst resonance scenarios generally can not be improved by a GM-increase. Nevertheless, in principle the concept considers all failure modes the underlying simulation is able to assess. Moreover, its flexible structure allows the adaption to all possible hazards with respect to ships in waves, for example by exchanging the deterministic element, here represented by the *Blume*-criterion, by another criterion.

In a further step, the present work is extended by a simulation-independent criterion. It specifically targets the insufficient stability cases in following seas, which are one of the most critical hazards as they often lead to capsize and total loss. There are two main reasons which motivate the development of such an additional criterion. One reason is that there is no accepted standard defining minimum requirements for numerical seakeeping simulations which makes it difficult to obtain standardised results. The second reason is that seakeeping simulations are relatively time and know-how intensive, why this technology is often not available at regulatory authorities as well as on many shipyards. To enable

a certain transfer of knowledge gained from the frequent and systematic application of simulations to a simplified criterion, which is easy to use, this can in turn increase ship safety on a wide basis.

The concept presented in this work intents to provide as good consistency as possible with the simulation based approach. Due to this reason, the principle structure is left unchanged. The only difference is that the limiting wave heights are no longer determined from simulated ship responses, but from a deterministic criterion which is based on hydrostatic lever arm calculations. The concept makes up a balance between the net-energy brought into the system and the remaining ability of the ship to compensate this energy in conditions, where the stability reaches its minimum in waves. This balance is made up with the extremes of the lever arm curve in wave trough and wave crest conditions, respectively. Additionally, a regression function takes care of the reduction of the limiting wave height in case of a resonance condition. For this purpose the natural roll period of a ship in waves must be calculated, which is a difficult task as this value depends on the amplitude as well as on the non-linear and transient lever arm curve. An approximate solution for this problem is developed based on an effective linearised stability, which better takes into account the real, mean lever arm curves compared to the simple use of GM.

The simplified criterion is calibrated with all samples available for the simulated approach. Regression coefficients ensure that the best possible agreement is achieved between both criteria. The last chapter in this work analysis in detail how good this agreement is and where differences occur. In general, the agreement is good, however some ships do not fully fit into the scheme. In such cases, often a failure mechanism other than pure-loss can be observed.

In summary, both criteria provide a framework to assess the ship safety with special focus on dynamic effects in waves. While the simulation based approach allows a general evaluation of many different failure modes, the simplified criterion focuses specifically on pure loss scenarios in following seas which are clearly related to insufficient stability. In case the investigation concentrates on this failure mode, with or without simulation, it is clearly possible to use the methodology as a minimum stability criterion, as increasing stability always improves the safety in these cases. The establishment of such type of criterion by the regulatory bodies could definitively improve the average intact safety of ships in the future. Additionally, the criterion can also be used as design aid during the development of hull forms as it allows to express the seakeeping behaviour by a single number, which makes hull designs comparable on an objective basis. Finally, the procedure seems to be suitable also for the use in on-board decision support systems which assist the crew by indicating safe and unsafe operating conditions.

For the future a set of criteria, based on the direct assessment of ship responses in the dynamic environment could lead to a further improvement of ship safety. Beside the minimum stability criterion as presented here, the future set of criteria should also

account for maximum stability limits in order to avoid excessive accelerations, as well as for problems of insufficient roll damping and for broaching of ships.

Bibliography

[1] Alaska Department of Environmental Conservation. Situation Report 8. 2006. URL `http://www.dec.state.ak.us`.

[2] Arndt, B. Ermittlung von Mindestwerten für die Stabilitaet. *Schiffstechnik*, Band 7, Heft 35, 1960.

[3] Arndt, B. Einige Berechnungen der Seegangsstabilität. *Schiffstechnik*, Band 9, Heft 48, pp. 157–160, 1962.

[4] Arndt, B. Ausarbeitung einer Stabilitätsvorschrift für die deutsche Bundesmarine. In *Jahrbuch der Schiffbautechnischen Gesellschaft*, Band 59, pp. 594–608. 1965.

[5] Associated Press. Ballast error lead to cargo ship's tipping. News Item, 2006.

[6] Bartsch, H. Statistische Methoden zur Untersuchung der Bewegungen eines Schiffes im Seegang. *Schiffstechnik*, Band 6, Nr. 30, p. 229, 1959.

[7] Billerbeck, H. et al. SinSee - Beurteilung der Schiffssicherheit in schwerem Seegang . *BMBF Statustagung Rostock*, 2005. Funded by the German Ministry for Research and Development.

[8] Blendermann, W. *Umgebungsbedingungen und Lastannahmen, Vorlesungsmanuskript*. Technische Universität Hamburg-Harburg, 2000.

[9] Blume, P. Experimentelle Bestimmung der Koeffizienten der wirksamen Rolldaempfung und ihre Anwendung zur Abschaetzung extremer Rollwinkel. *Schiffstechnik*, pp. 3–29, 1979.

[10] Blume, P. Development of New Stability Criteria for Modern Dry Cargo Vessels. In *Proceedings PRADS Conference*. 1987.

[11] Blume, P. and Hattendorff, H. G. Ergebnisse von Systematischen Modellversuchen zur Kentersicherheit. *Jahrbuch der Schiffbautechnischen Gesellschaft*, p. 219, 1984.

[12] Blume, P. and Hattendorff, H. G. Stabilitaet und Kentersicherheit Moderner Handelsschiffe. HSVA, Report S 165/83 and S 184/84, 1987.

[13] Boese, P. Eine einfache Methode zur Berechnung der Widerstandserhöhung eines Schiffes im Seegang. Institut für Schiffbau der Universität Hamburg, Bericht Nr. 258, 1970.

[14] Boie, C. Gedanken zur Sicherheit gegen Kentern. *HANSA International Maritime Journal*, p. 1821, 1962.

[15] Boie, C. Kenterunfälle der letzten Jahrzehnte. In *Jahrbuch der Schiffbautechnischen Gesellschaft*, Band 59, pp. 509–577. 1965.

[16] Bühr, W., Krüger, S. and Wanot, J. Offenes Methodenbanksystem für den Schiffbaulichen Entwurf. In *28. Fortbildungskurs, Institut für Schiffbau der Universität Hamburg*. 1994.

[17] Clauss, G., Hennig, J., Cramer, H. and Brink, K.-E. Validation of Numerical Motion Simulations by Direct Comparison with Time Series from Ship Model Tests in Deterministic Wave Sequences. In *OMAE2005-67123*. 2005.

[18] Cramer, H. and Krüger, S. Numerical capsizing simulations and their impact on ship design . *Jahrbuch der Schiffbautechnischen Gesellschaft*, 2001.

[19] Det Norske Veritas. *Rules for Ships, Part 5: High Speed, Light Craft and Naval Surface Craft, Chapter 14, Section 5*, 2008.

[20] Faltinsen, O. M., Minsaas, K. J., Liapis, N. and Skjørdal, S. O. Prediction of Resistance and Propulsion of a Ship in a Seaway. In *Thirteenth Symposium on Naval Hydrodynamics*. The Shipbuilding Research Association of Japan, 1980.

[21] Gadd, G. Bilge Keels and Bilge Vanes. National Physical Laboratories and Ship Division, 1964.

[22] Germanischer Lloyd. Ergebnisniederschrift Stabilitaet MS TRIER v. 8. 5.1967. Germanischer Lloyd /SeebG 1967.

[23] Grim, O. Beitrag zu dem Problem der Sicherheit des Schiffes im Seegang. *Schiff und Hafen*, 1961.

[24] Hass, C. *Darstellung des Stabilitaetsverhaltens von Schiffen verschiedener Typen und Groesse mittels statischer Berechnung und Simulation*. Master's thesis, Hamburg University of Technology, Institute of Ship Design and Ship Safety, 2001.

[25] Hasselmann, K. et al. Measurements of wind-wave growth and swell decay during the Joint North Sea Wave Project (JONSWAP). *Deutsche hydrographische Zeitschrift*, Reihe A (12), Ergaenzungsheft, 1973.

[26] Hennig, J. et al. Qualitative and Quantitative Validation of a Numerical Code for the Realistic Simulation of Various Ship Motion Scenarios. In *OMAE2006-92245*. 2006.

[27] Hoppe, H. Goal-Based Standards - A new Approach to the International Regulation of Ship Construction. *WMU Journal of Maritime Affairs, Vol.4, no.2.*, 2005.

[28] Ihms, M. *Bewertung der Kenterwahrscheinlichkeit von Schiffen durch numerische Simulation*. Master's thesis, Hamburg University of Technology, 2004.

[29] International Maritime Organization. *Code on Intact Stability for types of ships covered by IMO Instruments, 2002 Edition, Resolution A.749(18) as amended by resolution MSC.75(69)*. IMO, London, 2002.

[30] International Maritime Organization. REVISION OF THE INTACT STABILITY CODE, Report of the working group (Part 1). *SLF 49/WP.2*, 2006.

[31] International Maritime Organization (IMO). *International Convention for the Safety of Life at Sea, 2004 Edition*. IMO, London, 2004.

[32] International Maritime Organization (IMO). Statement by the Delegation of Singapore. *MSC 82/24/Add.2*, 2007.

[33] ISSC. Int. Ship and Offshore Structures Congress. 1994.

[34] Jensen, A. et al. Measurements of Velocities and Accelerations in Steep and Irregular Waves . In *Proceedings 10th International Symposium on Application of Laser Techniques to Fluid Dynamics*. 2000.

[35] Jiang, T. Hydrodynamische Detailuntersuchung zur Steigerung der Betriebssicherheit und Wirtschaftlichkeit von Seeschiffen, Teilvorhaben 1: Manövrierfragen bei großen Tankern, Zwischenbericht 2, Rationale Beschreibung des Seegangs in der Zeitebene. Germanischer Lloyd, 1988.

[36] Kanasashi Co., Ltd. Capacity Plan. URL `http://www.dec.state.ak.us`.

[37] Kastner, S. Kenterversuche mit einem Modell in natürlichem Seegang. *Schiffstechnik*, Band 9, Heft 48, 1962.

[38] Kastner, S. Modellversuche im achterlichen Seegang mit dem Kuestenmotorschiff Lohengrin. *HANSA International Maritime Journal*, p. 1212, 1964.

[39] Kroeger, P. Simulation der Rollbewegung von Schiffen. Institut fuer Schiffbau der Universitaet Hamburg, 1987.

[40] Krüger, S. Performance Based Stability . *DCAMM - Danish Center for Applied Mathematics and Mechanics, Lyngby, Ph.D.-course Stability of Ships*, 2002.

[41] KRÜGER, S., CRAMER, H., TELLKAMP, J. and FALK, J. Abschlußbericht zum BMBF Teilvorhaben Kentersicherheit im Seegang des Verbundprojektes ROLL-S. Flensburger Schiffbau-Gesellschaft mbH & Co. KG, 2002.

[42] KRÜGER, S., HINRICHS, R., KLUWE, F. and BILLERBECK, H. Towards the Development of Dynamic Stability Criteria. *HANSA International Maritime Journal*, Nr. 9, p. 204 ff., 2006.

[43] KRÜGER, S. and KLUWE, F. Development of Dynamic Stability Criteria from Seakeeping Simulations. In *Proceedings of the Ninth International Marine Design Conference (IMDC), Ann Arbour, Michigan*. 2006.

[44] KRÜGER, S. and KLUWE, F. A Simplified Method for the Estimation of the Natural Roll Frequency of Ships in Heavy Weather. *HANSA International Maritime Journal*, Nr. 9, 2008.

[45] LICHTENBERG, H. Untersuchung des Kenterverhaltens von Marinefahrzeugen durch Simulation. *Project Thesis, Hamburg University of Technology, Institute of Ship Design and Ship Safety*, 2004.

[46] LOAD AND RESPONSES COMMITTEE OF 23RD ITTC. Validation of Sea Keeping Computer Codes in the Frequency Domain (7.5-02 07-02.4). In *ITTC-Recommended Procedures and Guidelines*. 2002.

[47] LONGUET-HIGGINS. The Statistical Analysis of a Random Moving Surface. *Phil. Trans. Royal Society, London*, No. 966, p. 249, 1957.

[48] MITSUI O.S.K. LINES LTD. PUBLIC RELATIONS OFFICE. Incident with the Car Carrier Cougar Ace. Press Relaease, 2006.

[49] MITSUYASU ET AL. Observation of the directional spectrum of ocean waves using a cloverleaf buoy. *J. Physical Oceanogr. 5 (4)*, 1975.

[50] NATIONAL DATA BUOY CENTER. URL `http://www.ndbc.noaa.gov`.

[51] OCEANWEATHER INC. URL `http://www.oceanweather.com`.

[52] PAPANIKOLAOU, A. and SPANOS, D. Benchmark Study on Numerical Codes for the Predicition of Damage Ship Stability in Waves. In *Proceedings of the 10th International Ship Stability Workshop*. 2008.

[53] PAULLING, J. On Parametric Rolling of Ships. In *Proceedings of the 10th International Symposium on Practical Design of Ships and Other Floating Structures*. 2007.

[54] Penny, J., Eaton, A., Bishop, P. and Bloomfield, R. The Practicalities of Gola-Based Safety Regulation. In *Proceedings of the Ninth Safety-critical Systems Symposium (SSS01)*. Springer, 2001.

[55] Perez-Rojas, L. Review of the Ship Accidents Investigations Presented at the STAB Works/Conferences. In *Proceedings of the 10th International Ship Stability Workshop*. 2008.

[56] Petey, F. Ermittlung der Kentersicherheit lecker Schiffe im Seegang aus Bewegungssimulationen. Institut fuer Schiffbau der Universitaet Hamburg, 1988.

[57] Pierson, W. *A unified mathematical theory for the analysis, propagation and refraction of storm-generated ocean surface waves*. Master's thesis, New York University, College of Engineering, Department of Metereology, 1952.

[58] Register of Shipping of the USSR. *Interim Standards of stability for merchant sea-going vessels and coasters*. Morskol Transport, 1948.

[59] Roden, S. Modellversuche in natürlichem Seegang. *Jahrbuch der Schiffbautechnischen Gesellschaft*, Band 56, p. 133, 1962.

[60] Roden, S. Welche Ergebnisse liefern Kenterversuche mit Modellen ? *Schiffstechnik*, Band 9, Heft 48, p. 165, 1962.

[61] SAFEDOR. Design, Operation and Regulation for Safety; European Union research project of the FP6 Sustainable Surface Transport Programme. 2005-2008. URL `http://www.safedor.org`.

[62] Seattle Post - Intelligencer. Rescued crew of listing ship happy to be alive. Newspaper Article by Rachel D'Oro, 2006.

[63] Shin, Y. et al. Criteria for Parametric Roll of Large Containerships in Longitudinal Seas. *SNAME Annual Meeting*, 2004.

[64] Skjong, R., Bitner-Gregersen, E., Helmers, J. B. and Vanem, E. Hazard identification – Dynamic Environmental Loads. *Advanced Decision Support System for Ship Design, Operation and Training (ADOPT), Deliverable D2.4, European Union research project of the FP6 Sustainable Surface Transport Programme*, 2005.

[65] Söding, H. *Bewegungen und Belastungen der Schiffe im Seegang*. Vorlesungsmanuskript Nr. 18. Institut für Schiffbau der Universität Hamburg, 1982.

[66] Söding, H. Gutachten über die Belastungen des Schiffes E.L.M.A. Tres durch Seegang am Vormittag des 26.11.1981. Institut für Schiffbau der Universität Hamburg, 1982.

[67] SÖDING, H. *Leckstabilität im Seegang*. Bericht Nr. 429. Institut für Schiffbau der Universität Hamburg, 1982.

[68] SÖDING, H. Ermittlung der Kentergefahr aus Bewegungssimulationen. *Schiffstechnik*, Nr. 34, 1987.

[69] SÖDING, H. Simulation der Bewegung intakter und lecker Schiffe. In *23. Fortbildungskurs: Sicherheit gegen Sinken und Kentern*. Institut für Schiffbau der Universität Hamburg, 1987.

[70] SÖDING, H. Global Seaway Statistics. *Report Nr. 610, TU Hamburg- Harburg, Schriftenreihe Schiffbau*, 2001.

[71] SÖDING, H. Simulation of the Motions of Damaged Ships in Waves. *DCAMM - Danish Center for Applied Mathematics and Mechanics, Lyngby, Ph.D.-course Stability of Ships*, 2002.

[72] SÖDING, H. and TONGUC, E. Computing capsizing frequencies in a seaway. *Proc. of Stab. 1986, Gdansk, Vol II. Add 1, P. 52*, 1988.

[73] SPANOS, D. and PAPATZANAKIS, G. Review of Numerical Methods for the Prediction of Ship Motions in Waves in view of the ADOPT-DSS. *Advanced Decision Support System for Ship Design, Operation and Training (ADOPT), Deliverable D3.1, European Union research project of the FP6 Sustainable Surface Transport Programme*, 2006.

[74] STEMPINSKI, F. *Seegangsmodelle zur Simulation von Kenterprozessen, Diplomarbeit im Fach Meerestechnik*. Master's thesis, Technische Universität Berlin, 2003.

[75] UMEDA, N., MAKI, A. and ARAKI, M. Some Issues on Broaching Phenomenon in Following and Quartering Seas. In *Proceedings of the 10th International Ship Stability Workshop*. 2008.

[76] U.S. COAST GUARD. Cougar Ace situation update. Press Release, August 2, 2006.

[77] U.S. COAST GUARD. Pumping preparations progress as vessel moves north. Press Release, August 3, 2006.

[78] U.S. COAST GUARD. Cougar Ace summary of events. Press Release, July 26, 2006.

[79] U.S. COAST GUARD. Cougar Ace situation update; Initial vessel survey complete; life of naval architect lost in accident. Press Release, July 31, 2006.

[80] U.S. Coast Guard. Public Affairs Release: Cougar Ace and Ocean Tug Sea Victory Prepare to Depart Unalaska for Portland, Ore. Press Release, September 1, 2006.

[81] U.S.Coast Guard, Mitsui O.S.K. Lines, The O'Briens Group, Alaska Department of Environmental Conservation. Unified Command: M/V Cougar Ace. Website. URL `www.dec.state.ak.us`.

[82] Wagner, D. Kentersicherheit intakter Schiffe. *23. Fortbildungskurs, Institut für Schiffbau der Universität Hamburg*, 1987.

[83] Wendel, K. Sicherheit gegen Kentern. *VDI-Zeitung*, Nr. 32, 11. Nov. 1958.

[84] Young, I. and Holland, G. *Atlas of the oceans: Wind and wave climate*. Pergamon, Oxford, 1996.